METEO
FRANCE

Research **Report**
2017

Research Report 2017

Table of contents

The new Météo-France Objective and Performance Contract (COP) for the period 2017-2021 is launched. Research occupies a privileged place here as it supports all of the establishment's professions. It is the source of subsequent innovations in observation, numerical weather and climate prediction. It enables the institution to constantly improve the quality of its operational products and to open new projects to meet the expectations of society and public authorities.

But there is another element that leads us to reflect further on our scientific strategy. At the end of 2017, the Government launched its "Public Action 2022" initiative, which aims to transform public services in order to improve their quality, update their working environment and accompany the fall in public spending. Included in this reflection, Météo-France is building a new project for the establishment, by integrating the requested reduction in staff over the period, but maintaining its ambitions, those appearing in the COP and in particular those related to research.

At the international level, it will be a question of amplifying our policy of privileged cooperation with the ECMWF around the global ARPEGE/IFS model and consolidating the rapprochement with the ALADIN and Hirlam consortia within which the developments of high-resolution regional models are shared. Météo-France will also continue its policy of active participation in EUMETSAT and ESA programs. In particular, ADM-Aeolus will soon be operational, but also the preparation of the future MTG and EPS-SG satellites, which will carry new high-potential instruments. Météo-France will also continue its strong participation in European projects including Copernicus.

At the national level, Météo-France confirms its involvement in the scientific community, which is manifested through various links with numerous actors including the CNRS, CNES, Universities and its participation in AllEnvi. The establishment is a stakeholder in the AERIS and THEIA Data Poles, the Earth System Pole, Kalideos-Alpes under the aegis of the CNES, and participates in the construction of the IR ACTRIS-FR and CLIMERI-France. In particular, the AERIS data centre is an opportunity and a vector to facilitate access to the operational data of the institution to the world of research. And more locally, Météo-France reaffirms its support for the academic world in Toulouse, in a difficult context following the failure of the Idex.

In terms of its internal priorities, Météo-France will accentuate its long-term "seamless" orientation of its various numerical systems, targeting a single system, from mesoscale to the global level, integrating all compartments of the Earth System: atmosphere, waves, ocean, sea-ice, continental surfaces including hydrology, chemical composition of the atmosphere and in the case of climate, the carbon cycle. All of the main work carried out in the two CNRM and LACy laboratories, as well as in the Institution's thematic departments, is detailed in this document. We can nevertheless mention the major axes which are the forecasting of highly precipitating events, phenomena with a strong impact on our Mediterranean coasts, the forecasting of cyclones which have hit our overseas territories painfully, even tragically, or fog, a phenomenon with stakes for civil aviation and which is the subject of a particular point in the new COP. At the other end of the spectrum, under

the guidance of the IPCC, the CNRM has started simulations of the CMIP-6 exercise with a new version of the CNRM-CM6 climate system and an Earth System including the CNRM-ES carbon cycle. It is also a question of taking better account of the perspectives offered by Artificial Intelligence, in order to better enhance the overall forecasts, the numerous observations and to make the link with the impacts. In this rapidly changing context, the issue of the transfer to operational management is once again becoming an issue that will be at the heart of our thinking.

In connection with the dynamic cores and the perspective of the exascale, Météo-France participates in the Flagship project "Extrem Earth", being the representative of all European countries for the numerical modelling of weather. The target is the development of a convective scale global ocean-atmosphere model for exascale capacity calculators. If this Flagship were to succeed, it would be a major and structuring challenge for the entire European meteorological-climatic community. For the moment, Météo-France, which saw a rise in power of its computers in 2016 (2 x 2.5 Pflops), notes, both with satisfaction but also concern, that today the implementation of all scientific advances is leading to a saturation of both machines. The project to renew our computing resources in 2020 is therefore a major challenge, to continually convert research work into improvements to our digital systems, and ultimately, to better predict and prevent.

Before concluding, it should also be mentioned that Météo-France wished, in 2017, to clarify the organization of its research by creating a Research Department on the First of January 2018. It was a question of affirming the existence of a specific direction in connection with the actors of research and to formally recognize in our internal Organization Documents, the various "Unités Mixtes" whose supervision Météo-France shares and which materialize our strongest partnerships. These entities are the UMR CNRM, the UMR LACy and the UMS SAFIRE, but also the UMS of three Observatories of Universe Sciences: the UMS of the OMP in Toulouse, the OSUG in Grenoble and, since the First of January 2018, the OSU-R in Reunion Island.

This editorial cannot cover or summarize all the topics covered in this Research Report 2017. The detailed articles that follow are fascinating and illustrate perfectly the wide spectrum of our research activities, all essential to the establishment and its future.

Enjoy your reading.

Marc Pontaud
Director of Research, Météo-France

Numerical weather prediction

The most remarkable achievement in the area of numerical weather prediction is the completion of the use of the SURFEX surface model across all operational suites. SURFEX embodies the long-term investments of Météo-France research department in turbulent processes and surface-atmosphere interactions. It is a tile-type model now offering many surface types and layers, with the ability to handle their interactions. SURFEX has been the surface model of AROME since the beginning of that convective-scale system; it has also been the surface component of CNRM-CM, the coupled climate model of Météo-France, for example in the CMIP5 and subsequent contribution to the 5th IPCC assessment report. It has been introduced into the dedicated overseas versions of ALADIN, recently replaced by specific AROME configurations. In short, it has been a long standing objective to have it available also in the global short-range prediction systems based on ARPEGE: its ensemble assimilation, ensemble prediction, 4DVar data assimilation and higher-resolution configurations. Long standing here means some plans are close to be 15 years old, which is a way to say that this change has long been known to be a huge technical challenge. There always were more pressing things to do, more critical ones. The core of the difficulty was to enable a smooth and efficient key surface parameters update through the global data assimilation cycle. The ARPEGE suite had been one of the first global systems to benefit from such a feature, using optimal interpolation for analysing screen-level temperature and humidity, and correcting soil temperatures and water contents. Thanks to a commensurate dedicated effort, the many technical problems relating to a two-way interfacing of SURFEX with this system component in the main 4DVar suite as well as in the ensemble data assimilation have been tackled. Not everything is optimal yet, but this achievement opens a new era, given the many possibilities offered by SURFEX: it is a true investment that will yield benefits in the years to come. It is, for example, a significant step towards seamless data assimilation and modelling set of systems, since from now on, SURFEX is universally used. Many colleagues have, in the end, contributed to this achievement, meaning here not only the scientists from the Mesoscale Research group that developed the initial concept but also our colleagues from the operational departments of Météo-France and from the NWP group itself. However, this particular and difficult step successfully taken this year can only be dedicated to our colleague and friend Françoise Taillefer, who disappeared accidentally on the morning of the 7th of April 2017, having barely completed most of this work.

The following pages address other aspects of the ongoing research studies that, in the end, aim at improving the numerical forecasts provided by Météo-France both directly to citizens through its Open Data policy and indirectly through its expert forecasters. It must be remembered here, again, that the computer code behind these numerical tools is uniquely developed in strong, close cooperation with ECMWF and with more than 25 national hydrometeorological services from Europe and Northern Africa. This code benefits from, adding to it, scientific innovations but, at the same time, it is constantly adapted to make the most of current and upcoming high-performance computing architectures. This in itself also requires a deep sustained involvement of a large part of the NWP research group. Not all areas of progress are mentioned in the following pages. Together with the inclusion of the SURFEX surface model, many other changes have become operational in December 2017: a further increase in the number and diversity of observations assimilated by both AROME and ARPEGE, better initial conditions for several AROME configurations, a huge increase in the semi-processed output directed to forecasters and service users, a first step in ocean-atmosphere short-range coupled forecast, etc. Perhaps one of the most significant highlight of the usefulness and operational quality of the operational suite that results from all this work are the oversea AROME forecasts of tropical cyclones, in particular of the two cyclones that hit several Caribbean islands during the first days of September 2017, named Irma and Maria. These forecasts featured for example wind gusts predicted to reach more than 200 km/h, the model yet steadfastly coping with this and providing many other coherent extreme variables, that turned out to be observed along the right track and at about the right time.

①

On the representation of isentropic moist-air processes

It is usually assumed that the moist-air entropy can be represented in atmospheric science by the quantity e named equivalent potential temperature. A recent study published in the Journal of Atmospheric Science (October 2017, pages 3451-3471) invalidates this hypothesis by comparing the properties of θ_e with those of the potential temperature noted s which corresponds to the definition of the moist-air entropy and which is based on the third law of thermodynamics.

The two figures show isentropic stream functions computed with either θ_e (on the left) or θ_s (on the right). These figures are plotted by using outputs from the ALADIN model and for the Hurricane Dumilé located Northwest of Reunion Island in January 2013. These stream functions allow a synthetic description of the moist-air processes involved in the steam or Carnot machines forming the cyclones.

The ascending branches (upward black arrows) are associated with a decrease in θ_e between 1 and 4 km, whereas θ_s is a constant or increases with height. These behaviours are clearly incompatible, because the entropy is a state function and its variations between two points of the atmosphere cannot correspond at the same time to an increase and a decrease, depending on the chosen definition for computing it.

Therefore, one must trust in θ_s to represent the moist-air entropy, because it is the only definition which agrees with the third law of thermodynamics, a law discovered by Nernst and fully understood by Einstein and Planck at the beginning of the twentieth century. The study describes other properties for which the third law must be applied: to compute work functions or efficiency factors for steam or Carnot cycles, among other properties.
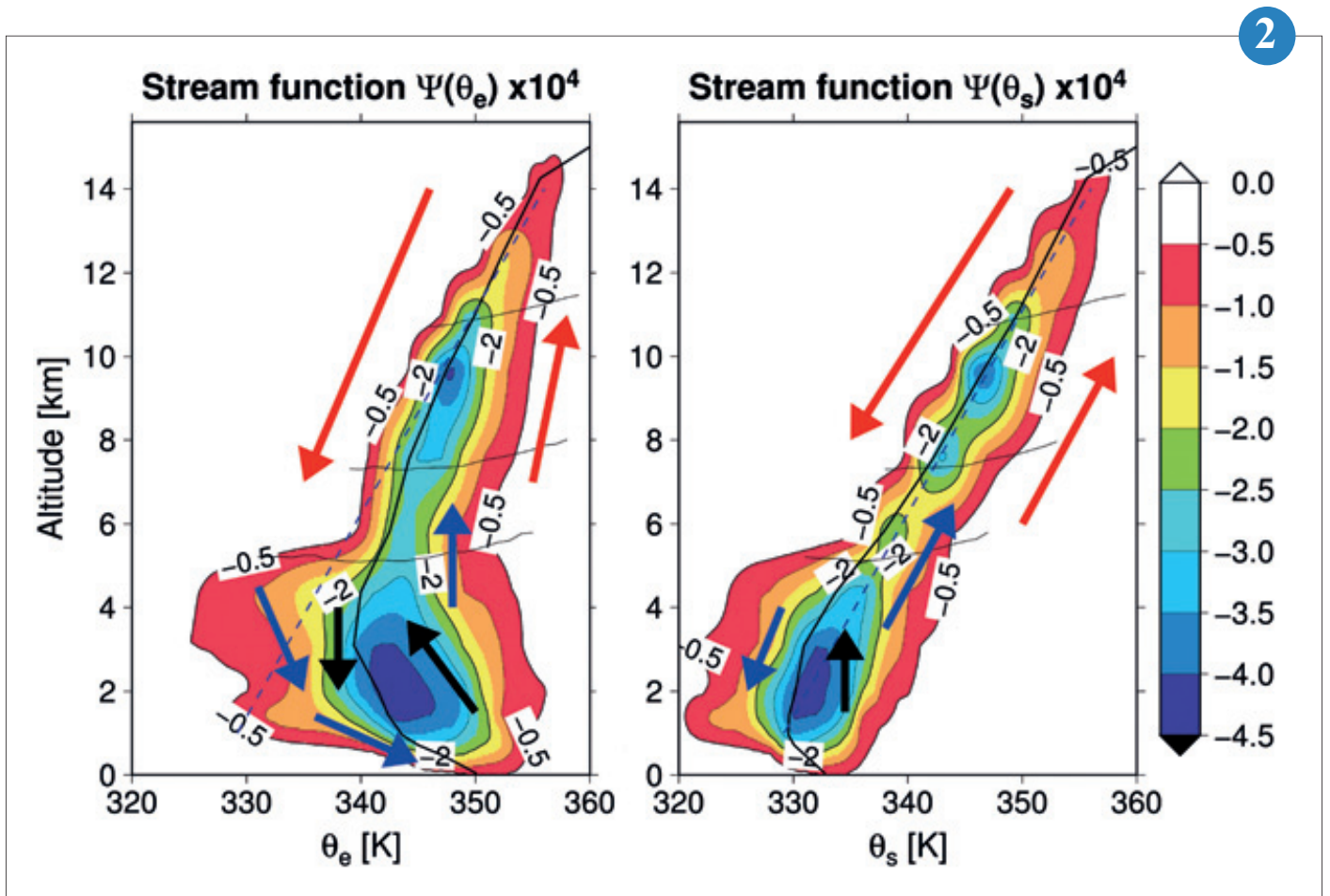
②

The isentropic stream functions Ψ computed with θ_e (on the left) or θ_s (on the right) in units of 10^4 kg/m^2/s.
The arrows indicate the mean circulation simulated by the model ALADIN for the cyclone Dumilé. The thin solid curves represent the mean freezing level (at about 5 km) and the lines of equal -12 and -38 Celsius temperatures (at about 8 and 11 km).

Local discrete space operators for reduced A-grid on the sphere

The aim of this research is to replace the spectral technique used in current operational forecast models of Météo-France, because it is not well suited for emerging massively parallel computers, due to the heavy amount of data communication require data each time-step. The method examined here keeps the current reduced lat-lon grid (with a quasi-uniform resolution, see Fig. a). The semi-structured aspect of the grid is exploited to build local (with few communications) but highly-accurate discrete space operators.

We have shown that, provided a particular care is exerted near poles, it is possible to define space operators with a uniform formal accuracy on the whole sphere. The stability of these space operators now needs to be demonstrated for all hydro-dynamical regimes occurring in real atmospheric conditions. This work is ongoing, by examining the behaviour of idealised two-dimensional forecasts with severe conditions, first outside poles (see Fig. b) and at poles themselves (ongoing work).

The next steps will then be to assess the stability for three-dimensional flows with severe conditions near poles, and to check the compatibility of these algorithms with the targeted new time-discretizations for operational models.

③

High-resolution Ocean-Waves-Atmosphere coupling contribution for tropical cyclone prediction

Ocean-Waves-Atmosphere (OWA) exchanges are not well represented in current Numerical Weather Prediction (NWP) systems, which can lead to large uncertainties in tropical cyclone track and intensity forecasts. In order to explore and better understand the impact of OWA interactions on tropical cyclone modelling, a fully coupled OWA system based on the atmospheric model Meso-NH, the wave model WaveWatch3 and the oceanic model CROCO (and alternatively NEMO-Indien) was designed and applied to the case of intense tropical cyclone Bejisa, which passed nearby Reunion Island (SW Indian Ocean) in January 2014.

The fully coupled simulation shows a good agreement with the available literature and observations. Two figures illustrate several representative parameters of the 3 components simulated by the coupled system. A horizontal resolution of 2 km is used for each model. Figure "a" (colours) shows the wind speed at 10 m, illustrating the well-known characteristics of a cyclone, i.e. the eye, the eyewall and the outer bands. The significant wave height (figure "a": contour) reaches more than 8 m at the front of the cyclone, in the eyewall where the effect of cyclone displacement cumulates with the increase of the wave fetch.

Figure "b" shows the ocean surface response during the cyclone. A cooling of about 2°C is attributed to an intense vertical mixing produced mainly by currents (figure "b": vectors), which are maximum in the left quadrants of the cyclone, where winds are also maximum. Sensitivity experiments used to highlight the impact of oceanic waves show that waves have limited impact on the track, the intensity evolution and the turbulent surface fluxes of the tropical cyclone. However, it is shown that using a fully coupled OWA system is essential to obtain consistent sea salt emissions and to properly reproduce their impact on heat and momentum fluxes.

④

Use of cloud radar data for Numerical Weather Prediction (NWP) model

Because of their high sensitivity to clouds and light to moderate precipitation, W-band cloud radars are very complementary to the traditional active sensors that are commonly used in meteorology (lidars and ground-based precipitation radars). Currently, these data are not used to initialise regional AROME class NWP models. To this end, a forward operator is needed to convert the physical fields predicted by AROME into reflectivity.

Therefore, a W-band reflectivity forward operator is designed in consistency with AROME and is devised for airborne and ground-based vertically pointing radars. To validate the forward operator, the Most Resembling Column (MRC) method is conceived to disentangle model spatial mismatches from errors in the forward operator. Each observed vertical profile is compared with the most resembling simulated one in a given neighbourhood.

This novel method is used to validate the forward operator using data collected in diverse conditions by the airborne cloud radar RASTA during the HyMeX first Special Observing Period. The MRC method is then applied to retrieve the optimal effective shapes of the predicted ice hydrometeor species. It is shown that treating snow and graupel particles as oblate spheroids, instead of spheres, leads to good agreement between the observations and simulations of the ice reflectivity levels.

The reflectivity forward operator developed here is the first step towards the assimilation of such data into AROME. It can also be used as a validation tool, for example to assess the benefits of the two-moment microphysical scheme LIMA over the one-moment microphysical scheme ICE3.

⑤

3

Grid point locations

a: Configuration of the reduced grid near a pole.
The number of points on the first latitude circle is 18, and progressively increases with distance from the pole.
B: Zoom of the potential vorticity field (abscissae: longitudes, ordinates: latitudes, in degrees) for an idealized forecast of barotropic instability flow, after 6 days of simulation.
The structure of the field is exactly matching that given in reference in the literature.
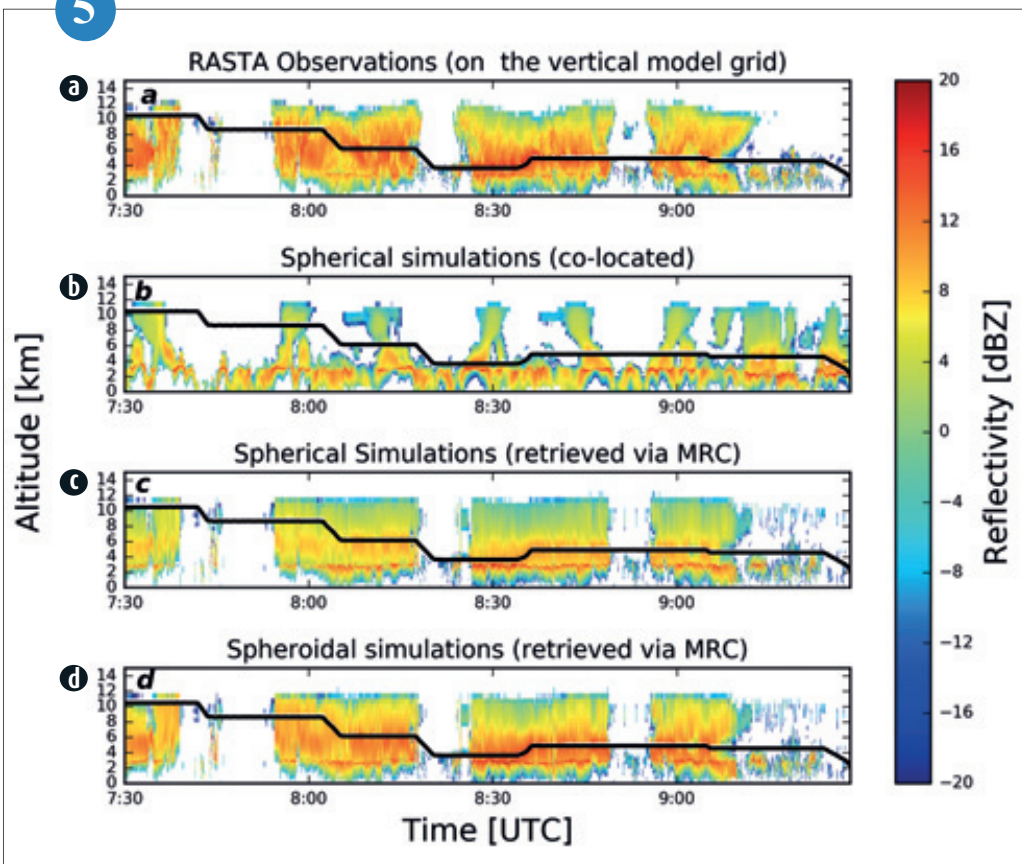
4

Bejisa : 02-01-2014 06:00
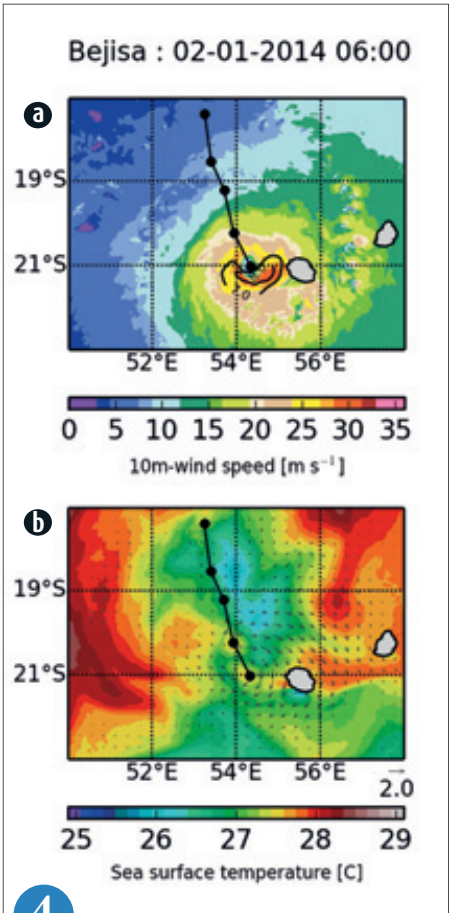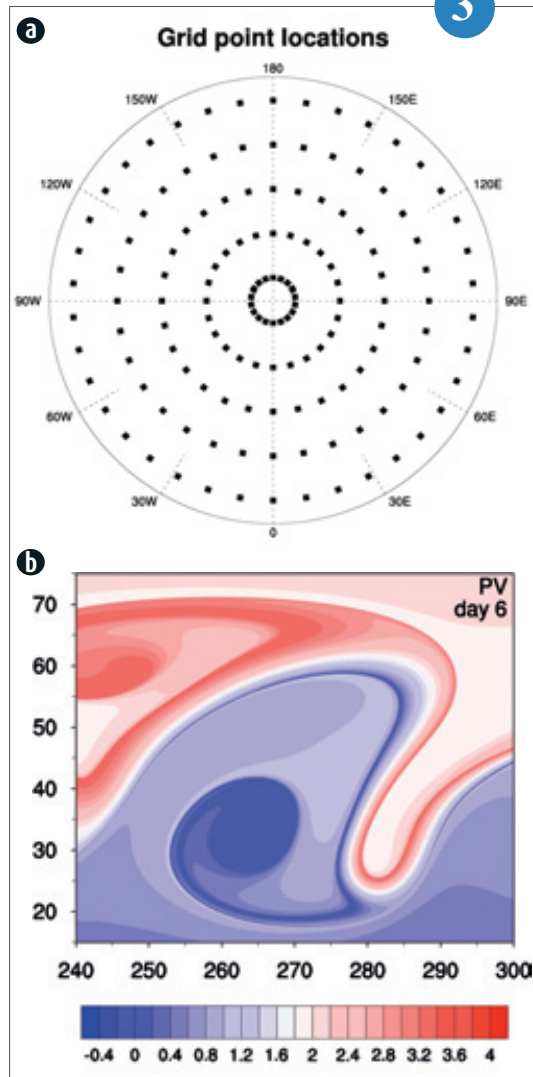
Instantaneous fields resulting from the coupled OWA simulation during the passage of tropical cyclone Bejisa near Reunion Island
a: 10m wind speed (colour) simulated by Meso-NH and significant wave height (contour) simulated by WW3.
b: sea surface temperature (colour) and surface currents (arrow) simulated by CROCO.

5

RASTA Observations (on the vertical model grid)

Spherical simulations (co-located)

Spherical Simulations (retrieved via MRC)

Spheroidal simulations (retrieved via MRC)

Time-height cross section of the reflectivity observed by RASTA (Figure a) along the aircraft track on 26 October 2016.
The corresponding co-located simulated profiles are shown in Figure b.
The simulated profiles retrieved by the MRC method are shown in Figure c when snow and graupel particles are considered spherical and in Figure d when they are both treated as oblate spheroids.

Using the cloud radar "Basta of Bourbon" (BOB) for climatology studies and evaluation of the operational model AROME-Indian Ocean

LACy acquired a 95 GHz cloud radar BASTA in 2016. This radar, deployed on the new observation site of "Observatoire de Physique de l'Atmosphère de La Réunion (OPAR)" located at Reunion Island University, will be used in synergy with the aerosol lidar MARLEY (Mobile Aerosol Raman Lidar for troposphEre surveY) and a set of weather sensors (2DVD, weather station, all-sky camera, radiometer, ...) to investigate tropical cloud properties. This new experimental site, which is intended to complement observations made at the Maïdo atmospheric station - the latter is mostly dedicated to the observation of the upper troposphere - will shortly become one of the main reference sites in the southern hemisphere for cloud observations.

Data collected during the first year of exploitation of the radar (Nov 2016 - Oct 2017) were analyzed to produce a climatology of clouds developing in the northern region of Reunion Island. This climatology was confronted with AROME-Indian Ocean model forecasts over the same period to assess the model's ability to accurately forecast the occurrence and vertical distribution of clouds in this part of the island. Observations show the existence of a marked seasonal cycle that is relatively well captured by the model. The latter nevertheless seems to underestimate the thickness of the low cloud layer in summer and winter, and to overestimate the thickness of the cirrus layer developing during the austral summer.

6

Impact of the increase of aircraft data in AROME-France

In Europe, EUMETNET manages commercial aircraft data purchase and dissemination (E-AMDAR operational service). On request of Météo-France, the number of these observations was increased in France from beginning of May to mid-June 2017. More data were assimilated by NWP models. This E-AMDAR trial was an opportunity to check that the assimilation of additional aircraft data increases AROME-France forecast skills. To do so, a data-denial test suite has been run (assimilation and forecasts) on May 2017. The extra data being organized in vertical profiles (ascents and descents flights) at French airports but not being flagged as "extra", a significant part of the work was to identify additional observations. Every profile has been associated with an airport (French or not) and was assigned with a status: "routine" or "extra" using "normal" periods such as April 2017 or May 2016 as a reference for "routine". Suppressing all "extra" profiles yields a 15% decrease of the European aircraft data, or a 12% of all aircraft data used by the operational AROME-France (see Figure a). The impact on the quality of AROME forecasts, when removing extra data on May 2017 is reduced. It is only detected at 12h and 18h networks. It is rarely significant. A slight improvement of the 24-h wind and temperature forecasts is assessed on a geographical domain that closely encircles the metropolitan area (see Figure b).

7

a: This diagram shows the impact of two methods to identify "extra" profiles of E-AMDAR data (at French airports). The red part shows the amount of "extra" data removed in the data-denial experiment. The green part is made of "routine" profiles. The other E-AMDAR data (in blue and brown) are not affected by data selection. As are the data from the USA (grey): they are not modified in the data-denial experiment.
b: Estimate of the impact of the withdrawal of additional E-AMDAR observations in AROME-France forecasts when comparing to radiosoundings.
The 12Z-based 24-hour forecast bias and root mean squared error (RMSE) are shown as a function of pressure levels. 12Z is the base time that exhibits larger impacts. Here, the operational (in blue) appears slightly better than the test (in red): lower RMSE and lower bias, between 850 and 250 hPa. The impact is significant only for 2 levels (stars) in mid-troposphere.

Climatology of the vertical distribution of cloud fraction in Saint-Denis (Reunion Island)
observed by the radar BASTA during a typical summer (a) and winter (b) day. Vertical distribution
of the cloud fraction observed by BASTA and predicted by AROME-Indian Ocean in summer (c) and winter (d).
Analyses are based on a full year of observation / forecasts.
▼
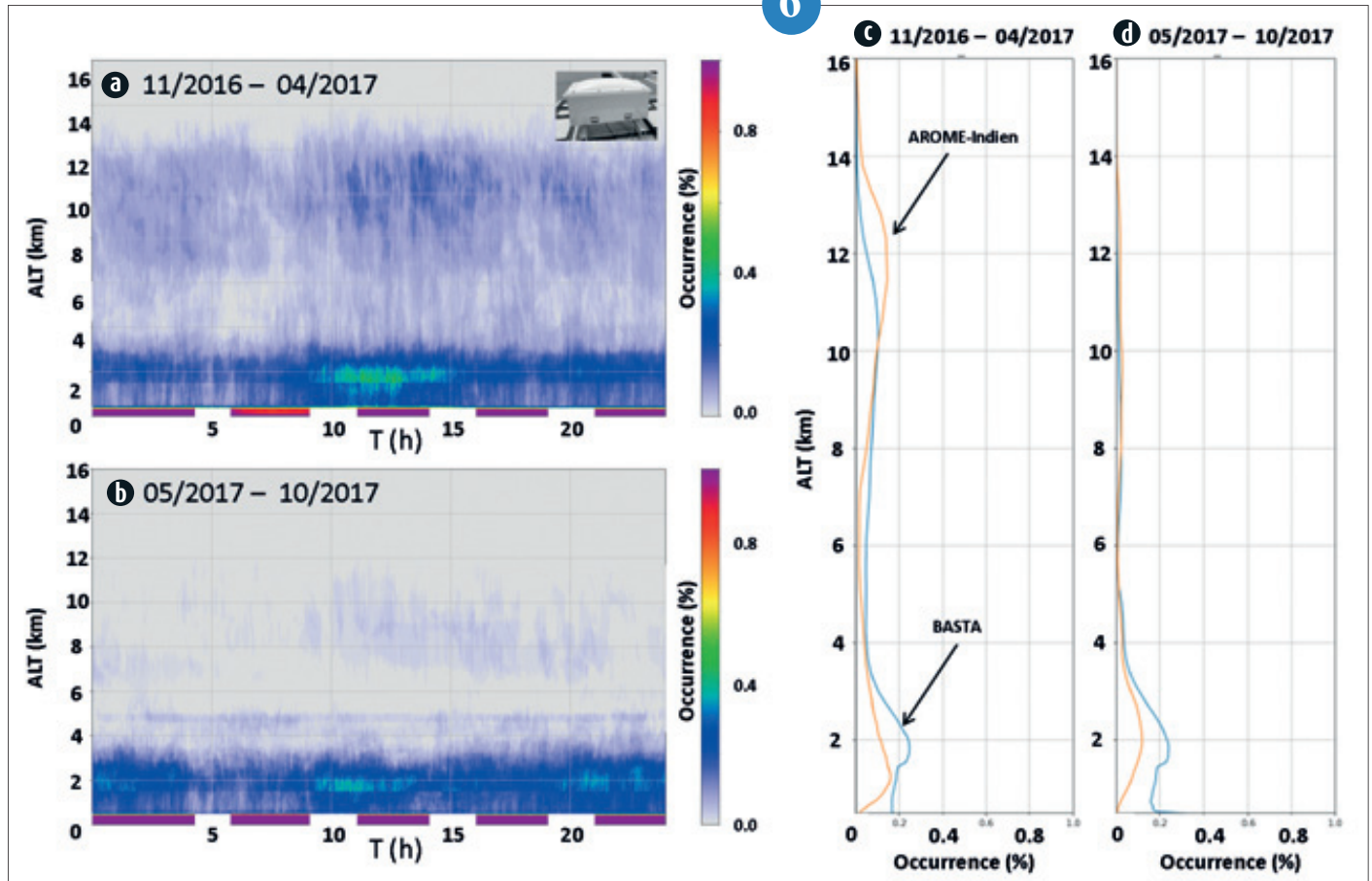
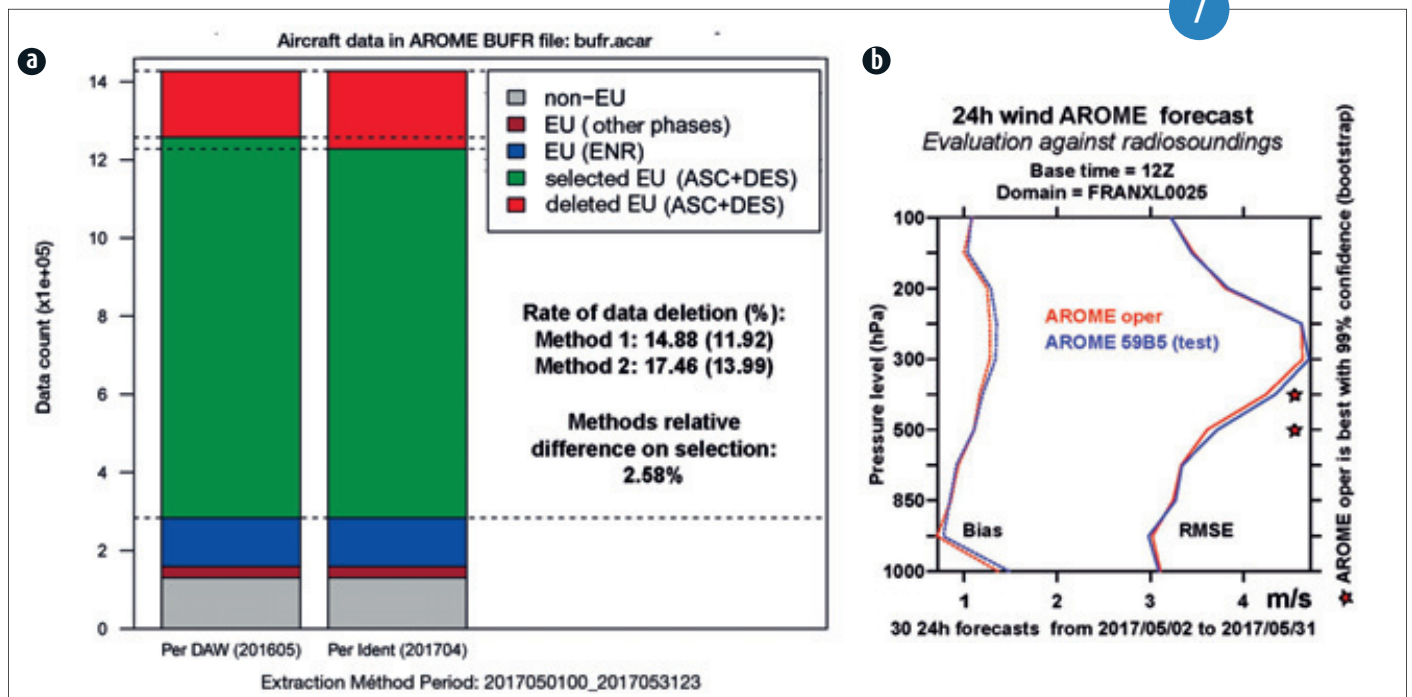# Towards the assimilation of ground-based microwave radiometers into the AROME model: an Alpine valley case study

Ground-based microwave radiometers (MWR) provide continuous measurements of temperature and humidity profiles as well as liquid water path both in clear and cloudy-sky conditions. Their information content is located in the boundary layer known to be the most under-sampled part of the atmosphere in current networks. A research action is currently under progress at CNRM to evaluate the benefit of these new observations to improve the initialisation of the AROME forecasts particularly during stable boundary layer conditions.

During the Passy-2015 field experiment, a ground-based microwave radiometer has been deployed at the bottom of an Alpine Valley and was collocated with radio-soundings launched at a high temporal frequency (every 3 hours). Limitations of the 1.3 km horizontal resolution AROME model to represent well stable layers and the orography led to a large underestimation of the surface cooling. One dimensional variational assimilation (1DVAR) experiments similar to the operational assimilation scheme have been carried out by combining microwave radiometer observations and 1h AROME forecasts. The forecast error was significantly reduced thanks to the 1D assimilation of MWR observations from 8 K to 0.5 K close to the surface in clear-sky. During low cloud conditions, the forecast error of the cloud-based temperature inversion was also divided by two. Thanks to the high temporal resolution of the observations (a few minutes), the representation of the boundary layer diurnal cycle in the model is greatly improved. These results show the potential benefit that could be brought by the assimilation of MWR observations into the AROME model.
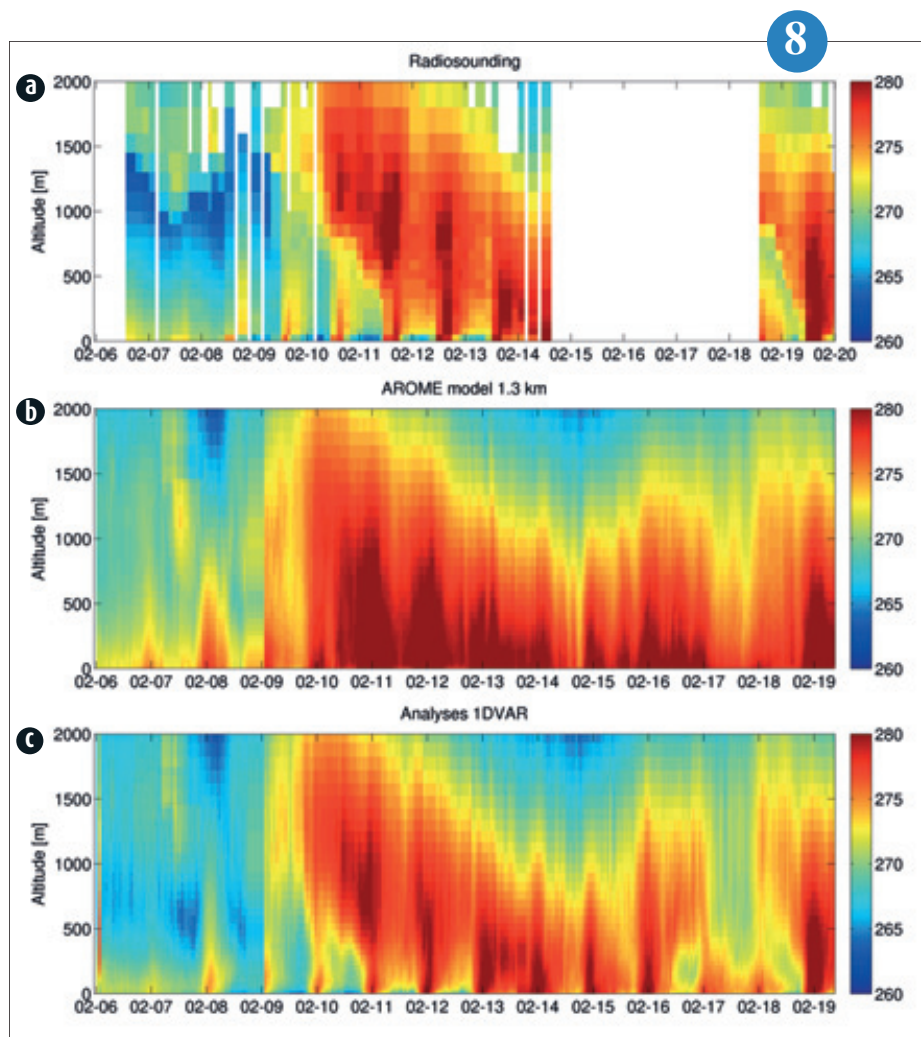
8

Assimilation of IASI radiances on earth in AROME

The French sensor IASI (Infrared Atmospheric Sounding Interferometer) is on board European polar-orbiting satellites MetOp and provides users with 8461 measurements in each sounded pixel. IASI measures information on atmospheric profiles of temperature and humidity, and on surface temperature and emissivity, among others.

Following the methodology developed at CNRM for microwave sensors and imagers, it was possible to set up a retrieval process for land surface temperatures from IASI using surface emissivity atlases provided by the University of Wisconsin. Infrared measurement is sensitive to the presence of cloud in the sounded pixel. In clear sky condition, land surface temperature in the pixel can be retrieved from the observations at given wavelengths which are sensitive to the surface. This methodology is now available in the global model ARPEGE and in the convective scale model AROME. The figure illustrates the land surface temperature retrieved from IASI in clear sky condition, and the cloud cover in cloudy condition, in AROME-France. Thanks to this more realistic land surface information, the assimilation of IASI is improved, leading to a better description of the lower layers of the troposphere above continents.

The synergy between land surface temperatures retrieved from various sensors will be evaluated so that these temperatures can be used in the surface analysis process. It will provide more realistic information on surface temperature to the assimilation of satellite observations and to the forecast model.

9

Time series of temperature profiles
from radio-soundings (a) from 1h AROME forecasts;
(b) after 1D assimilation of ground-based microwave radiometer observations into AROME;
(c) during the Passy-2015 experiment from 02/06/2015 to 02/20/2015.
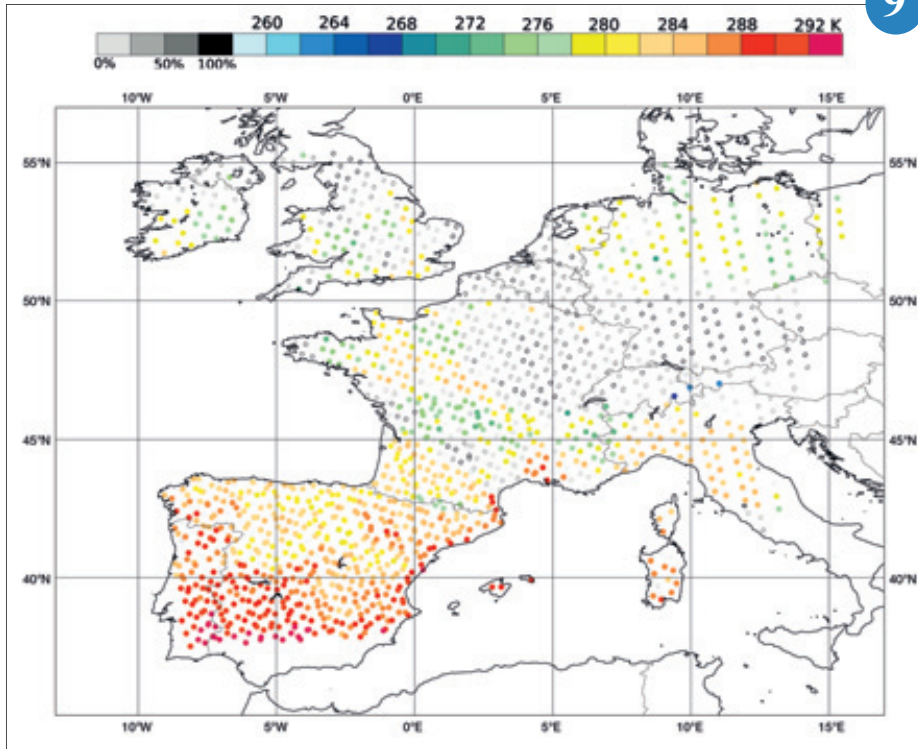
Land surface temperatures retrieved from IASI in clear sky pixels (colour scale, temperature is in Kelvin) and cloud cover within IASI pixel (grey scale, percentage) in AROME-France, 8 October 2017 at 21 UTC.

Prototype of 3DEnVar assimilation scheme for AROME

The operational AROME suite makes use of hourly cycled assimilation/forecast steps based on a 3DVar. One weakness of this assimilation scheme is that the forecast error covariances are modelized and climatologically calibrated: correlations are homogeneous over the domain and variances stay static. As a consequence, analysis increments (differences between the analysed and the background states), obtained after the assimilation of several observations, do not depend on the meteorological situation.

3DEnVar schemes aim in replacing these climatological covariances, either by covariances deduced from an ensemble of forecast, or by a linear combination of both using a hybrid formulation. Localization of the sampled covariances, which consists in progressively removing spatial correlations with distance, is needed in order to reduce spurious sampling noise. Figure 1 shows that the retrieved increments, although more noisy than those deduced from the 3DVar, clearly display spatial structures linked to the flux. Forecast scores after 5 weeks of cycled assimilations show significative improvements when running AROME with a 3.8 km resolution.

Researches are ongoing on implementing different localization schemes and on the use of the EnVar in its 4D version. In parallel, an ensemble of assimilation based on AROME will run operationally, allowing to provide sampled covariances of forecast errors in real time. The final goal is to improve forecasts at the operational resolution of 1.3 km.

Horizontal cross sections at 900 hPa of temperature increments (in K) retrieved by (a) the 3DVar, and by (b) the 3DEnVar, the 6th of February, 2016. Both cases consider the same guess (3h AROME forecast at 3.8 km resolution).
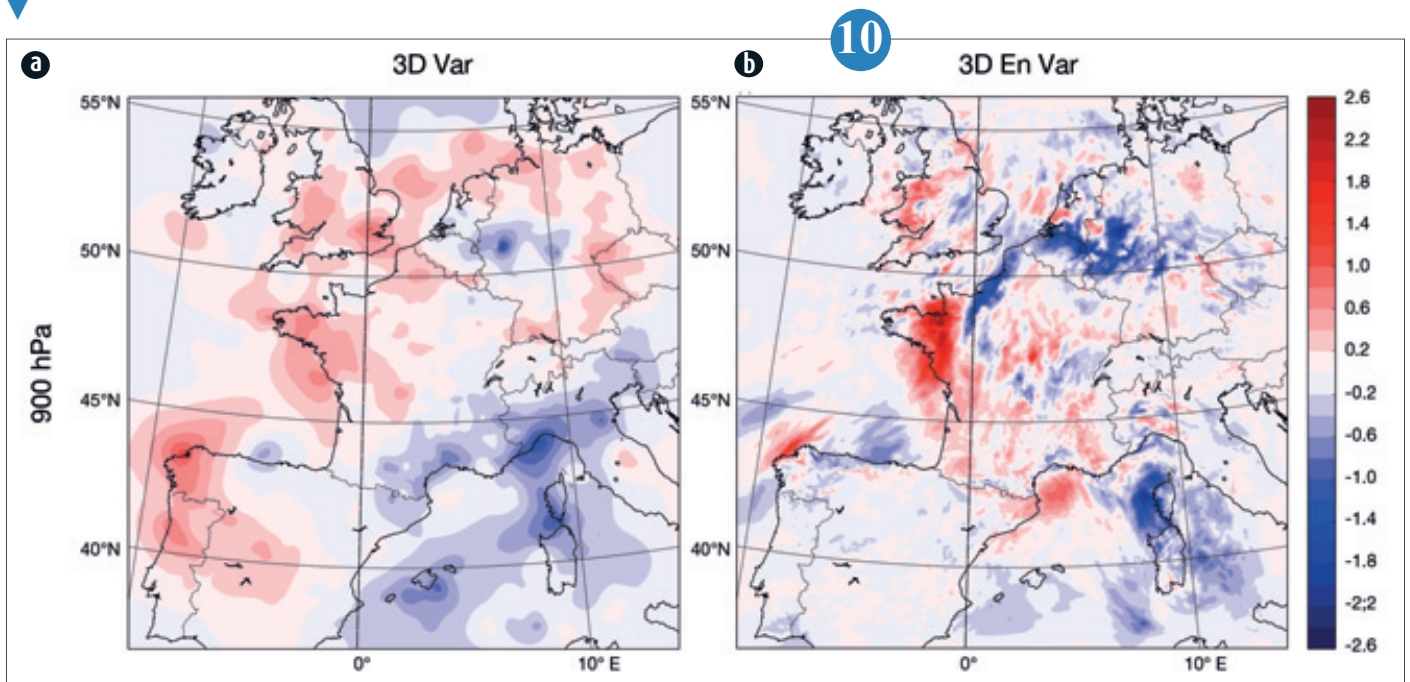
PEARO, size and resolution sensitivity

A key aspect when developing high-resolution ensemble prediction systems (EPSs) is the compromise between ensemble size and model resolution. Therefore, an important consideration for the design of future ensemble configurations and how best to deploy increased computing power is the relative benefits of enhanced resolution and ensemble size.

In this context, the AROME-France convective-scale EPS (AROME-EPS), which operationally runs 12 perturbed members at 2.5 km horizontal resolution, has been compared to two auxiliary ensemble configurations, which are run at a resolution of 2.5 km and 1.3 km with 34 and 12 members respectively.

Results indicate that increasing model resolution is more beneficial at very short ranges, whereas increasing the ensemble size has a larger impact at longer forecast ranges, as predictability decreases and more members are required to better sample the larger uncertainty. Time-lagging of three successive ensemble productions also appears as a competitive approach to increase the ensemble size at no additional cost. The performance of the time-lagged 36-member ensemble is generally close to or even better than the performance of the single 34-member ensemble for the whole forecast range and for different surface weather variables.

Given the relative costs and skills of the different EPS configurations it is suggested that resources should be primarily spent on increasing ensemble size, by combining both additional members and time-lagged EPS productions. In addition, the performance of the 1.3-km ensemble should be further examined, especially for cases of high-impact weather.

11

EFI AROME

The prediction of high-impact weather is a key issue, owing to their impact on the society, the economy and the environment. The French high-resolution ensemble prediction system AROME-EPS, which runs with a 2.5 km resolution over France, has strong potential to forecast such events.

In particular, the Extreme Forecast Index (EFI), introduced by Lalaurette (2003), is commonly used to compare an ensemble forecast to a reference model climatology, in order to measure the severity of the current weather forecast.

A first study examined the feasibility and the relevance of EFI computations within the AROME-EPS, with the main difficulty being the very small sample available to compute the model climate, provided by the two-year operational archive (available from August 10, 2015). Since this sample is not sufficient to provide a reliable climate, additional temporal and spatial sampling methods are combined in order to improve the model climate estimate.

The results obtained over a few cases of severe weather are encouraging: areas of strong EFI are often consistent with the strongest observations and the Météo-France « vigilance » maps, especially for winter storms and heavy precipitation.

In addition, objective verification scores computed for EFI relative to the operational warning procedure show that this index is able to properly discriminate between false alarms and non-detections. Hence, it could be relevant in an operational context to anticipate remarkable weather events.

In the short term, a regular monitoring of EFI by forecasters could be suggested. It is also expected that EFI will become more accurate in the future owing to a larger climate sample.

12
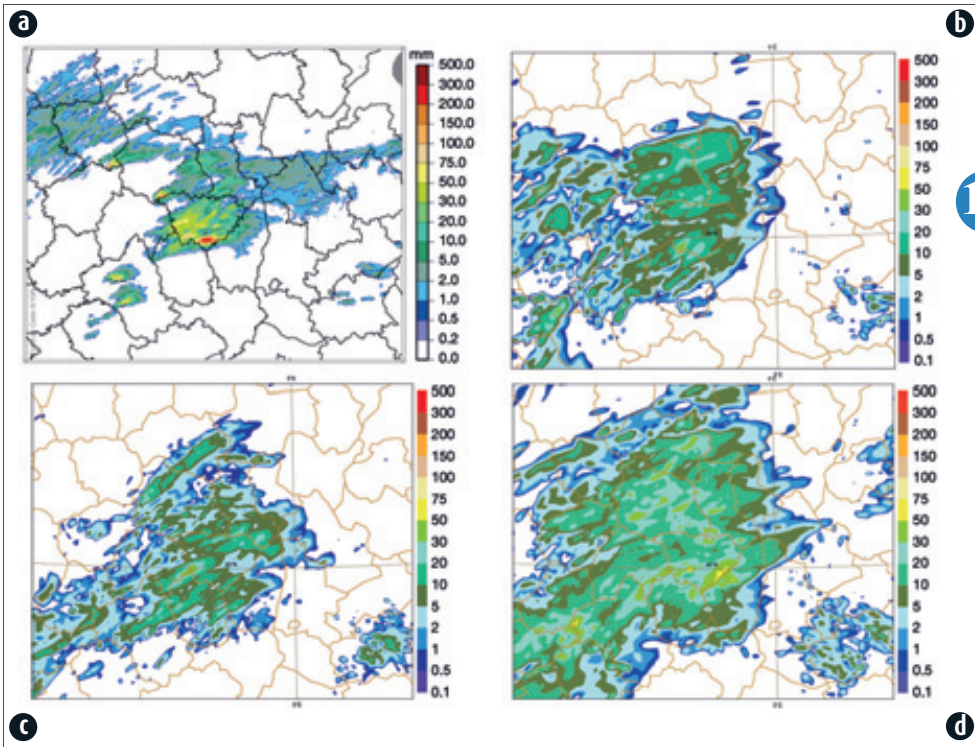
6h accumulated precipitation,
valid on 13 June 2017 at 21 UTC:
a: Observations;
b: Maximum percentile of the operational
AROME-EPS;
c: Maximum percentile of the 1.3 km AROME-EPS
(12 members);
d: Maximum percentile of the 34-member
AROME-EPS (2.5 km resolution).
All AROME-EPS experiments are issued on 12 June
at 21 UTC.
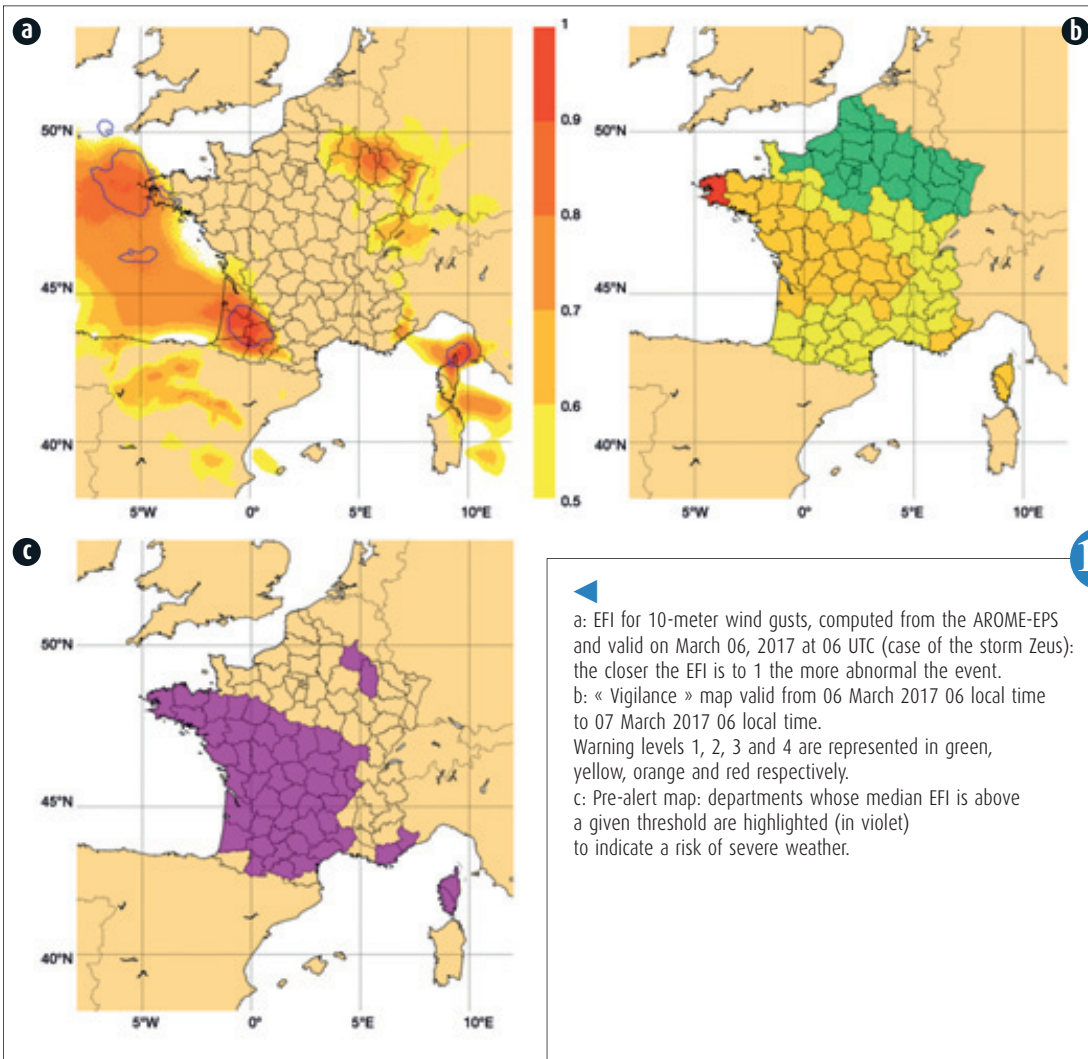
a: EFI for 10-meter wind gusts, computed from the AROME-EPS
and valid on March 06, 2017 at 06 UTC (case of the storm Zeus):
the closer the EFI is to 1 the more abnormal the event.
b: « Vigilance » map valid from 06 March 2017 06 local time
to 07 March 2017 06 local time.
Warning levels 1, 2, 3 and 4 are represented in green,
yellow, orange and red respectively.
c: Pre-alert map: departments whose median EFI is above
a given threshold are highlighted (in violet)
to indicate a risk of severe weather.

Process studies and modelling

The articles in this chapter are examples of the researches conducted at Météo-France in 2017 on the understanding and modelling of meteorological phenomena involved in high impact weather and of their interactions with the surfaces. Their overarching goal is to improve the modelling of physical processes in weather and climate numerical prediction models of Météo-France, and to develop efficient weather and climate services.

The study presented here on the intensification of extreme rainfall in the Sahel over the past 35 years, published in the journal Nature, illustrates how the understanding of the underlying processes makes it possible to interpret trends observed in satellite observation series and find signals in climate projections. This type of approach is applied to other high-impact weather, as hereby illustrated for heat waves.

For these process studies and the improvement of the process description in climate or weather models, high-resolution modelling is a key tool. The articles on turbulence modelling and the development of turbulence indicators for offshore wind farms are illustrations at both ends of the resolution range used for these studies (0.5m to 2.5km). These very high-resolution simulations, such as the one presented in Figure, are also used to prepare and evaluate the benefit of hectometer resolution envisioned for the next generation of limited-area numerical weather prediction systems. This high resolution requires improving the description of surfaces and interactions at the interfaces with the atmosphere, as illustrated hereby for different types of surfaces (urbanized surfaces, natural surfaces, ocean).

①

Intensification of deep convection and extreme rainfall in the Sahel over the past 35 years

In the Sahel, most of the precipitation comes from mesoscale (MCS) systems such as squall lines. These MCS are among the most intense in the world and a major cause of recurring and devastating floods.

Many studies indicate that extreme precipitations have increased in relation to global warming. However, in the Sahel as generally in the tropics, in-situ observations are rare. In addition, models are struggling to simulate MCS, which leads to highly uncertain projections of rainfall extremes. On the other hand, the METEOSAT satellite archive has allowed us to identify a strong intensification in the

Sahel over the last 25 years, with a tripling of the number of MCS whose temperature is lower than -70ºC (see figure).

This trend is only partially related to the rain recovery that followed the droughts of the 80s. It does not involve a local warming either because in the Sahel, we observe a cooling during the monsoon season (which is mainly driven by the increase of precipitation since 1982). This trend is, however, highly correlated with global warming, which, at the regional scale of West Africa, mainly affects the Sahara. This southern gradient (cooling in the Sahel, warming in the Sahara) induces an

intensification of the wind shear which favours the development of intense MCS, capable of generating within a few hours strong convergences of humidity and violent rains. These regional changes are consistent with the trend observed on the extremes and may explain them.

Future climate projections indicate an increase in this temperature gradient between the Sahel and Sahara, which suggests that the increase in the frequency of extreme Sahelian rainfall events could continue.

②

The AROME-NEMO coupled system for heavy precipitation event forecast in the Mediterranean region

The Mediterranean Sea is a significant source of heat and moisture for the convective systems at the origin of heavy precipitation events that frequently affect the basin.

In order to improve the representation of the air-sea interactions that occur at fine-scale, the coupling between the AROME weather forecast system and the NEMO ocean model was developed. The two models exchange information (sea surface temperature, surface currents – heat, water and momentum fluxes) interactively thanks to the SURFEX-OASIS coupling interface, with a exchange frequency of one

hour. The coupled system was applied with a domain that covers the Western Mediterranean Sea and with a ~2.5km-resolution in the two component models, on two Mediterranean heavy precipitation events that affected the South-East of France during the first field campaign (SOP1) of the HyMeX program: IOP13 (12-15 October 2012) and IOP16a/b (26-28 October 2012).

The results of the coupled simulation compared to those of an atmosphere-only (AROME) simulation driven by a constant sea surface temperature equal to the initial field, show the

sensitivity of the precipitation forecast to the coupling with ocean, in terms of intensity and location. Water budgets allow to quantify the coupling impact on the sea surface evaporation that feeds the mesoscale convective systems, with for example during IOP13 a decrease of 10% in evaporation due to sea surface cooling and ocean vertical mixing.

③
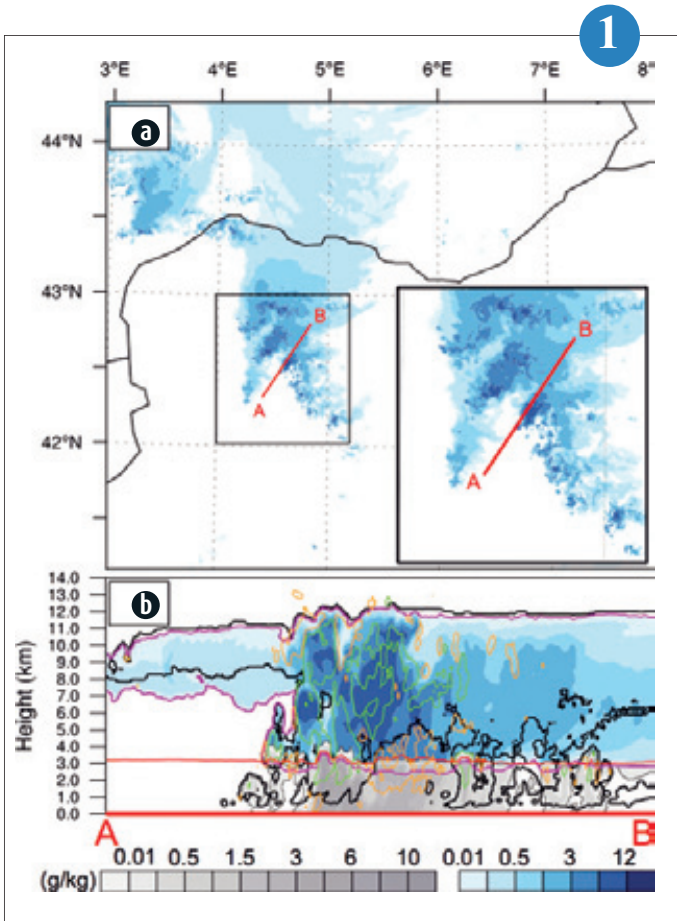
Meso-NH simulation at 150m horizontal resolution of the Mediterranean heavy precipitation event of 26 October 2012 observed during the HyMeX SOP1 field campaign, initialized from the AROME operational analysis:
a: Ice content at 6 km above sea level;
b: Vertical section along segment AB for liquid rain content (grey scale), ice precipitation content (blue scale and magenta isoline) and cloud content (black isoline) with the 0°C isotherm (red isoline), and upward (above 5 m/s, green isolines) and downward (less than -2m/s, orange isolines) velocities.
The resolution of 150 m enables to describe convective cells forming the convective mesoscale system at different stages: cells at the cumulus stage, well-developed convective towers reaching an altitude of 12 km and generating very heavy rainfall, and a large stratiform part extending downstream, according to the upper-level flow.

a: Architecture of the AROME-NEMO coupled system and domain over the Western Mediterranean basin.
b, c: Accumulated amounts of precipitation between 26 October 2012 00 UTC and 27 October 2012 00UTC (POI 16a) in the coupled forecast (CPL) and in the AROME-WMED (atmosphere-only) forecast (NOCPL) forced with a constant sea surface temperature; both starting on 25 October 2012 at 00UTC. Observed values are indicated with circles.

a: Map of significant trends of the most intense MCS cloud cover (MCS size greater than 25000 km² and using a temperature threshold of - 70°C) at 18h (UTC).
Trends are expressed as a percentage change per decade, relative to the 35-year mean (contours).
b: Time series of the number (per day) of these intense MCS over the Sahelian domain (purple rectangle in figure (a)).

Estimation of turbulence indicators for offshore wind farms using the meso-scale model AROME

In support of off-shore wind farm projects, Météo-France had created and computed atmospheric turbulence indicators for the atmospheric layer between 40 and 160 m along the coastal areas of the North Sea, Channel and Atlantic.

The turbulence intensity, the 100 m gusts and the vertical wind shear exponent, were identified as the most suitable indicators in this context. The production of the turbulence and gust intensity indicators required a study phase since these two indicators are not basic outputs of the AROME numerical weather model at 100 m height.

Their computation method has been chosen to produce values consistent with values issue to their current definition in wind-farm projects; their quality was assessed by comparison with calculations made on the basis of observations. The scientific knowledge on atmospheric turbulence and its representation in AROME were thus exploited at best.

Several indicators, potentially respecting the criteria presented in previous section, were computed from hourly AROME data at the 0.025° horizontal resolution over the 2000-2015 period. The selected indicators were those that have been considered to be the closest to those computed with available wind observations. One of the difficulties and limitations of the approach lies in the low availability of wind observations at high levels and moreover on sea.

Statistics were then established from these different indicators of turbulence, to provide an estimate and a climatology of atmospheric turbulence between 40 and 160 m on the western coast of France.

④

Improving the turbulence in the stable boundary layer

Improving the representation of the atmospheric turbulence in the nocturnal stable boundary layer is a key feature for fog forecast, as well as frozen surfaces, temperature inversions and pollution peaks especially in winter.

The turbulence parameterization currently used in the Meso-NH and AROME models operates with a mixing length, an important parameter which describes the typical eddies size. A new expression for the mixing length has been formulated. This expression adds a wind shear term to an existing formulation based on the buoyancy. The buoyancy and the wind shear limit the eddies size in the presence of positive atmospheric static stability.

For the model inter-comparison GABLS1 case, the Meso-NH simulation with the old mixing length overestimates the turbulent mixing intensity, which leads to overestimate the boundary layer height as shown on the potential temperature (Figure a) and wind speed (Figure b) profiles with respect to the reference LES. Taking into account the wind shear in the mixing length expression reduces these biases.

This work could improve the turbulent mixing intensity modeled by numerical weather forecast models.

⑤

Modelling of human behaviours related to building energy consumption and corresponding CO_2 emissions in urban areas

Urban areas account for about half of the world population, energy consumption and CO_2 emissions. The urban parameterisation TEB calculates the energy exchange between urban areas and the atmosphere. It includes a building energy model, which calculates the energy demand related to heating and air conditioning as a function of the meteorological conditions, building characteristics (e.g. structural wall material, presence of insulation, glazing ratio), as well as human behaviours (e.g. design temperature for heating). In order to initialise TEB with these parameters, a database on urban tissue (mapuce.orbisgis.org) has been compiled in cooperation with geomaticians, architects and sociologists. Information on human behaviours has been retrieved via a combination of surveys and census data.

A large variety of building use (e.g. housing, office, retail) exists at urban district scale, especially in French and European city centres. TEB has been improved to represent this variety and the associated behaviours. It is now able to simulate building energy consumption (Fig. a). In a further step, the CO_2 fluxes related to heating, traffic and urban vegetation have been included. They have been evaluated against the observations made during the CAPITOUL1 campaign in the centre of Toulouse, southern France. The more detailed representation of building use and human behaviours allows to better represent the daily cycle of CO_2 flux compared with a constant heating design temperature of 19 °C in the entire building stock (Fig. b).

This research and development will allow to quantify the impact of climate change mitigation and adaptation measures on CO_2 fluxes in urban areas.

⑥
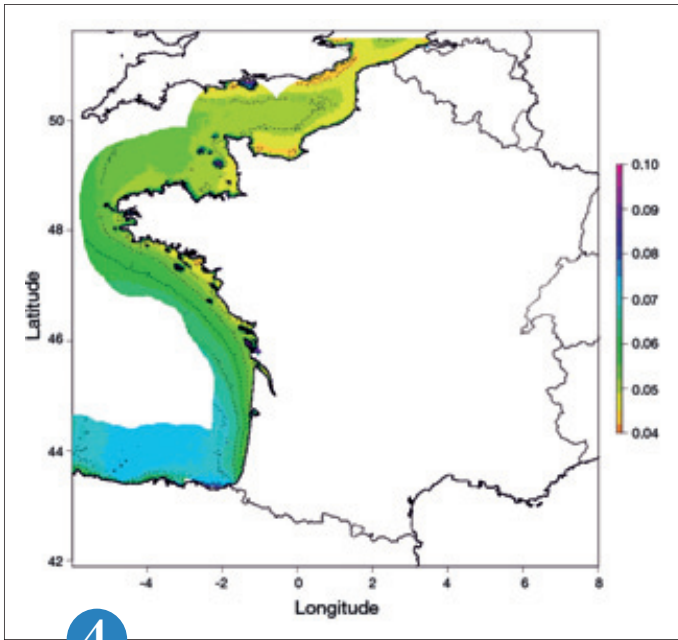
◄ Map of the average turbulence intensity at the 160 m level on the coastal strip, calculated from the AROME data (2000-2015).

Potential temperature (a) and wind speed (b) vertical profiles, averaged over one hour, resulted from a tridimensional LES (reference) and two single-column simulations with the old and the new mixing length on the models inter-comparison case GABLS1. ▼
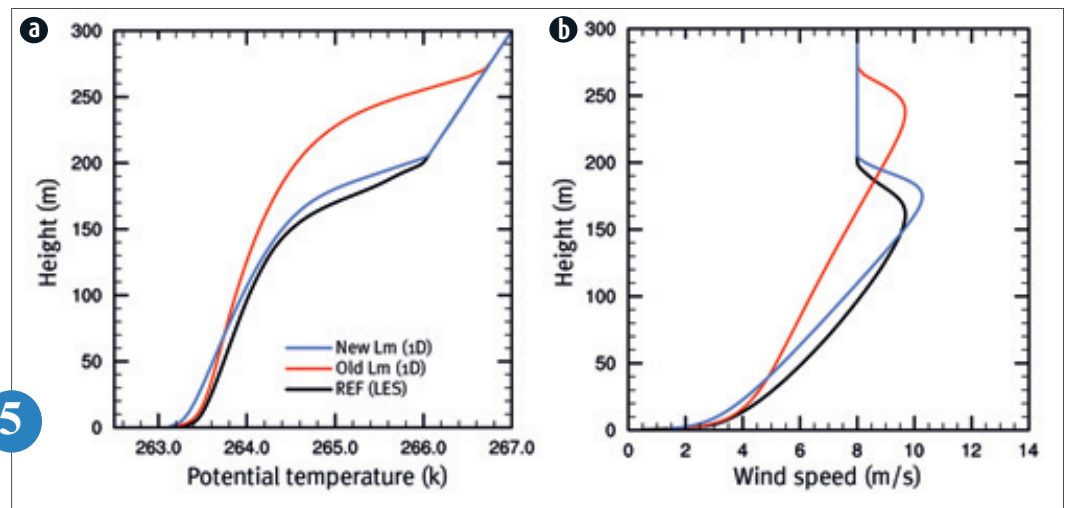
a: Spatial distribution of the heat flux related to building energy consumption simulated with TEB for the city of Toulouse, southern France.
The heat flux is averaged for the winter 2004/2005 season, which was part of the CAPITOUL observation campaign.
b: Average daily cycle of the CO_2 flux for the same period at the location of the observation tower, which is depicted by the black cross in (a).

▼
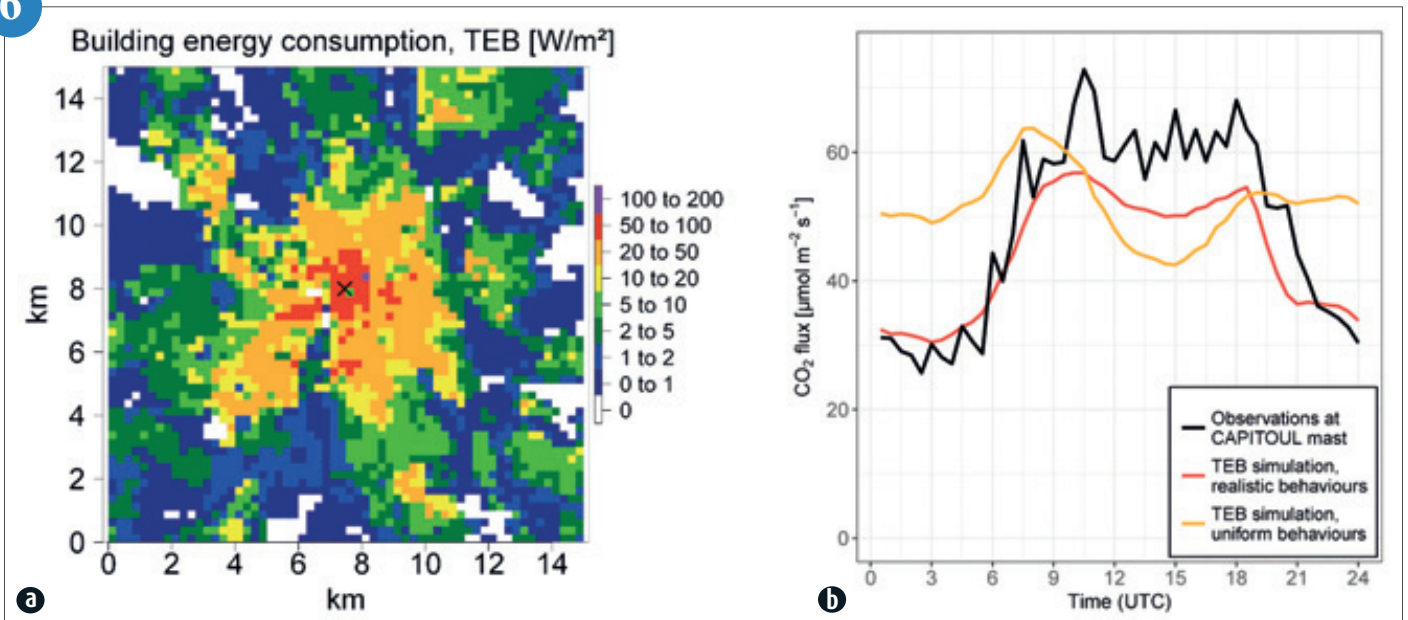
Towards a new radiative transfer scheme in Météo-France models

The transmission of solar radiation through the atmosphere is critical in meteorology. The radiative codes used at Météo-France to represent this physical process historically come from the ECMWF, but the last update dates back to 2002. That is why the recently developed radiative code ecRad is now being implemented.

The main differences between this new code and the original one are 1) the use of the 14-spectral bands RRTM model in comparison with the original 6-band model; 2) the implementation of a new aerosol climatology based on recent satellite observations; 3) the revision of aerosols optical properties. The figure compares shortwave radiative fluxes measured and simulated by the model Méso-NH at Carpentras for clear-sky conditions. Fluxes computed based on aerosol climatology significantly differ from the observations. In addition, both codes show great differences in surface fluxes even with identical aerosol load, which highlights the impact of the prescribed aerosol optical properties. Simulations without aerosols are closer to the observations, likely because aerosol load this day was much less than in average. Simulations without ozone point to the significant radiative forcing of this gas, and how this forcing differs between both codes.

These results overall underline the sensitivity of simulated fluxes to the radiative code, and shed light on the need for an improved representation of aerosol and active gas radiative forcing. This issue will be tackled by using prognostic rather than climatological values for these radiatively active elements, in view of refining the surface energy balance. The new radiative code will also serve as a basis for the development of a solar photovoltaic power forecast product.

7

7

Differences between simulated and measured shortwave downward radiative fluxes at Carpentras on July 3rd 2017 at local noon
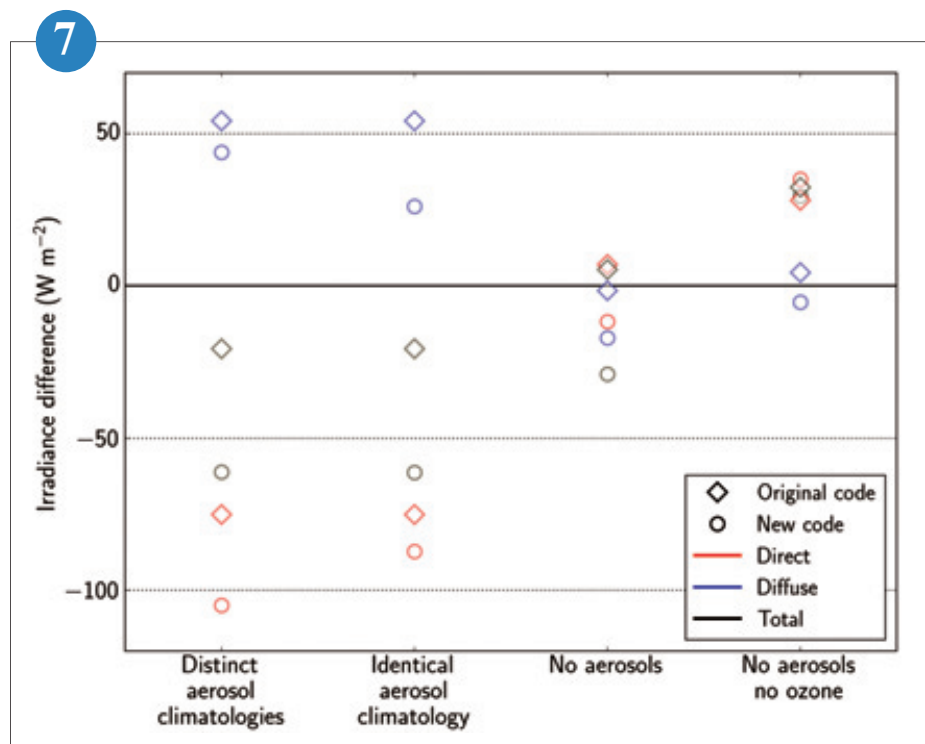Measurements are obtained with a pyranometer and simulations were performed with Meso-NH using the original and new radiative codes.

Climatic trend of Sahelian heat waves

In the Sahel, the annual cycle of temperature peaks in spring (April-May), just before the arrival of the monsoon rains. The monthly-mean daily maximum temperatures Tmax (minimum Tmin) are then about 40°C (30°C). It is also during this time of the year that the global warming is the strongest, reaching more than 2°C in 60 years for the night-time minima (Tmin). The springtime Sahelian heat waves are developing in a very hot climate and which warms up strongly. Therefore, they correspond to events with potentially severe societal repercussions.

They are defined here as synoptic-to-seasonal meteorological events, and night-time and daytime waves are studied separately. We analysed how the average climate trend affects these heat waves that we previously detected from observations.

Global warming is generally stronger in the northern Sahel, and at the first order, the trends observed for the waves are relatively close to this average trend. It is slightly lower (higher) for daytime (night-time) heat waves (see figure). These differences involve distinct atmospheric circulations and physical processes, with a role of water vapour on the intensification of these waves that calls for dedicated studies. Beyond this, the dominant influence of the mean climatic warming on heat waves shows that it is first necessary to better understand the Sahelian average climate, its annual cycle and trends and to improve their modelling (climate simulations indeed display a very wide dispersion in spring).

8

BEST, April–May, 1950–2012

(a) Clim. Tmax trend

(b) Clim. Tmin trend

(c) HWmax Tmax trend

(d) HWmin Tmin trend

(e) HWmax–Clim. Tmax trend

(f) HWmin–Clim. Tmin trend
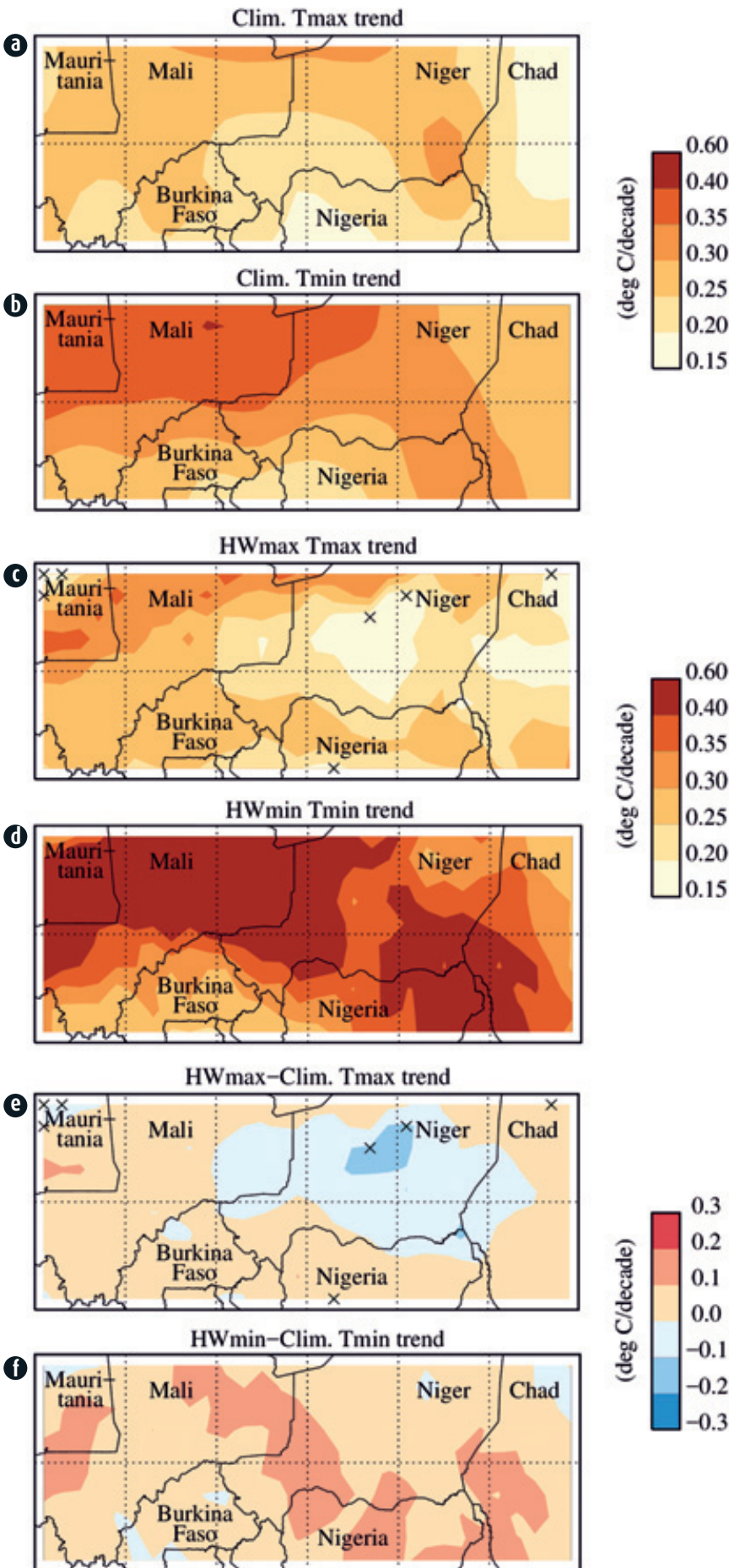
◄
Maps of climatological trends of daily (a) maximum
and (b) minimum temperatures (Tmax and Tmin)
computed over April-May for 1950-2012;
(c) and (d) same as (a) and (b), except for Tmax (Tmin)
of daytime (night-time) heat waves;
(e) and (f): difference between climatological
and heat wave trends (e=c-a, f=d-b).

Disaggregation of satellite LAI for a better description of the dynamics of vegetation covers •

The dynamics of vegetation growth on land surfaces is closely related to atmospheric conditions and is impacted by the climate variability. Vegetation covers takes part of the global climate change through the feedback on water, energy and carbon budgets. The Leaf Area Index, which represents the canopy leaf density, is a good indicator of the plant growth. Using satellite observations, LAI can be retrieved at the global scale at a resolution of about 1 km. Yet, over mixed pixels with several types of vegetation (forest, grassland, etc.), the satellite observation provides the averaged LAI and the LAI of each vegetation type is unknown.

An LAI disaggregation method was developed. It provides every 10 days global maps of LAI for each vegetation type. This new data set was used to study the evolution of individual vegetation types over the last two decades. Although the trend analysis shows a general greening of land surfaces, there are large discrepancies among vegetation types and regions of the globe. For instance, the global greening is very large for conifer forests and summer crops, and quite small for winter crops and grasslands. Besides, forests have been greening in the North-Eastern part of Europe while crops and grasslands have been browning (negative trends) in this region.

This new data set will be valuable for the improvement of global vegetation monitoring, analysis of climate change impacts and evaluation of land surface models used to elaborate future climate scenarios.

9

ECOCLIMAP-SG, a new database for the surface parameters

ECOCLIMAP is a kilometric global database describing the ecosystems at the terrestrial surface. It's integrated in SURFEX that gathers several physical models and allows to simulate the evolution of the considered environment (soil, water, ...). It's used by all the models in Météo France. Indeed, SURFEX is coupled with the meso-scale atmospheric models Meso-NH, AROME and ALADIN along with the climatic global model CNRM-CM and soon the numerical weather forecast model ARPEGE-PNT. The first version of ECOCLIMAP was published in 2003, an update on Europe was produced in 2012.

The high resolution modelling is developing and requires a finer description of the surface. A more regular update also represents a strong issue. ECOCLIMAP-SG (Second Generation) answers to these two needs. Before, the definition of parameters closely relied on the land cover map. Now, this map is at 300m resolution

Trend of Leaf Area Index (LAI) over the period 1999–2015 for different types of vegetation cover
Values represent mean LAI, mean trend and geographic discrepancy.

▼

9
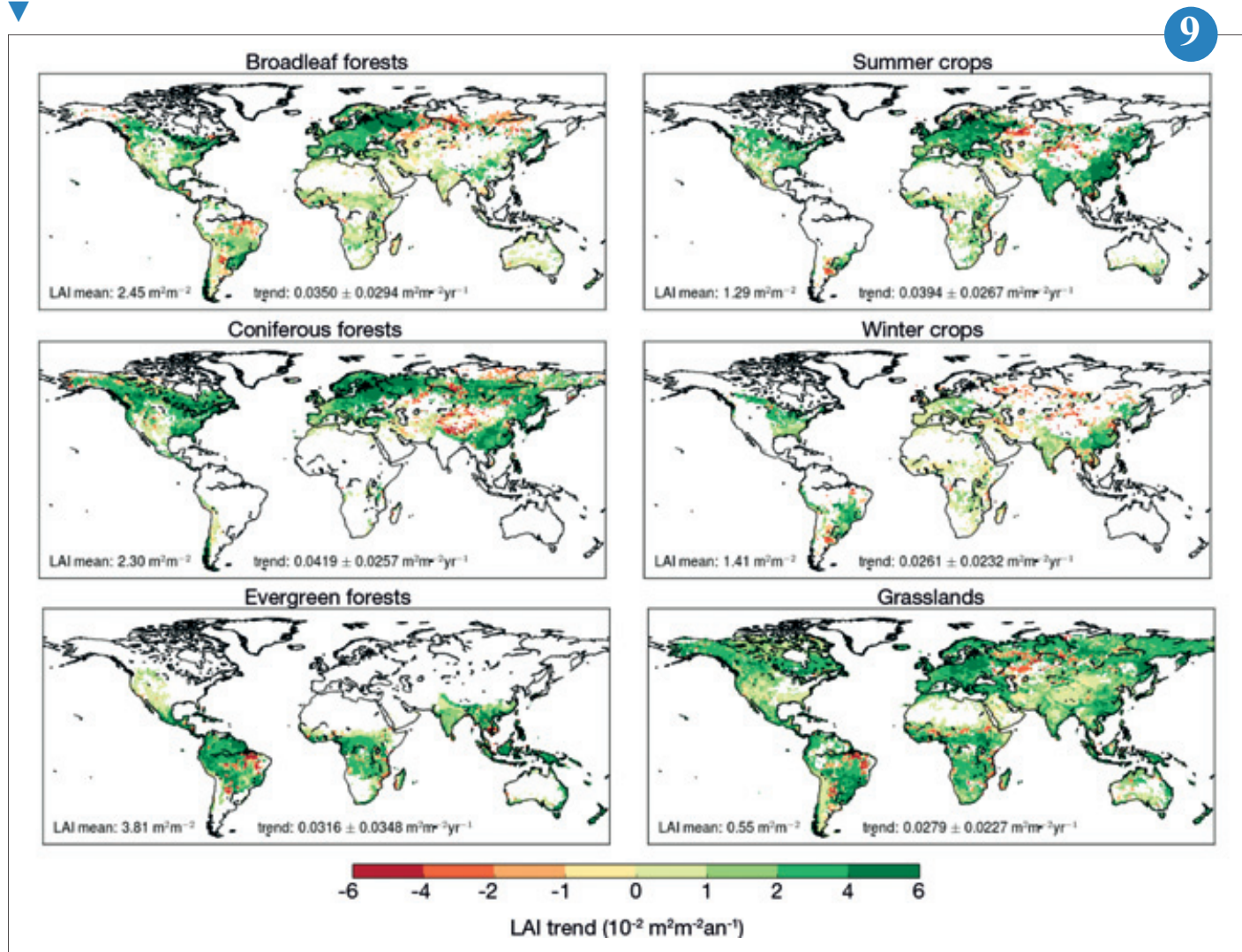
a: The ECOCLIMAP-SG land cover map at 300m resolution.
b, c: Results in the hydrological application
SIM: discharge ratio (best = 1) and NASH criterion (best = 1).
ECO1 = ECOCLIMAP1. ECO2 = ECOCLIMAP2.
ECOSG = ECOCLIMAP-SG.

and associated with some maps of parameters coming from independent satellite data (leaf area index, albedo, height of trees...).

The first tests were realised in offline mode (ie lead by observations or analyses) for the hydrological applications SIM-France and SURFEX-TRIP at the global scale. The first results for SIM showed a clear improvement of the scores on the rivers discharges.

Other tests are also in progress in coupled mode with Meso-NH and AROME-France. It aims at estimating the sensitivity of these simulations to changes in the surface parameters, and if necessary to propose to adjust some of these parameters, even the calculations including them into SURFEX, on which uncertainties exist.
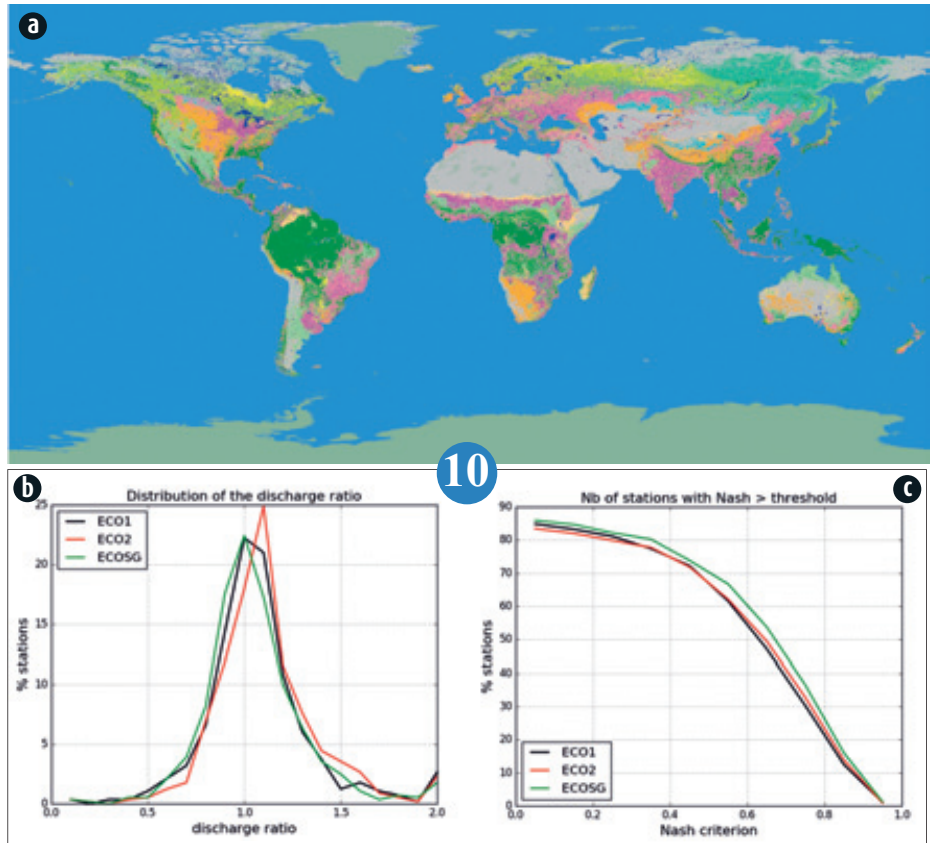
Assessment of the energy budget of land surfaces by satellite for a better characterization of the vegetation at the global scale

Vegetation and plant growth depend on the solar radiation that reaches the Earth's surface in the frequency spectrum useful for the photosynthesis (400-700nm) called the Photosynthetic Active Radiation (PAR). With a growing number of satellite missions observing the Earth, it is now more and more possible to have a comprehensive monitoring of the energy budget in the PAR domain as it constraints the rate of photosynthesis. A two-stream model of the energy budget in which all the incident angles are considered (diffuse illumination) has been developed to assess the consistency of available satellite observations for vegetation monitoring at the global scale.

Using satellite observations, the diffuse energy budget is slightly underestimated in Europe but stays within the theoretical uncertainty boundaries, showing that the observations are suitable to monitor the vegetation dynamics. The uncertainty analysis shows that the "effective" Leaf Area Index (LAI) plays a major role in the energy budget. The effective LAI is composed of the observed "true" LAI and of a clumping factor representing the spatial heterogeneity of the foliage (or how much the vegetation is folded). This clumping has a significant impact on the fraction of radiation that actually goes through the vegetation. From the available observations, it is

then possible to estimate this clumping effect and relate it to two physical characteristics of the vegetation: crown density and radius. This newly retrieved map of vegetation characteristics improves the spatial distribution and time dynamics of the energy budget. Studies are underway to assign values to each vegetation type so that the energy budget in ISBA can be further improved.

Vegetation characteristics retrieved
from satellite observations: density [m^{-2}] multiplied
by the square of the crown density [m].
The map of the combination of these two vegetation
parameters exhibits strong similarities
with the ECOCLIMAP land cover map that is used in ISBA.
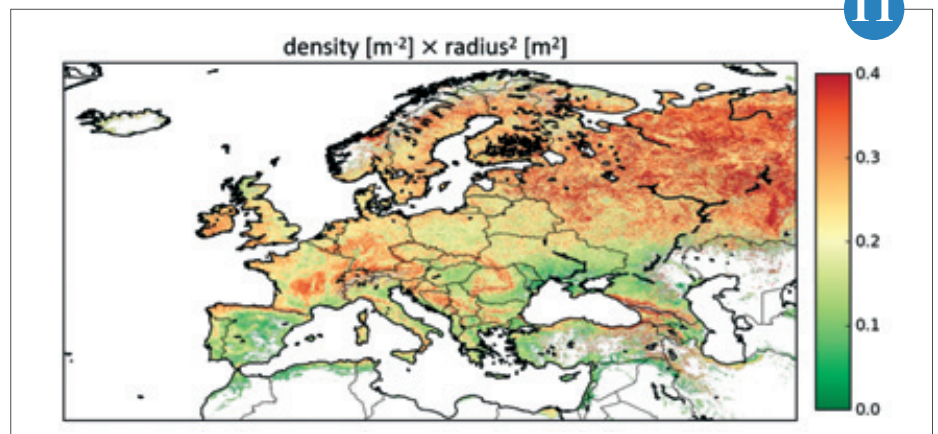
Atmospheric composition: aerosols, microphysics and chemistry

Air pollution causes nearly 50,000 premature deaths per year in France and about 10 times more in Europe, representing a major health challenge. This justifies measures to improve air quality but also, within the scope of Météo-France's activities, research activities to better understand and model the atmospheric composition of the lower layers of the atmosphere, with the aim of increasingly reliable forecasts to alert populations and public authorities.

Météo-France's MOCAGE research and forecasting model is part of the operational air quality forecasting systems of the national platform Prév' Air and the European CAMS_50 European project. In 2017, a representation of olive and grass pollens, which are among the most allergenic, was implemented in the model. Also, a study combining modelling and Lidar observations focused specifically on the 2016-2017 winter, which saw several remarkable episodes of fine particle matter pollution associated with very low inversion layers. Traditionally used in offline mode, MOCAGE is now one of the three online chemistry models in ECMWF's IFS weather prediction model. This approach makes it possible to inter-compare models in the same framework, and opens new perspective for very high spatial resolution applications.

It is also necessary to represent atmospheric composition in climate models, particularly aerosols, because of their interactions with cloud microphysics and radiation. This is reflected in the development of the simplified Tactic scheme within ARPEGE and ALADIN-Climat, which provides a realistic representation of aerosols at a moderate numerical cost. This approach will allow for the first time to conduct many long simulations with interactive aerosols as part of the international exercise CMIP6.

1

The TACTIC aerosol scheme for aerosols-climate interactions

Aerosols play an essential role in the climate system due to their interactions with radiation and clouds, and the ensuing radiative forcing is still submitted to large uncertainties.

In order to better understand these interactions and to be able to quantify the impact of aerosols on global and regional climate, a prognostic aerosol scheme called TACTIC has now been included in the CNRM climate models. This scheme, developed for several years at CNRM jointly with ECMWF, enables us to represent the main natural and anthropogenic aerosol types realistically with an affordable cost for long climate simulations. The attached figure represents the aerosols included in TACTIC, and the parameterizations of the different associated processes. The work carried out in 2017 has notably lead to a significant improvement in the representation of natural emissions (sea salt and desert dust), as well as the one of the sulfur cycle by taking into account the chemical reactions generating sulfate aerosols. A similar module allowing the formation of nitrate and ammonium aerosols whose contribution to anthropogenic aerosol forcing might increase by the end of the 21st century has also been added. All these aerosols thus produced in TACTIC can interact with radiation and clouds within the model, and have impacts on global and regional climate.

The TACTIC scheme will be included in the global (CNRM-ESM) and regional (CNRM-RCSM) climate simulations of CNRM which will be carried out for the international exercises CMIP6 and Med-CORDEX.

2

Friday 23 February 2018 00UTC CAMS Analysis t-017 VT: Thursday 22 February 2018 07UTC
Model: ENSEMBLE Median Height level: Surface Parameter: PM10 Aerosol [µg/m3]
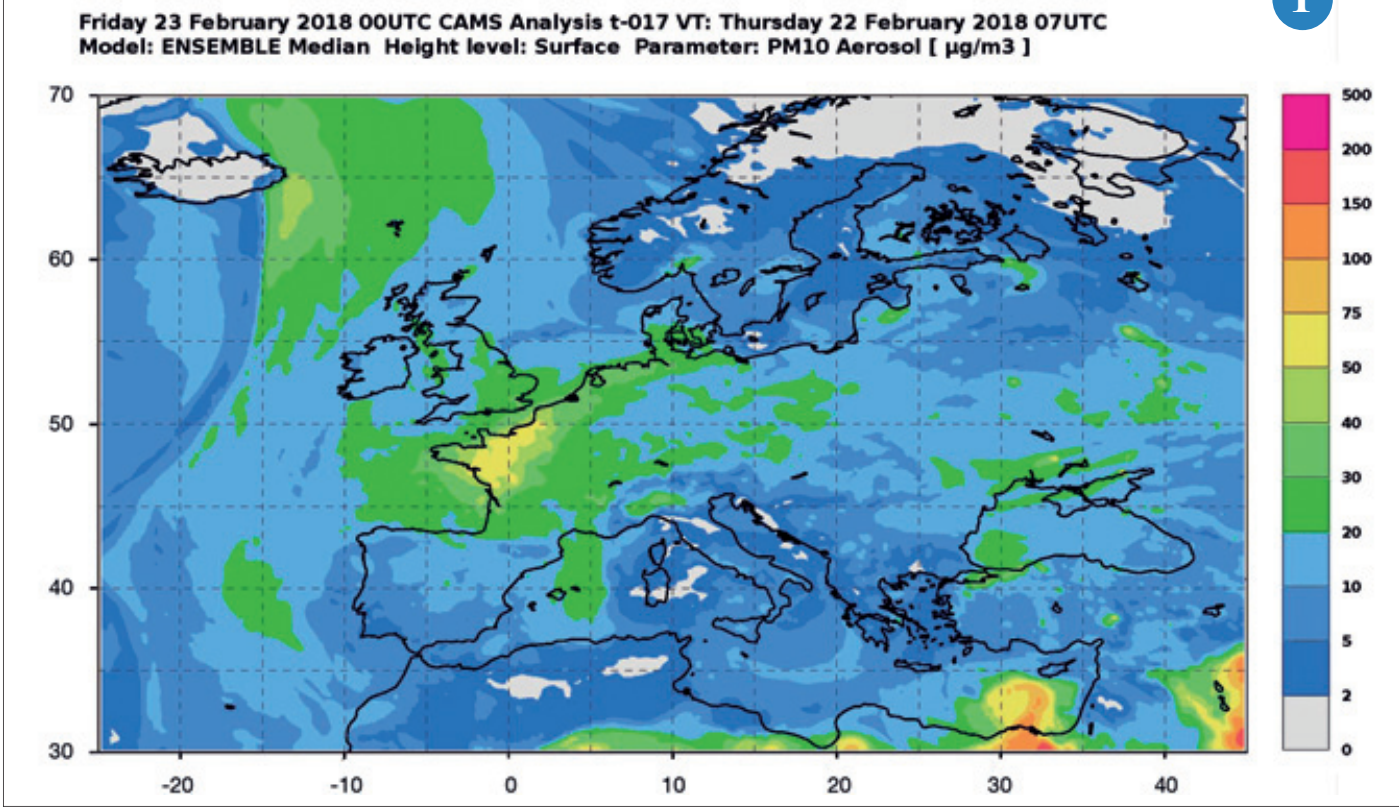
▲ Fine particulate matter (PM10) pollution episode in Western France. The overall analysis of the PM10 concentration on the Europe domain for 22/02/2018 was produced as part of the European Copernicus CAMS_50 project led by Météo-France. The set consists of 7 models, including the MOCAGE model developed at CNRM.

The TACTIC scheme included in the CNRM-ESM and CNRM-RCSM climate models.▼
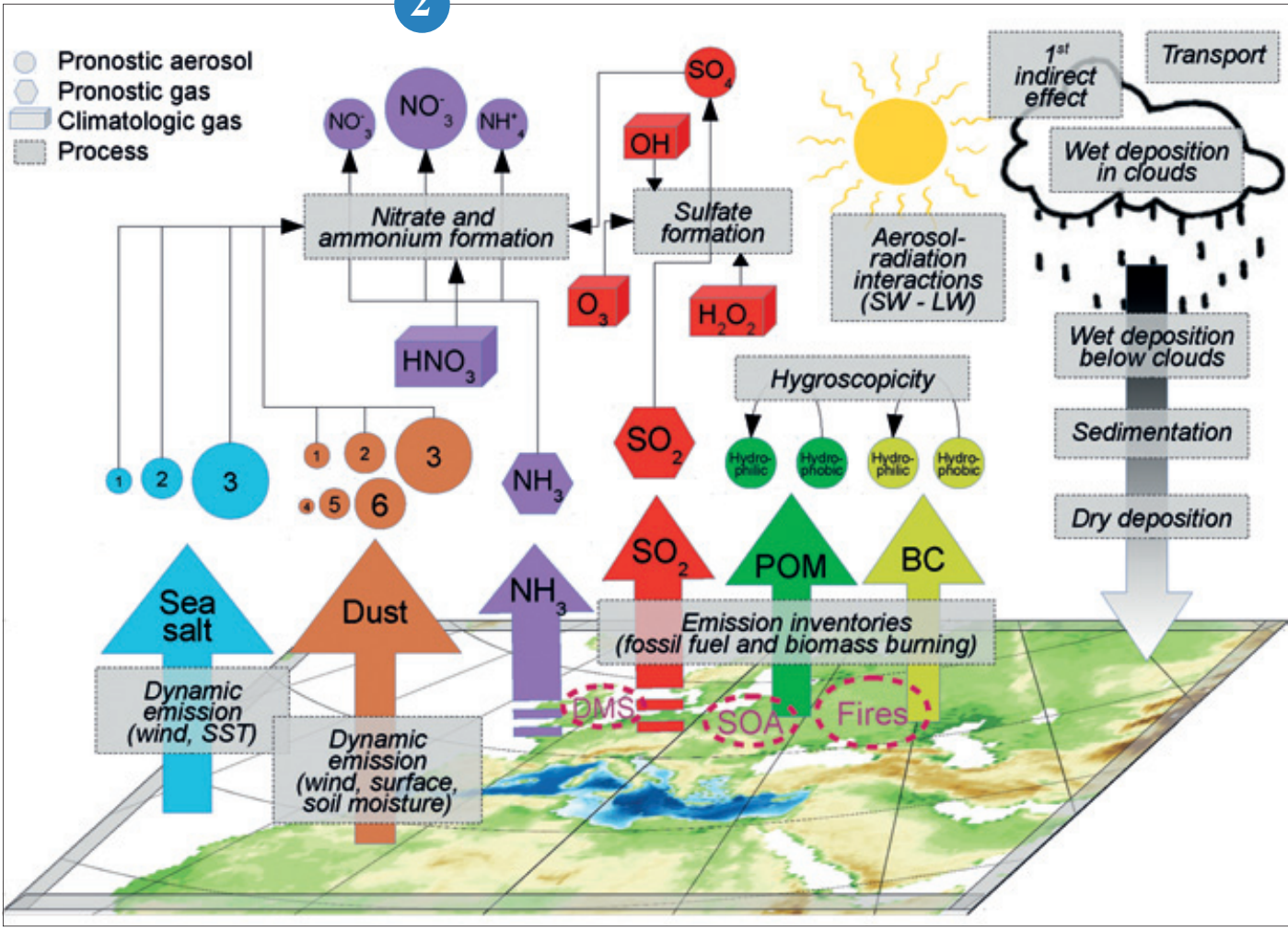
The chemistry module from MOCAGE model implemented in ECMWF IFS forecast model

In the frame of the European program Copernicus, ECMWF develops and improves continuously its daily forecasts of air composition at the global scale from surface up to 65 km altitude.

Three chemistry modules representing both tropospheric and stratospheric chemical processes are now implemented in ECMWF IFS operational weather forecast model. One of them comes from MOCAGE model. MOCAGE is the model developed by Météo-France that is used for research purposes and also for operational air quality forecasts over France and Europe. Recently, an extensive evaluation of the three chemistry modules implemented in IFS has been done by comparing the air composition simulated over one year (2011) to a large variety of ground-based, airborne and satellite-borne observations. The figure illustrates the performances of the three chemistry modules (colours) for different species (signs), obtained by comparison with data from several aircraft campaigns. It shows that all three IFS configurations give realistic results against measurements, but with differences depending on the considered chemical species and chemistry module.

This extensive evaluation work gives insights to better understand the quality and drawbacks of each chemistry module and serves as a basis to improve them.

③

Forecasting peaks of winter particulate pollution in the presence of low inversion layers

Since the adoption of the LAURE law in 1996, forecasting pollution peaks has been a major public health issue. During the winter, fine particles (PM10 and PM2.5) are one of the main sources of pollution. Their peaks in atmospheric concentrations are all the more difficult to model because they are usually associated with a very low inversion layer, which traps pollutants on the ground. It is therefore essential to determine precisely the maximum height at which emissions can be injected into the MOCAGE chemical transport model.

A study carried out on the episodes of fine particle pollution in winter 2016/2017 made it possible to objectively correlate very low boundary layer heights measured by a lidar at Trappes at high concentrations (Fig.) of PM10 on the ground over the Paris agglomeration. The two peaks observed between 30 November and 10 December, at more than 100 µg/m³, are thus bound to a boundary layer not exceeding 200 metres in height. Conversely, when the boundary layer is well developed in early November, measured concentrations are low.

As part of the air quality forecasts with the MOCAGE model, emissions are distributed over the 5 levels of the model closest to the ground, i.e. a height of about 500 metres. During the winter 2016/2017 episodes, part of the emissions are injected above the inversion layer, and therefore not trapped, preventing the model from correctly predicting these peaks. By reducing the number of injection levels to 3 (about 180 m), MOCAGE correctly simulates peaks (orange curve).

A diagnostic of the height of the boundary layer will therefore be introduced in the MOCAGE model to limit the number of injection level of emissions according to it.

④

Forecasting of olive and grass pollen atmospheric concentrations on a European scale

In 2013, Météo-France participated in the first global deterministic prediction of atmospheric concentrations of birch pollen in Europe. As part of the European Copernicus CAMS_50 project, these forecasts have been extended to olive and grass pollen, recognised by WHO as among the most allergenic and therefore strategic public health issues.

Emission flows are calculated by two parameterizations developed by the FMI, using wind, humidity and precipitation fields. For olive trees, the heat accumulation since the beginning of the year is also taken into account. The emission starts as soon as the warming exceeds a threshold (geographically variable) and stops as soon as the maximum number of grains that an olive tree can emit is reached. For grasses, the parameterisation is based on an emission probability around dates deduced from past observations.

These forecasts have been validated for the 2014 season, and have been operational since the 2016 season, with the CAMS_50 project providing daily 96-hour forecasts of 7 transport and chemistry models, including the MOCAGE model from Météo-France, and an overall forecast. Models are forced by the meteorological fields of the ECMWF operational model. The spatial-temporal redistribution of olive pollen is correctly modelled by MOCAGE and remains close to the median ensemble (Fig a). Similarly, model/ observation comparisons show a good determination of the start date for grass pollination, but with some overestimates of peaks as a function of location (Fig b).

Next year, the extension to ambrosia pollen is planned.

⑤
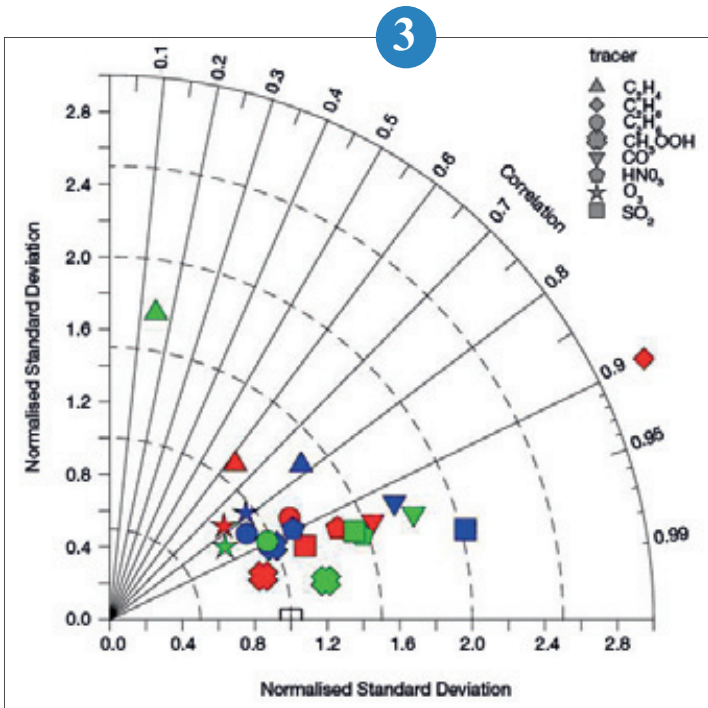
3

Taylor diagram showing, for several chemical species,
the error and the correlation between the results of IFS simulations
and the data gathered during aircraft field campaigns.
The closest the model is to the black rectangle located at the bottom of the figure,
the best the model is. The three colours correspond to the three chemistry modules
and the species to the different signs.

PM10 concentrations (µg/m³) measured (in blue) and predicted
by the MOCAGE model (in orange) on the ground in Paris (top)
and height of the boundary layer (in km) measured by the lidar of Trappes (bottom).
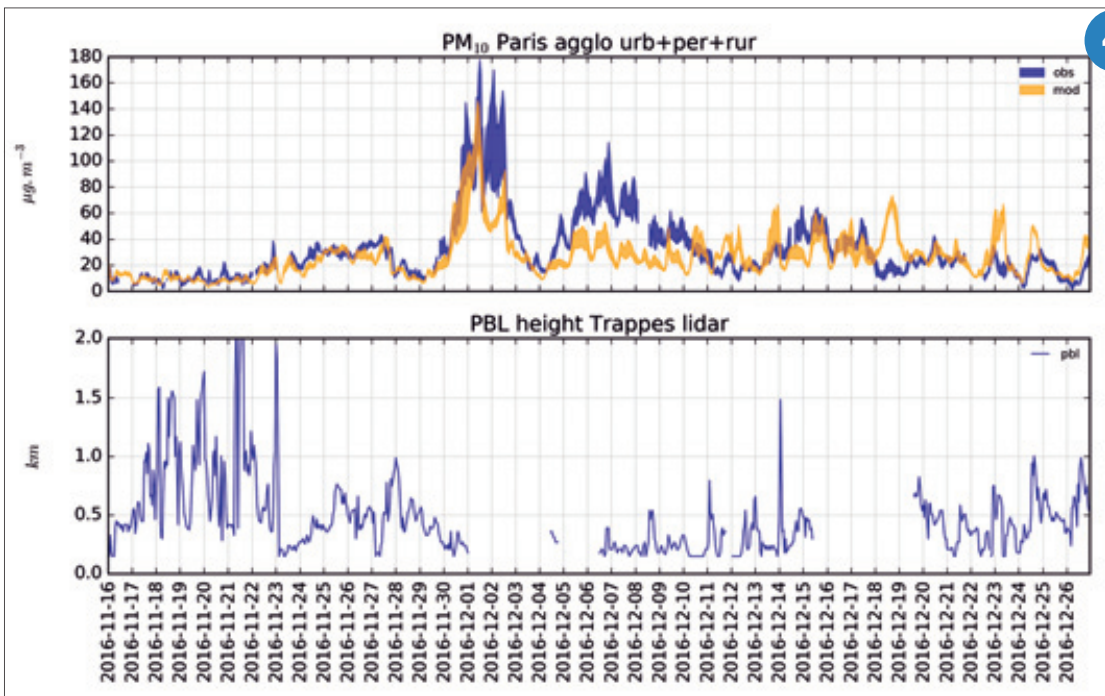
4

a: Correlation between
observations and pollen
concentrations of olive trees
predicted by the 7 models over
Europe during the 2014 season,
as well as the average
and median of the models.
b: Surface atmospheric
concentrations of grass pollen
(in grain/m3) at Nice forecasted
by the MOCAGE model (curve)
and observed (point) during
the 2014 season
(March 1 to August 31).
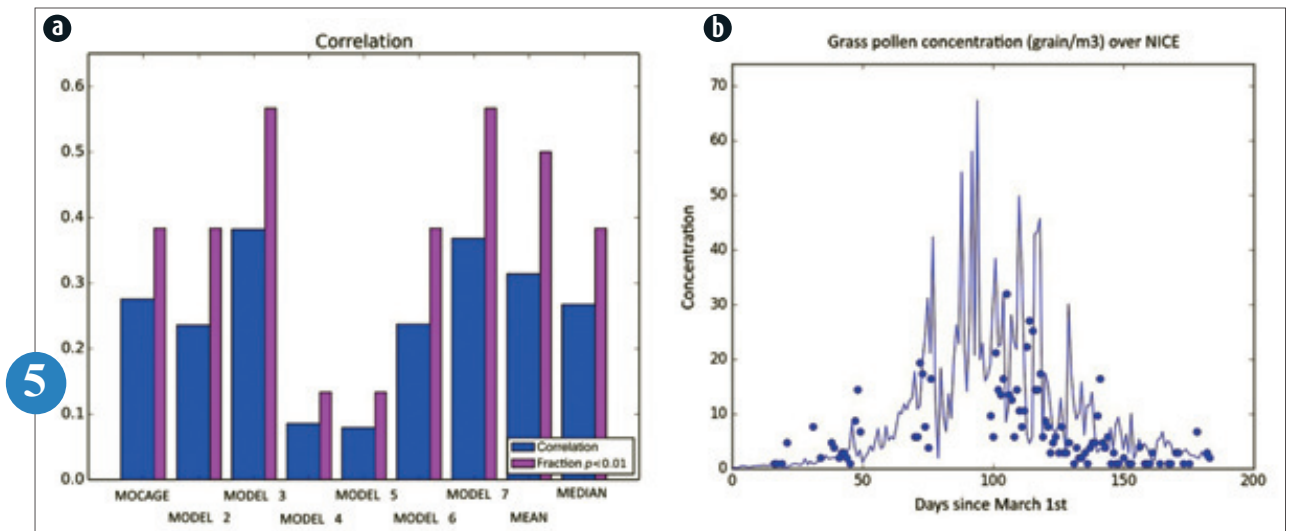
5

Ozone evolution in the upper troposphere at northern mid-latitudes, as seen by IAGOS

Atmospheric ozone plays a major role in several environmental issues. Its impact on the surface temperature reaches its maximum when it is located at the interface between troposphere and stratosphere, named UTLS.

Since 1994, the IAGOS observation system performs in situ measurements for several chemical species, including ozone, on board commercial aircraft. The measurements mainly take place in the UTLS of the northern hemisphere. Their vertical resolution is well suited for analysing the air composition in this thin layer, located between 9 and 14 km above sea level in the mid-latitudes. It makes the IAGOS dataset a major tool for evaluating the ability of models to reproduce the evolution of the UTLS chemical composition, and for validating the estimations performed by remote sensing instruments.

The analysis of this 20-year time series highlighted an increase in the upper tropospheric (UT) ozone burden, over all the well-sampled regions (from eastern United-States to north-eastern Asia). The comparison with other observation datasets (satellites, ozone sondes, surface stations) shows that this ozone enhancement takes place through the whole free troposphere, but remains stronger near the top. It is at least partly influenced by a long-term enhancement of the exchange processes between troposphere and stratosphere, coupled with the stratospheric ozone recovery.

The incoming implementation of other chemical species into the IAGOS system measurements, and the extension of their geographical coverage thanks to new partnerships with aircraft companies in the Pacific sector, will likely add further understanding to this analysis.

6

a: Map of the regions highlighted in the present study: western North America (WNAm); eastern United-States (EUS); North Atlantic (NAt); western Europe (Eur); western Mediterranean basin (WMed); Middle East (MidE); Siberia (Sib); north-eastern Asia (NEAs).

b: Time series of ozone mixing ratio (ppb) in the UT, in the 8 regions of this study
The monthly means are represented by the thin line. For each month, the interval between the lower and the higher values (percentiles 5 and 95 respectively) is filled in red. The available yearly means are illustrated by the bold line with black circles.
Note that northwest America is not sampled over a period long enough to derive robust trends.

Upper tropospheric O₃
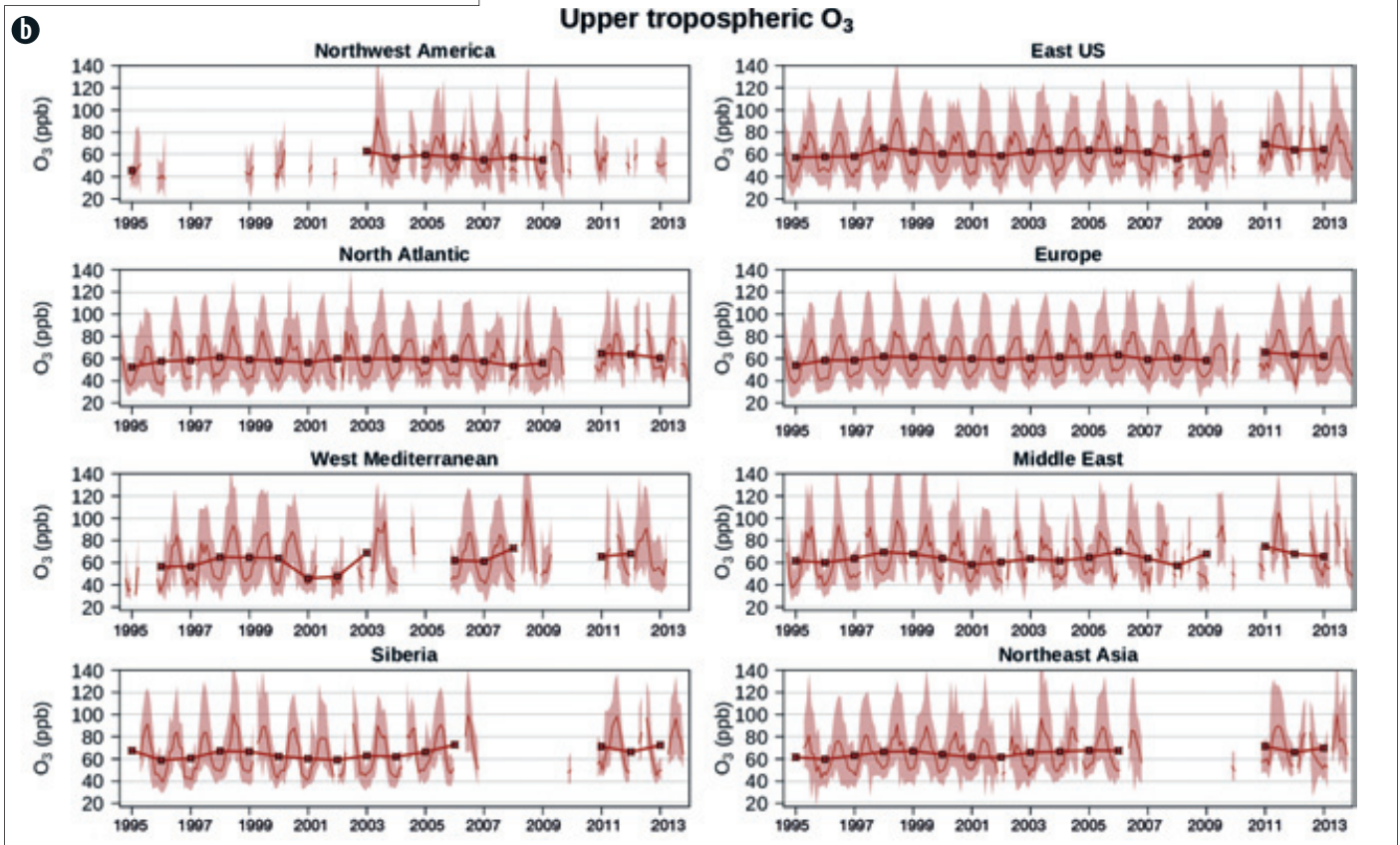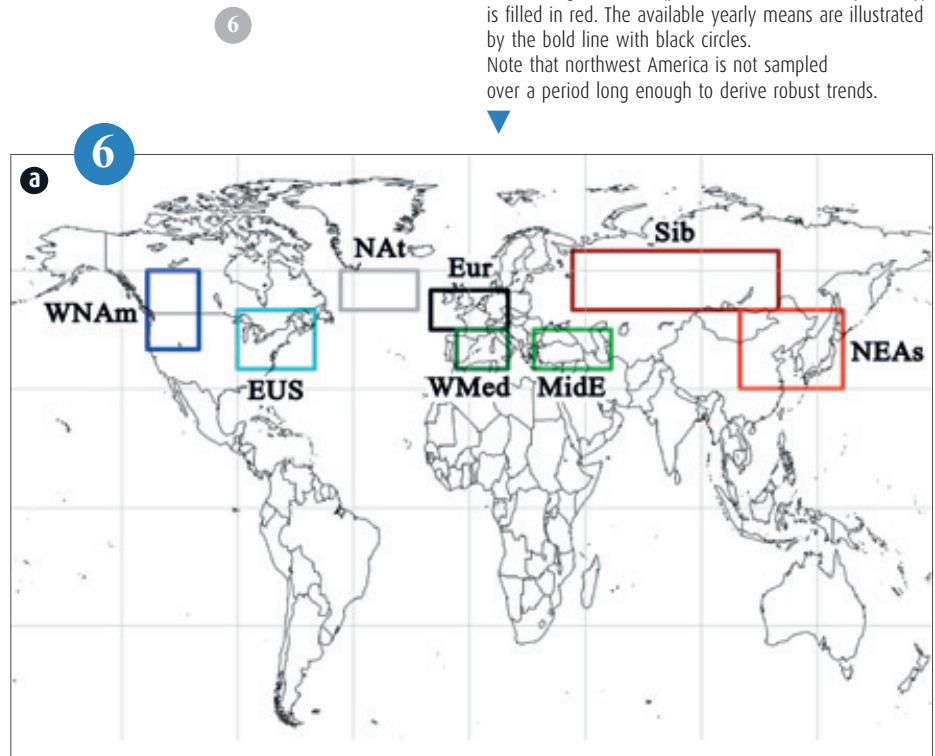
Climate

During the North Atlantic hurricane season of 2017, the Caribbean was severely struck by the three hurricanes Irma, José and Maria, resulting in loss of life and extensive damage. A few months earlier, during an early heat wave, mainland France experienced the warmest day (26.4°C) on June 21st for a month of June since the beginning of the weather observations.

Météo-France is in charge of forecasting such extreme events and also contributes to the progress of knowledge on their recent and future changes in the context of global warming. It is in this spirit that this year CNRM carried out high-resolution global climate simulations on the Antilles with ARPEGE-Climat. These new simulations will be used by CNRM and the Antilles-Guyana inter-regional directorate within the FEDER CA3F project to assess the link between global climate warming and changes in cyclone frequency and characteristics. Still in terms of extremes, this year's research activities also focused on the impacts of storms in France in the 20th century and the evolution of heavy rainfall events in the French Mediterranean. Also, as a result of recent work, it will now be possible to extend the real-time characterization of heat waves by estimating their likely evolution a few days ahead, based on weather forecasts.

The use of seasonal forecasts can provide information on the probability of occurrence of extreme events such as heat waves or cold waves in our regions, a few months in advance. Météo-France's seasonal forecasting system capitalizes on the CNRM-CM global coupled climate system model initialized by re-analyses. After a development phase of more than 4 years, version 6 of this model will make it possible to carry out a new set of climate simulations which will serve as a basis of the 6th IPCC assessment report.

1

▲
Satellite image from the GOES13 satellite, 06/09/2017 at 12h00 UTC: after hitting the island of Saint-Barthélemy, hurricane Irma is moving westward and threatens the island of Saint-Martin.
© Météo-France.

Study of climate

Impact of the North Atlantic cold anomaly on summer 2015 in Europe

Starting in winter 2014-15, a cold anomaly persisted for nearly two years both at the surface and in the 700 first meters of the North Atlantic Ocean between Iceland and Newfoundland. Using Météo-France seasonal prediction system 5, CNRM revisited the hypothesis that this cold anomaly had an influence on the occurrence of an abnormally warm summer in 2015 (Duchez et al. 2016). Several sets of ensemble predictions were initialized from 1 May 2015 conditions and run to cover the June to August (JJA) summer season, introducing a surface relaxation of the NEMO ocean component towards the Mercator-Ocean GLORYS2V3 ocean reanalysis. Relaxation is either restricted to the area of the cold anomaly or covers the entire globe.

By comparing the ensemble distributions for summer 2015 to a reference period of 1993 to 2014, Fig. shows that System 5 without relaxation fails to reproduce the warm near-surface temperature anomaly found over Central Europe (CE), and that ocean relaxation over the cold anomaly region (RANO) does not significantly shift the temperature distribution over Europe towards warmer values. With a global ocean relaxation (RGLO), the model manages to represent a warm anomaly more consistent with reference data, mainly during July and August. However, the response in terms of atmospheric circulation patterns in the coupled system is weak and suggests that other processes were at play during the heat wave observed over the area of interest.

Follow-up studies will consist in exploring other sources of predictability (such as the land surface) and extending the analysis to sub-seasonal time scales.

2

Data Rescue in West Indian Ocean

World Meteorological Organization (WMO) launched the Indian Ocean Data Rescue Initiative (INDARE) in order to accelerate recovering of climate records and to improve the quality of climate datasets from Indian Ocean area. In fact all the international and national climate data bases are still poor in pre-1961 meteorological data from this geographical area.

In 2017, following the request from WMO, Météo-France developed a Data Rescue implementation plan for the recovery of climate records from Madagascar, involving both meteorological service of Madagascar (DGM) and Météo-France.

A first work of searching and analysing led to recovering, sorting and cataloguing the digital publications available on line, containing historical meteorological observations for Madagascar, Mayotte and Comores over the period 1864-1961.

In 2017, in a framework of a partnership between Météo-France and the French National Archives (Archives nationales), 33 boxes of climate hard-copy archives related to West Indian Ocean over the period 1864-1961, originating from the historical Collection of the French meteorological services, have been made available to Météo-France.

Météo-France quickly started several tasks like preserving, restoring, inventorying and then imaging of monthly reports of 26 meteorological stations over the period 1947-1961. The first objective of the Météo-France's action, aiming at inventorying and sharing resources with other meteorological services and with international projects, will continue during the next two years.

3

Heat wave characterization in early mode

A "seamless" approach combining observations and forecasts has been developed to capture in real time the probable characteristics of a current or forecasted heat wave and to allow its qualification in comparison with past events.

It is based on a method of identifying heat waves applicable to any time series of daily temperatures. A set of thresholds constructed from the series' distribution is used to identify the occurrence of an episode, determine the start and end dates, and estimate the severity.

This method is implemented on a temperature indicator in France, consisting of the average daily temperature of thirty cities distributed homogeneously over the territory. In the forecasting mode, this indicator is based on the statistical adaptations of the 14-day ensemble forecasts for these same cities, prepared by the European Centre for Medium-Range Weather Forecasts (ECMWF). The fifty-one series made up of the abutment of the series observed with each realization of the model are then injected into the heat wave identification algorithm. The share of the realizations detecting a heat wave makes it possible to appreciate its probability, but also to estimate its probable characteristics: duration, peak of maximum heat and overall severity.

Through the use of a national temperature indicator, the approach remains global in France. To qualify the geographical specificities of the episodes, the method will soon be available at the regional and departmental levels, based on observed and expected daily temperature indicators for these same areas.

4

▲

Impact of ocean relaxation on the area of the anomaly
(RANO, in red) or global relaxation (RGLO, in green)
on the distribution (box-and-whiskers)
of monthly mean 2-meter temperature (T2m)
over Central Europe (CE) in ensemble seasonal predictions
of summer 2015 with System 5 (reference, in blue),
according to the forecast month
Reference data (ERA-Interim) are shown as a black line
for 2015, and the yellow distribution for 1993-2014.
System 5 climatologies for 1993-2014 with and without
global relaxation are shown in light blue and light green,
respectively.

▲ Monthly climate report for the Vohemar station in Madagascar, January 1960

▶
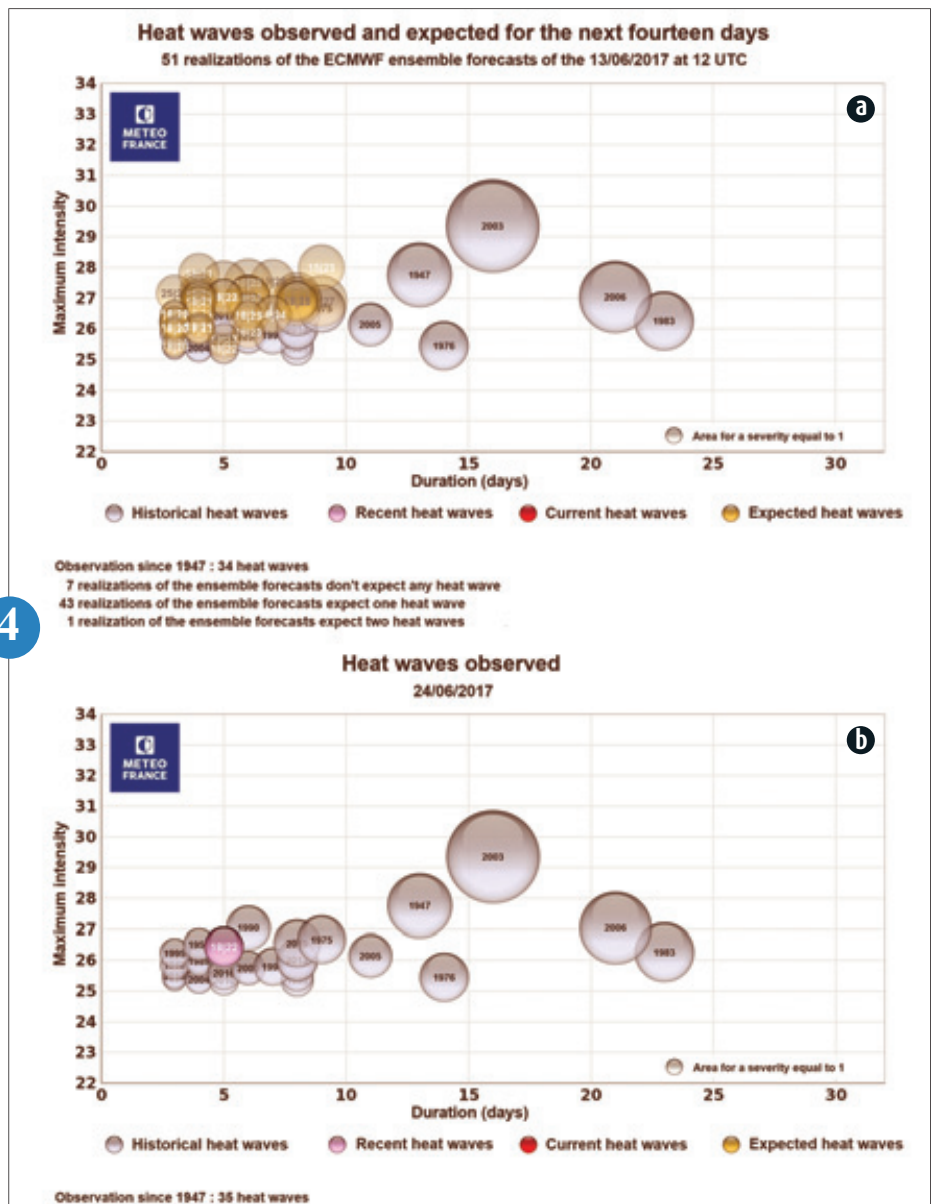
Ensemble forecasts on June 13, 2017 at 12 UTC
of the heatwave that will start on the 18th June (figure a)
and a posteriori characterization of the episode (figure b):
the episode duration and the maximum value
of the temperature indicator are respectively represented
on the abscissa axis and on the ordinate axis.
The symbol area is proportional
to the overall severity of the event.

Optimal interpolation of daily temperatures in Ile-de-France, taking into account urban fraction

Minimum and maximum daily 2-m air temperature maps have been developed taking into account land use. Derived parameters, such as heating and cooling degree days, can be deduced from these daily maps.

A screened regression equation is computed each day between 2000 and 2015, linking altitude and urban fraction to temperature measurements. Its relevance is further verified by cross validation. The deviations from this regression are then interpolated by kriging on a fine grid, where the altitude and the urban fraction are already known. Minimum temperatures very often depend on the urban fraction, this dependency being more frequent in spring and summer. Maximum temperatures depend mainly on altitude.

From these temperatures, heating and cooling degree days can be deduced on the same fine mesh grid, corresponding to the energy devoted to the maintenance of thermal comfort. One can notice a considerable difference (30% in urban zone) between maps of cooling degree days deduced from ordinary kriging of temperature and those using urban fraction and altitude. Other climatological parameters (monthly and seasonal averages) will be analysed.

This work will help to describe the urban heat island in Paris. It can be improved by adding, once available and validated, measurements from denser networks in urban zones.

5

Detection and impact analysis of winter windstorms affecting France over the XXth century

During winter, Atlantic storms may reach European western coast, France in particular, often causing extended damage due to wind gusts. In the recent years wind storms climatology has constantly improved. Nevertheless, wind impact of a storm is still difficult to characterise.

The newly provided ECMWF reanalysis for the XXth century is used here to study wind storm climatology thanks to an automated tracking algorithm. At the same time, a Loss Index is computed which combines the destructive power of the wind (V3) related to its quantile 95% with the population density. This Loss Index (LI) is used to select a set of 1500 days corresponding to the highest values of the LI for that are representative of the storm activity for France. Then, given one storm track, the wind field is extracted within circles of influence of the storm, and this allows to compute the spatial LI field all along the storm evolution (see Fig. a). Considering storms that reached France, we observe that they may be separated in two classes, a first one for the storms that stay always on the Northern side of the Jet, and a second one for the storms that cross the Atlantic Jet from South to North. This latter class has often been studied as a

typical case favouring fast deepening cyclogenesis. We compute the average LI associated with these storms for the period centred on the Jet crossing moment (see Fig. b). We can see that the impact of the storm is maximum just after the crossing which appears to be also the moment when the storm is the closest to France. Using this century-long dataset we notice that the storms which cross the jet close to France are also the ones which cause the most damages over France.

6

Climate change

Observed increase in extreme daily rainfall in the French Mediterranean

Heavy precipitation events observed in the French Mediterranean regions are among the most severe weather events affecting mainland France. Several studies investigated how such events could respond to anthropogenic climate change, using numerical climate models. Here we focus on the observed evolution of these events, taking advantage of the available 55 years of record.

The most homogeneous daily rainfall series (about 70 weather stations all over the French Mediterranean) are combined together to produce a regional index of relative intensity of annual maximum daily rainfall. Possible changes in intensity are then assessed from this regional index.

Results show a statistically significant increase of daily rainfall intensity, estimated at +22 % [+7 to +39 %] between 1961 and 2015. Significance holds for more than 15 years. The wide confidence range highlights the high variability of heavy precipitation events. Using Clausius-Clapeyron units (CC, which corresponds to +6.8 %/K), the estimated increase is close to 2xCC. However, given uncertainties, observations are consistent with an increase following or even smaller than the CC rate – i.e. values simulated by global climate models. Results obtained with other indicators such as the number of events, their surface, or the total volume of water precipitated above a threshold, consistently point toward an intensification of the most extreme events over the last decades.

This study adds a new line of evidence suggesting more extreme events in a warmer climate – a diagnosis that is particularly relevant for adaptation. Future work includes extending this study to other regions, and using the proposed regional index in a climate monitoring perspective.

7
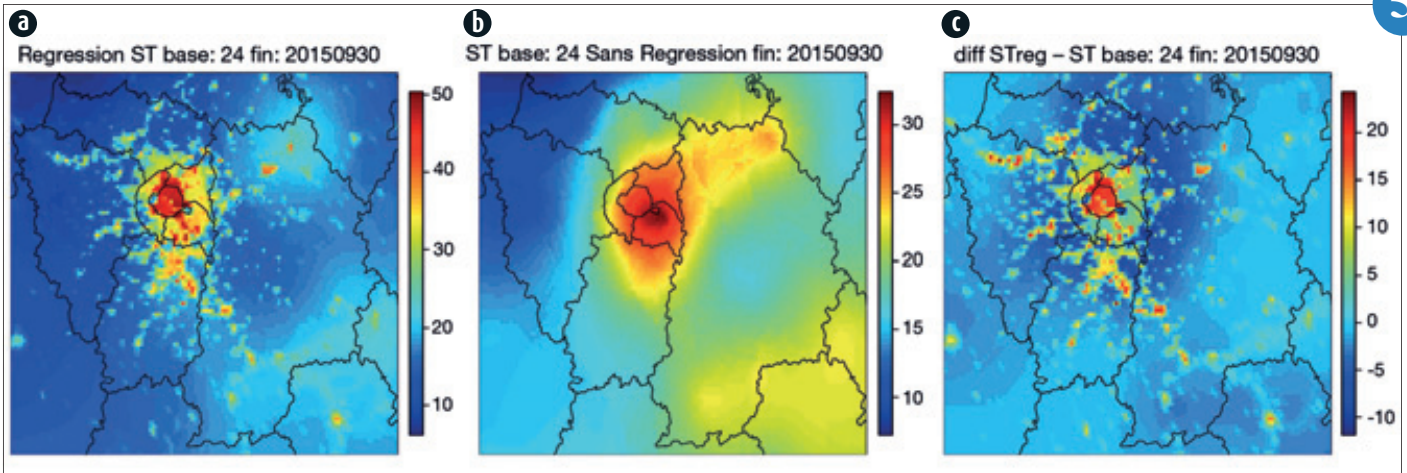
a: Unified cooling degree-days, calculated with a 24 °C threshold from spatialized minimum and maximum temperatures, taking into account relief and urban occupancy metadata when relevant.

b: Unified cooling degree-days, calculated with a 24 °C threshold from spatialized minimum and maximum temperatures by a simple geometric kriging.

c: Difference between the unified cooling degree-days calculated with a 24 °C threshold from spatialized minimum and maximum temperatures, taking into account relief and urban occupation metadata when relevant, and those obtained by simple geometric kriging. Urban areas and high-altitude areas (to a lesser extent) are highlighted.
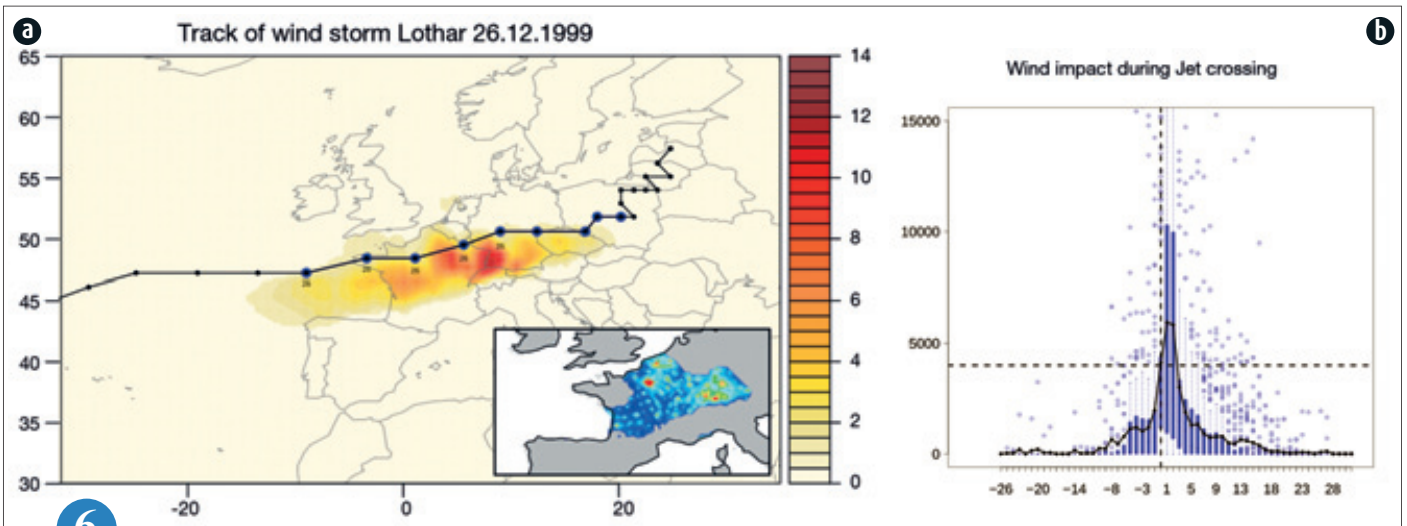
a: Track of the famous Lothar wind storm, 21 Dec 1999, as detected with the tracking algorithm. Shading colours indicates a meteorological index based on the wind with relation to its quantile 95%. Insert: Same index combined with population density.

b: Averaged values of Loss Index for storms reaching France for the track time-steps around the moment the storm crosses the Atlantic Jet.
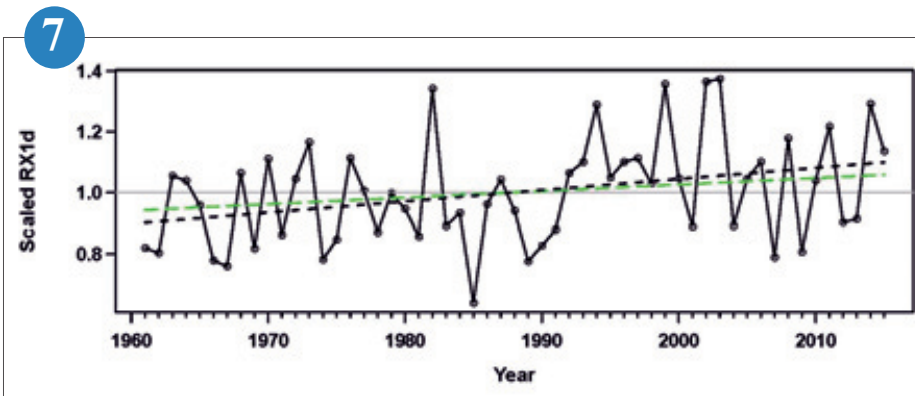
Time-series of the proposed regional index
of heavy precipitation intensity,
over the period 1961-2015.
This index is derived from normalized annual maxima
of daily rainfall, and is therefore unit-less
(1 corresponds to the mean intensity).
Dashed black: linear trend as estimated
from this regional index.
Dashed green: linear trend as expected following
the Clausius-Clapeyron relationship (+6.8 %/K,
i.e. +11.8 % over the period given
the observed warming of +1.7K).

Response of tropical cyclone induced rainfall to climate change over the Atlantic basin

Tropical cyclones are known to generate very high winds and storm surges due to cyclonic swells. In addition to these two effects, heavy rainfalls accompanying the systems may cause catastrophic floods and landslides. With climate warming, the water vapor that the atmosphere may contain is expected to increase following the Clausius-Clapeyron formula. This increase is estimated to be around 7 %/K. This could result in a rainfall increase of the same amount within extreme events.
A study has been conducted at CNRM to investigate water budgets in simulated hurricanes. Two periods were compared: present conditions and a warming scenario (RCP8.5). A rotated-stretched version of the CNRM-CM5 model was used, with a pole of interest located in the tropical Atlantic, allowing a local resolution of 50kms necessary for hurricane simulation.

Tracks of modelled hurricanes were obtained from an object-based tracking algorithm. Water budget components were calculated for each hurricane rainfall percentile. By aggregating rainfall over variable size domains, we showed that for small size domains, the rainfall increase could largely exceed the expected rate of 7 %/K, in relation to changes in moisture convergence inside the hurricanes. Robustness of these results to changes in the CNRM-CM physics that were developed for the CMIP6 phase should be addressed in future studies, particularly by investigating the ensemble runs produced for the FEDER C3AF project.

8

Study of climate change in the French Antilles: regional climate, tropical cyclones and sea states

The interdisciplinary collaborative (Universities of the French West Indies and of Montpellier, BRGM and Météo-France) C3AF project funded by the European Regional Development Fund aims at studying hazards associated with climate change in the French Antilles (tropical cyclones, swells, sea level rise, floods, landslides, erosion) and their environmental and socioeconomic impacts in the islands.
At Météo-France, researchers study future changes in North Atlantic tropical cyclone activity and in the associated swells that hit Antillean coasts. ARPEGE-Climat atmospheric model simulations at very high resolution in the Atlantic cyclonic basin allow tracking tropical storms and hurricanes in order to detect possible changes in their frequency, intensity and geographical distribution. These simulations are also used to drive wave models (MFWAM, WaveWatch 3) in order to estimate changes in cyclonic wave climate. These latter models also allowed reproducing some recent events such as hurricane Matthew in 2016. In addition, analyses of historical precipitation records in the French Antilles and of the associated atmospheric dynamics from both observations and numerical simulations are currently under way.
Late 2017, the first analyses of all tropical-cyclone tracks and their changes, as well as regional sea states, will be available. On the other hand, the C3AF consortium has included in its time table the study of impacts from hurricanes Irma and Maria (September 2017), which have triggered much questioning within the public in regard to their possible links with climate change.

9

Seasonal forecast

Seasonal forecasting and stratosphere dynamics

Seasonal forecasting aims at exploiting the fact that slow evolving, and thus potentially predictable in the long range, components may condition the climate of a forthcoming season. Among these components, the stratospheric equatorial jet is a potential predictor. We have extended the vertical resolution of the version of Arpege model used for Copernicus seasonal forecasts from 91 to 137 vertical levels, in order to better represent the stratosphere dynamics. Two re-forecast experiments (7-month range, 140 member ensem-

bles) have been carried out for summer and winter seasons. Figures a (winter) and b (summer) show that 30 hPa zonal wind along the equator is highly predictable till month 7. The mean zonal wind at 30 hPa, 60°N, which characterizes in winter the occurrence of stratospheric sudden warmings, exhibits a time correlation of 0.42 (137 level version) against 0.26 (91 level version) in DJF, and 0.76 against 0.73 in JJA. However, no such improvement is obtained with tropospheric scores, except North Atlantic oscillation (NAO) index which

exhibits a correlation of 0.73 against 0.67. The difference between the last two scores is not statistically significant anyway. Given the computation cost of such a vertical resolution increase, the next version of the seasonal forecast model (in 2019) will be rather based on a higher horizontal resolution in the ocean.

10
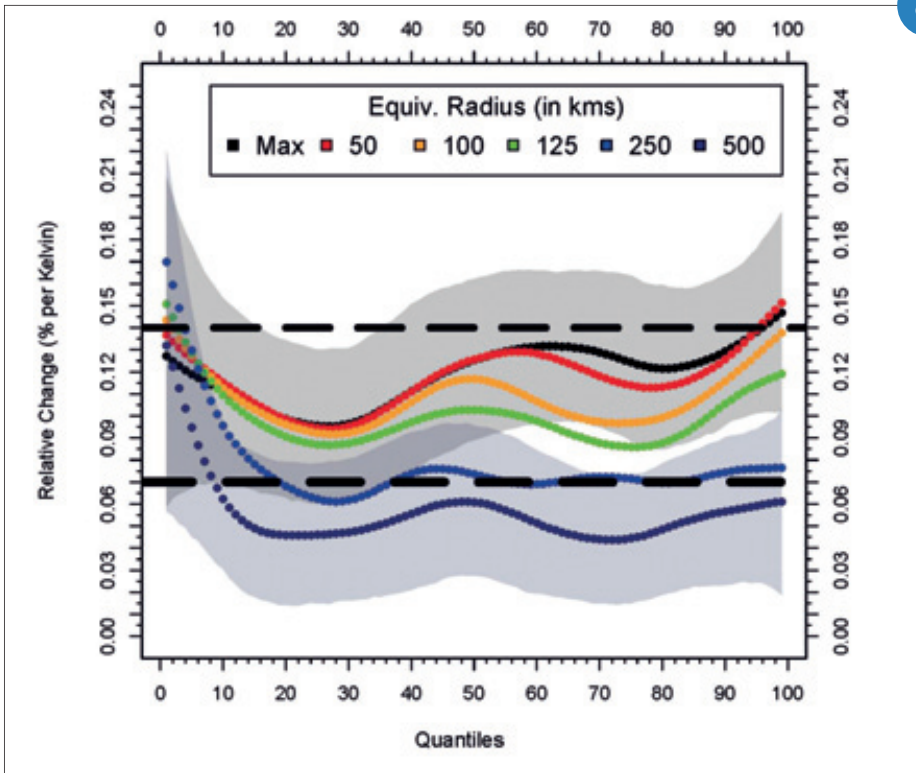
Relative change of rainfall quantiles
for 6 spatial aggregation domains
Equivalent size of the domains has been reported
in the upper frame. Changes have been normalized
by the mean SST change over the tropical Atlantic basin.
Horizontal dashed bold lines correspond to rates
of changes of respectively one and two Clausius-Clapeyron
rate of change (7 %/K). Units are percent by Kelvin.

Example of a category 4 hurricane
on the Saffir-Simpson scale during the month of August,
from an AMIP-type ensemble simulation
from the ARPEGE-Climat model stretched
over the tropical Atlantic (15 to 150 km resolution).
Model physics is as in the version used
for IPCC's CMIP6 exercise.
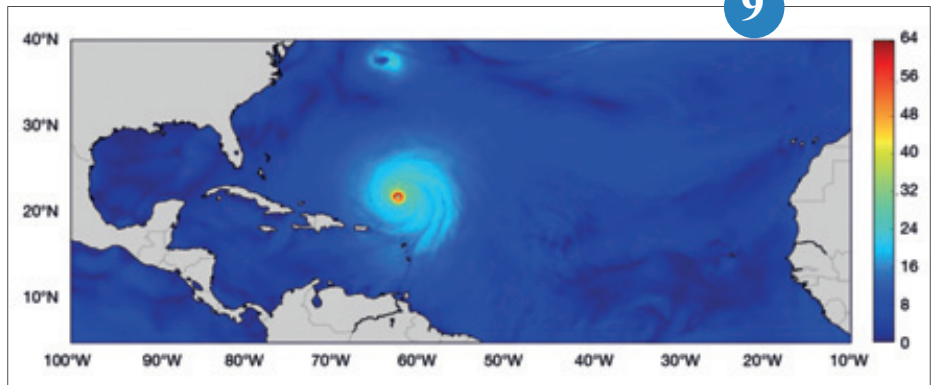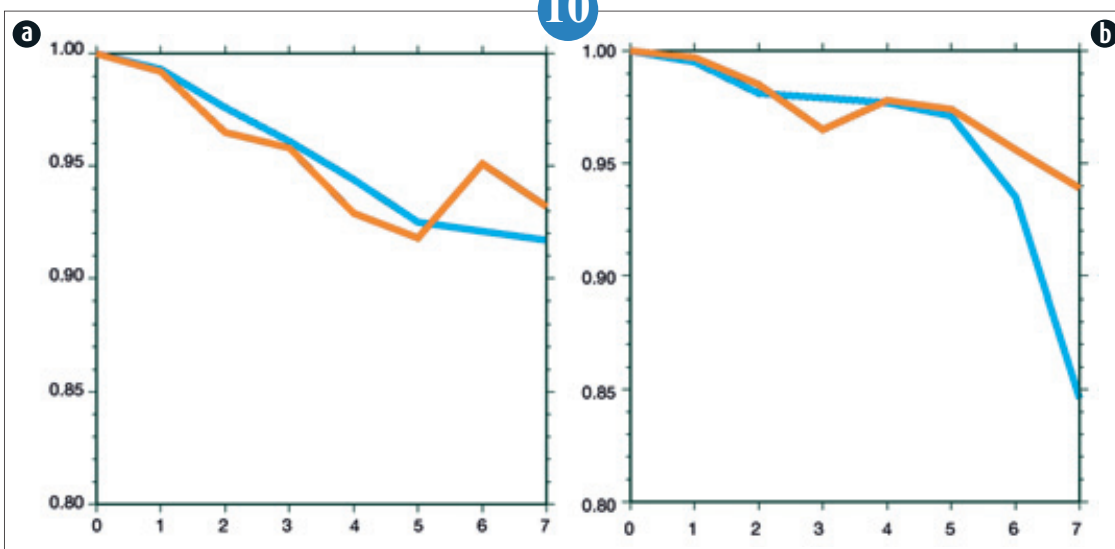
a, b : Correlation coefficient
between forecast
and observation for mean zonal
wind along equator at 30 hPa,
as a function of time lag
(month) for 1st November
start dates (a)
and 1st May start dates (b) ;
red line for Arpege
with 137 vertical levels,
blue line for 91 vertical levels.

Seasonal predictability of heat wave and cold spell over Europe

In the frame of the Copernicus Climate Change contract C3S/433 on the seasonal forecast, the DCSC department has developed new « state of art » products for users in respect with model skills in seasonal forecasting. In the « Proof of Concept » phase of the C3S program, the issue of the probability of extreme event occurrence has been addressed, in particular for heat wave and cold spell over Europe by considering the anomaly of the number of heat wave days (or cold spell days) for the next three months.

Following the results coming from recent projects as the ACASIS project over the Western Africa and the Extremoscope project over France, the heat wave events (respectively cold spells) has been defined in each grid point from an indicator based on the mean temperature by merging a statistical approach (exceed of the percentile 90 for heat wave or percentile 10 for cold spell), an absolute one (threshold of 20°C for heat wave or +3°C for cold spell) and a minimum duration (three consecutive days).

The climatological reference of the number of heat wave (cold spells) has been calculated from ERA Interim reanalysis since 1979 over a large domain covering the whole Europe and the Mediterranean coasts. The seasonal predictability has been assessed with the Météo-France model system 5 from the initialisation starting in May for the heat waves and November for the cold spells. Probabilistic scores (Receiver Operating Characteristic) have been calculated with debiased temperature datasets from a quantile mapping method on the hind-cast period (1991-2014) of the Météo-France System 5 model. Areas of better skills have been identified for heat wave predictability on Central and Eastern Europe and cold spell on Western and Northern Europe. These results are consistency with the seasonal forecast skills of the mean temperature in summer and winter over Europe and allow to better tailor climate information for the user needs.

These products have been also experimented in forecast mode for the years 2015 and 2016 and will be soon available with the C3S seasonal forecast models.

11

Climate monitoring and seasonal forecast of general circulation over North Atlantic and Europe

Weather regimes and modes of variability are tools made by climate researchers for climate analysis. They synthesize the dynamics of the atmosphere by a reduced number of indicators, which therefore facilitate the understanding of mean circulation impacts at different time scales, from one day, to one month, to one season.

However these tools remain rarely used operationally by meteorologists and climatologists, for a lack of homogeneous definitions which could be applied at different timescales (past climate re-analyses, recent analyses, forecasts up to seasonal), and also because of a lack of graphical representations adapted to users.

This was a motivation for DCSC to develop products based on weather regimes and modes of variability over North Atlantic and Europe. They aim to address climate monitoring and seasonal forecast issues. Regimes and modes have been calculated from ERA-Interim reanalysis fields, in order to define fixed spatial patterns, helping interpretation at different timescales. A specific work has been conducted, in particular in the COPERNICUS framework, to define graphical representations adapted to seasonal forecast.

Among the available products, there are data and graphics on past or future situations, at different time-steps, from daily (for regimes exclusively), to monthly or seasonal, in reference to climatology. There are also maps showing the mean impacts of regimes and modes on the European climate, in terms of temperature and precipitations. Some graphical products show simultaneous evolution of modes or regimes and temperature or precipitations in France (Figure).

For seasonal forecast, because they rely on large scale information given by models, regimes and modes take advantage of a generally better predictability that impact parameters themselves. Soon they would be made available on the set of COPERNICUS seasonal forecast models.

For more information:
http://dcsc-avh-net.meteo.fr/avh/
and http://seasonal.meteo.fr/.

12
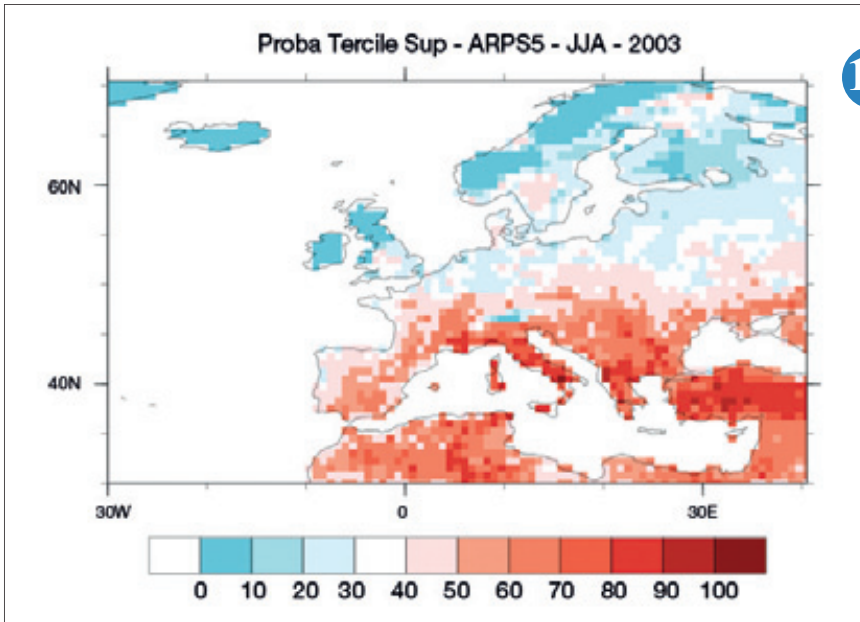
Probability of the upper tercile for the number
of heat wave days over Europe
for the summer 2003 (June to August),
from the Météo-France System 5 model,
initiated in May
In red, the regions where the model forecasted
a strong probability of a number of heat wave days
upper than the climatology.
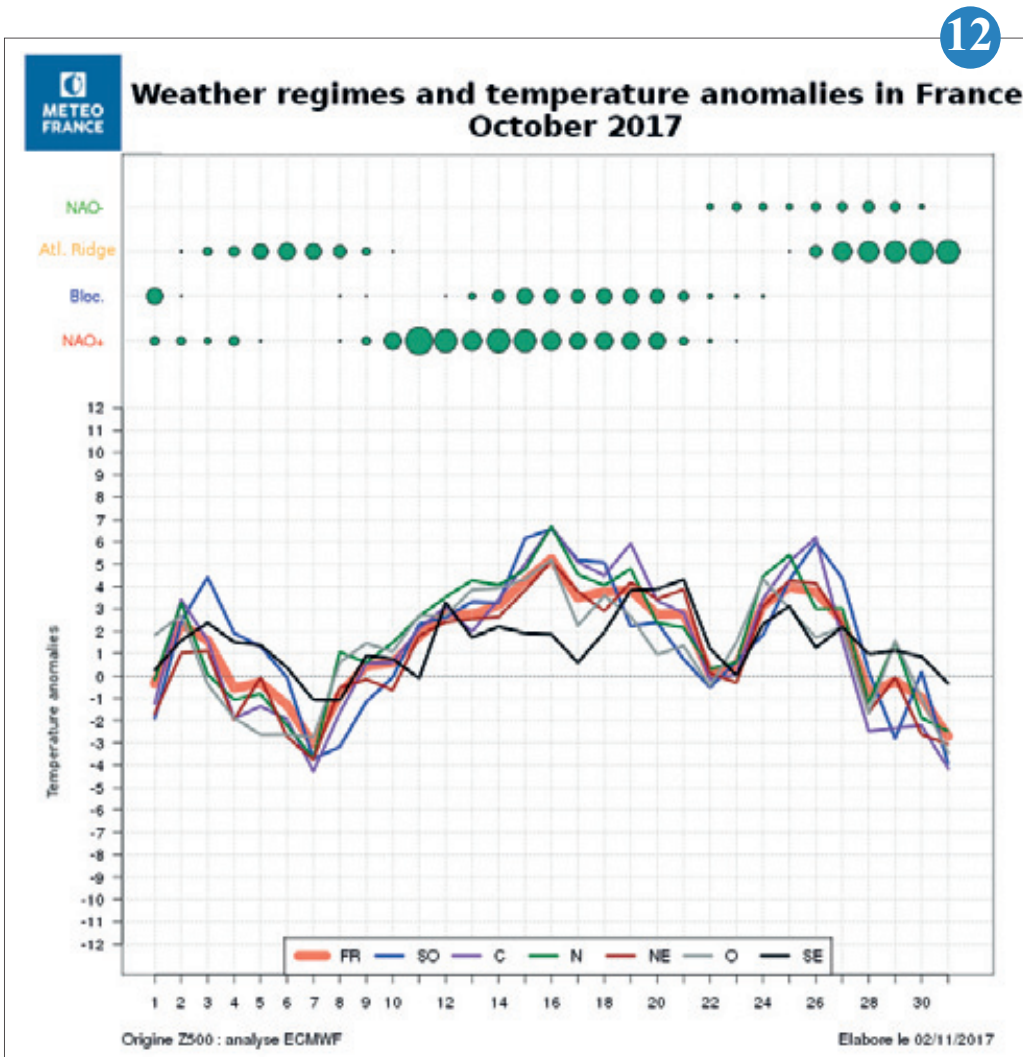
Real-time daily monitoring (available at D+1)
of weather regimes and temperature
anomalies in France
For each day is plotted the correlation
between regime's centroids
(NAO-, Atlantic Ridge, Scandinavian Blocking,
NAO+) and the daily Z500 field
over North Atlantic and Europe.

Cryosphere and Hydrology

The water cycle is an active component of the climate system, providing a link between the atmosphere, the ocean and land surfaces. Weather predictions and climate projections by means of numerical models are only relevant if the energy and water fluxes at the interfaces between these compartments are appropriately represented in the models, at all time scales. Furthermore, the fate of water on land surfaces is essential for ecosystem and human societies. In the liquid phase, water contributes to river discharge, including floods. All natural systems where water is present in the solid phase (ice) constitute what is referred to as the "cryosphere", bringing together glaciers, seasonal snow on the ground, permafrost, but also lake, river and sea ice. The cryosphere plays a major role in the climate system at all space and time scales, and is related to prominent natural hazards in mountain regions such as snow avalanches.

CNRM carries out a wide range of research activities in order to better observe (in-situ and by satellite), understand and model the various aspects of the water cycle on land surfaces. The Snow Research Centre maintains two dedicated observatories in the Northern Alps, the Col de Porte at 1325m in the Chartreuse massif, and the Col du Lac Blanc at 2700m in the Grandes Rousses massif. These observations make it possible to measure the long term trends of snow conditions in mountain regions (see Figure). This is complementary to modelling efforts into the long term projections of the impact of climate change of the mountain cryosphere, carried out in collaboration with the Climatology and Climate Services Division of Météo-France. In addition, such observations play a pivotal role to develop and evaluate numerical models of the snowpack. Their increased level of complexity is necessary to improve the forecast capabilities, thereby providing better support to operational forecasting duties of Météo-France, especially in the field of avalanche hazard warning. This is also required to test and address knowledge gaps regarding the interactions between snow on the ground and its surrounding environment. At a much wider scale, research carried out at CNRM aims at improving the modelling tools used to perform climate simulations at the global scale. This concerns in particular the way permafrost, that is permanently frozen ground. Permafrost plays a crucial role in the climate system, in particular due to greenhouse gas compounds which it hosts (in particular methane and carbon dioxide), and which may be released when permafrost thaws under the influence of ongoing climate change. Adequately modelling how permafrost evolves, depends on the ability of the land surface model to simulate the behaviour of carbon compounds stored in the ground, but also its thermal regime, which is driven by its own properties, atmospheric conditions, and the presence of snow and vegetation. All of these components also play a major role by regulating the water cycle at the scale of the country, the monitoring and forecasting of which requires to not only address surface, but also subsurface processes. CNRM researchers contribute to the development of a national-wide modelling platform for large scale hydrology including aquifers.

All of these research activities contribute to improving scientific and technical knowledge within the national and international scientific community. However, be it through the development of global models contributing to IPCC assessments, or smaller-scale models directly employed for operational hydrological or avalanche forecasting activities, all of these challenged being driven by societal needs. In many cases, CNRM staff operating in the field of the cryosphere and hydrology plays an important role note only addressing research questions, but also contribute to the innovation process by which academic knowledge is converted into forecasting tools used for delivering operational services.

(1)

Current and future evolution of the snowpack in the Pyrenees

In the frame of the ClimPy Interreg project, aiming to enhance the Pyrenean Climate Change Observatory (OPCC in French) and the knowledge on climate change in the Pyrenees, Météo-France (DCSC -climate services department- with CNRM/CEN- research unit on snow- and DIRSO - Southwestern Regional Department) focuses on the evolution of the snowpack at different time scales. First, an inventory of snow height series on the French Pyrenees has been achieved and around 40 one have been selected, according to quality criteria on length and missing data ratio, to be used in climate trend analysis. A new method for data control and reconstitution has been defined from a specific configuration of the CROCUS snowpack model using

an assimilation process based on snow height data. Once completed, these snow series will contribute on the climate trend analysis over the last decades. Moreover, another action has been initiated on the current climate with AEMET (Spain National Meteorological Service) to share the climatological databases on the Pyrenees and to a snowpack reanalysis with the SAFRAN-CROCUS model, evaluated from homogenised series and teledectection data. On the future climate, a new dataset of bias corrected projection have been prepared on the Pyrenees area from the Eurocordex ensemble and the new downscaling method, named ADAMONT. Tailored indices have been defined to highlight the changes on impact

parameters for snow resort activities: winter mean temperature, winter precipitation amount, snow rate precipitation, snowpack mean or duration, snow-height day number over thresholds, snow water equivalent. These indices will be soon available on the OPCC geoportal website and the national climate services websites DRIAS and Climat[HD].

(2)
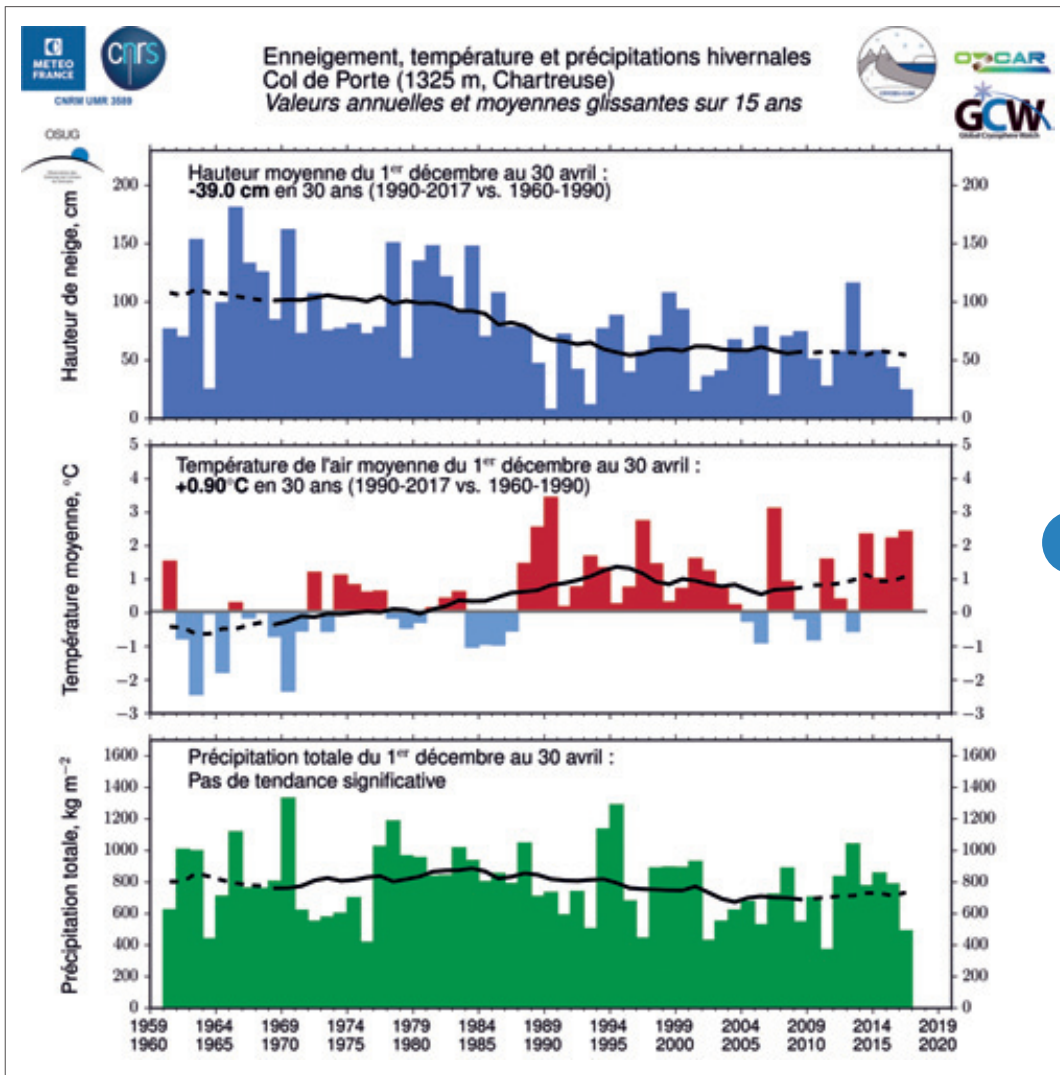
Overview of measurements performed at Col de Porte, 1325 m altitude, from 1959 to 2017. The upper plot illustrates changes in mean winter snow depth, the middle plot shows changes in winter temperature, and the lower plot shows changes in total winter precipitation. All of these variables exhibit significant inter-annual variability will significant decreasing trend in snow depth, significant increasing trend in winter air temperature, and insignificant trend in total winter precipitation.
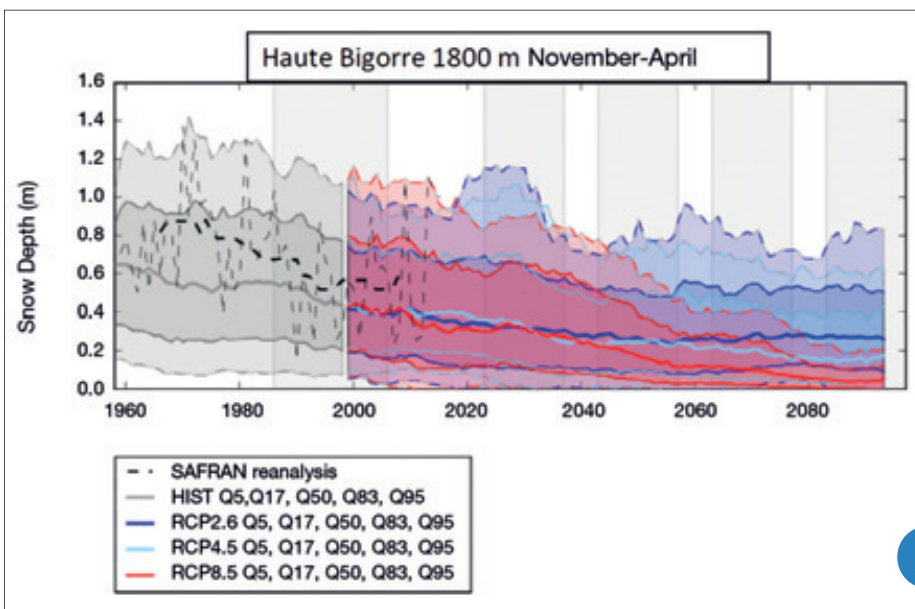
Evolution of winter snow height mean
from 1960 to 2100 at 1800 m
on the Haute Bigorre area (France)
from the SAFRAN-CROCUS reanalysis
(annual data on grey dotted line,
15 years mean on black dotted line) and the EUROCORDEX
ensemble including the historical run (grey),
the RCP 2.6 (dark blue), the RCP 4.5 (light blue),
the RCP 8.5 (red). For each RCP scenario,
the statistical distribution has been represented
with the median and extreme percentiles (5, 17, 83, 95)
of 15 years mean values, aiming to evaluate
the uncertainties and inter-annual variability.

A new model estimating the impact of light-absorbing impurities deposition on snowpack evolution

Light-absorbing impurities deposited on the snowpack (mineral dust, black carbon, soot, atmospheric particles, organic debris, etc.) darken the snow. By modifying its ability to reflect solar radiation, this directly accelerates snow melt. This also indirectly affects the evolution of the snowpack physical properties.

A detailed representation of light-absorbing impurities deposition, evolution in the snowpack (increased concentration by compaction, scavenging by melt water, etc.) and impact on the energy budget and solar radiation absorption have recently been implemented in the multi-layer detailed snowpack model Crocus. Modelling experiments have been carried out using data acquired at the Col de Porte experimental site (1325 m, Chartreuse) during 2013-2014 winter. The model simulates snowpack evolution reasonably in term of snow depth, snow water equivalent and radiative properties (albedo). It makes it possible to quantify the impacts of light-absorbing impurities on snow physics. For instance, during the snow season 2013-2014 affected by several deposition of Saharan mineral dust, the simulations highlight that the melt-out date of the snowpack is advanced by 9 days compared to a clean snowpack.

These results open many prospects to better understand and quantify the impact of atmospheric impurities on snow physics in the contexts of the interactions between the climate and the cryosphere, of water resources management and of avalanche forecasting.

③

Snowpack simulations with a multi-physical ensemble system

The detailed snowpack model SURFEX/ISBA-Crocus is commonly used in support of operational avalanche hazard forecasting as well as in climate change impact studies.

Despite the physical basis of the model, it suffers from errors and approximations in the empirical parameterizations of a number of processes. It is difficult to identify a unique and optimal configuration because there is equifinality between these parameterizations: different model configurations can lead to a similar overall skill.

New options were implemented for several processes (fresh snow density, metamorphism, radiative transfer, turbulent fluxes, thermal conductivity, liquid water retention, compaction, etc.) It allows building a new multi-physical ensemble system called ESCROC (Ensemble System Crocus). Optimization methods were designed to select a sub-ensemble of 35 equiprobable members. The obtained spread is able to explain about 2/3 of total error in snowpack simulations on the instrumented site of Col de Porte (1325 m, Chartreuse).

The new system ESCROC opens the door to a wide range of applications. It allows quantifying the contribution of snow model uncertainty in future projections of snow cover (about 20 % of total uncertainty for one given emission scenario). It will allow accounting for model uncertainty in the future operational numerical system in support of avalanche hazard forecasting, being combined with meteorological ensembles and an ensemble algorithm for the assimilation of snowpack observations.

④

Col du Lac Blanc: a site for snow observing and modelling in high mountains

Since 1990, Météo-France and IRSTEA have been managing the experimental site of the Col du Lac Blanc located at 2 700 m altitude in the Grandes Rousses massif in the French Alps. By its location, the site may be considered as a natural wind tunnel and not surprisingly was mainly dedicated to observation and modelling studies on wind-induced snow transport.

One of our ambitions for the Col du Lac Blanc site is that it remains a reliable reference site for high mountain observations. For this task, monitoring and evaluation studies of the site measurements are carried out daily. The site hosts regularly pilot experiments to test new approaches or measurements prototypes. Thanks to the site measurement facilities, innovative research for understanding and modelling wind induced transport are carried out towards a realistic representation of wind-induced snow transport in different models; this phenomenon plays a major role for the seasonal evolution of the snowpack and for avalanche occurrences. Some evaluation studies of the Numerical weather Prediction AROME model against relevant in-situ measurements have been conducted and allow to consider the potential added value of AROME fields such as wind gusts to map wind-induced snow transport (the attached figure shows AROME wind forecasts evaluated against in-situ measurement at Col du Lac Blanc). The site is also increasingly used to improve the use of remote sensing data in high mountains.

⑤
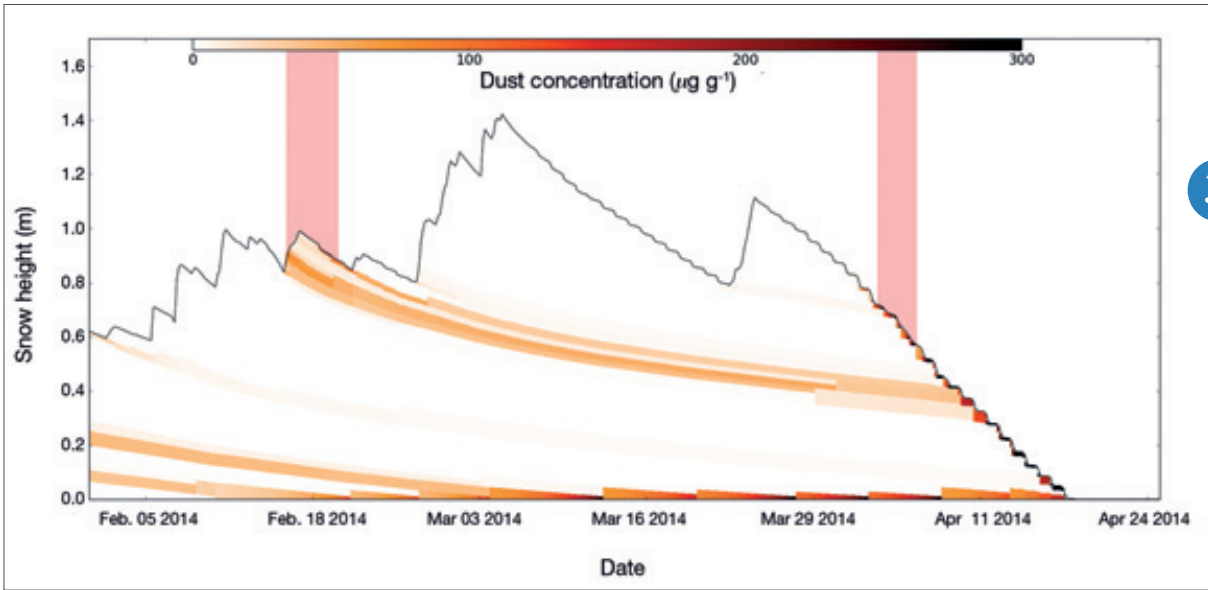
Simulated mineral dust concentration profile for the second half of 2013/2014 snow season at Col de Porte (1325 m, Chartreuse)
The simulation is carried out with the Crocus snowpack model using ALADIN-Climate dust deposition fluxes.
The two major Saharan dust events are represented by the red areas.
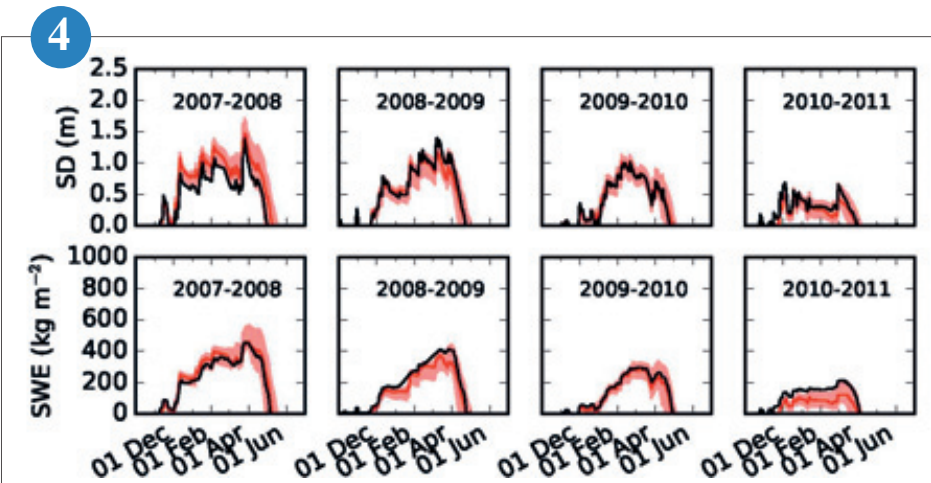
Snow depth (SD) and snow water equivalent (SWE) observed (in black) and simulated
by 35 equiprobable members of the ESCROC system during 4 winter seasons from 2007 to 2011.
The red envelope represents the uncertainty
of the parameterizations in the snowpack model
(difference between 5th and 95th percentiles
of the ensemble) and the red line
represents the ensemble median.
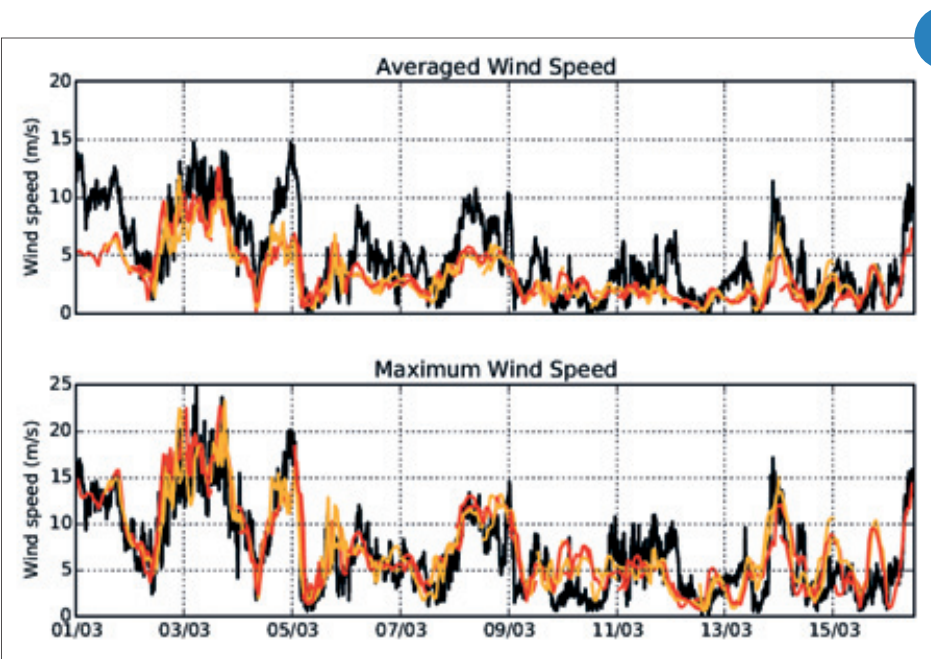
Mean (top) and maximum (bottom)
wind speed at « Col du Lac Blanc »:
Observations (black) and short range forecasts
from AROME model (00h00 UTC: red;
12 h00 UTC: in orange) for the period ranging
from March 1st to March 16th 2016.

Permafrost and Climate Change

The thawing of permafrost, the permanently frozen ground, in the arctic and boreal regions is an important consequence of the current climate warming trend. These frozen soils contain vast amount of carbon that could be released to the atmosphere in the form of CO_2 and CH_4 as the thawed organic matter becomes available to microbial degradation. These greenhouse gas emissions would feedback to the climate system, amplifying the warming. Permafrost thawing was described as a key process to the fate of the planet at the 2012 Doha climate conference.

How fast this carbon will be released and under what form is highly dependent on snow cover, soil temperature, and soil moisture, methane being produced in waterlogged soils. In order to correctly represent climate change effect in the high latitudes a climate model has to correctly represent the processes leading to the emissions of CO_2 and CH_4. Until recently, ISBA the land surface model of the CNRM only represented the exchange of energy, water and CO_2 between the soil, vegetation and atmosphere. CH_4 emissions were not taken into account. We built a new soil organic carbon model that represents the vertical dynamics of soil organic matter (including advection and cryoturbation) and the decomposition processes releasing CO_2 and CH_4 as a function of soil temperature, soil water and ice content, soil oxygen content and snowpack evolution. The model also represents the diffusion of these three gases in the soil. It was validated on two well-instrumented sites in Greenland and one site in Siberia. Model results indicate that the amount of carbon stored in the soil plays a crucial role in the rate of emissions besides the physical parameters as soil temperature and water content.

6

Aqui-FR, the future hydrogeological French modelling platform

The Aqui-FR project aims at producing groundwater levels and river flow forecasts at time scales ranging from 10 days to the season, and up until climatic projections. It is based on existing hydrogeological models already used by stakeholders, and favours their development was the still lack. That way, the Aqui-FR project is designed as a promoting tool of the hydrogeological works carried out in France.

The first phase of the project led to the consolidation of the structure of the platform and its scientific validation through the calculation of performance scores related to the groundwater levels and river flow reproduction. The exploitation of the platform started, and an historical reanalysis of the groundwater levels from 1958 to 2017 (period of atmospheric reanalysis SAFRAN) was undertaken over the current covered domain.

In order to compare the filling of the aquifers over space and time, the SPLI (developed by the BRGM consistently with the SPI) is used. It gives qualitative information, spread throughout 7 classes, of the groundwater level relative to its history (see figure). The temporal evolution over the whole domain as well as its spatial distribution of the SPLI during two extreme events is represented on the figure as an example.

The next phase of this project, along with the inclusion of new regional models, is going to focus on seasonal forecasts and the study of the benefits of aquifer modelling in terms of reliability with a spatial focus on low flow forecast (both for river flows and groundwater levels).

7
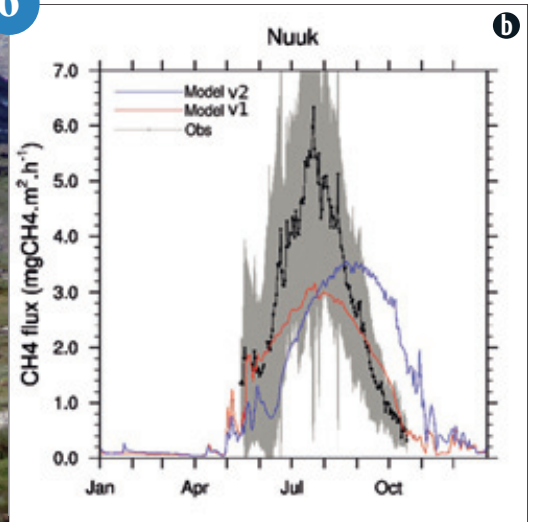
a: July 2017 view of the Kobblefjord fen measuring site in Greenland (operated by University of Aarhus and the Danish Centre for Environment and Energy).
b: Seasonal evolution of the methane flux observed (black curve) and simulated by 2 versions of ISBA (blue and red curves).
The grey surface represents the dispersion between the 5 soil chambers.

Temporal evolution of the Standardized Piezometric
Level Index over the Aqui-FR domain as well
as its spatial distribution during a dry period in 1973
and in a wet period in 2001
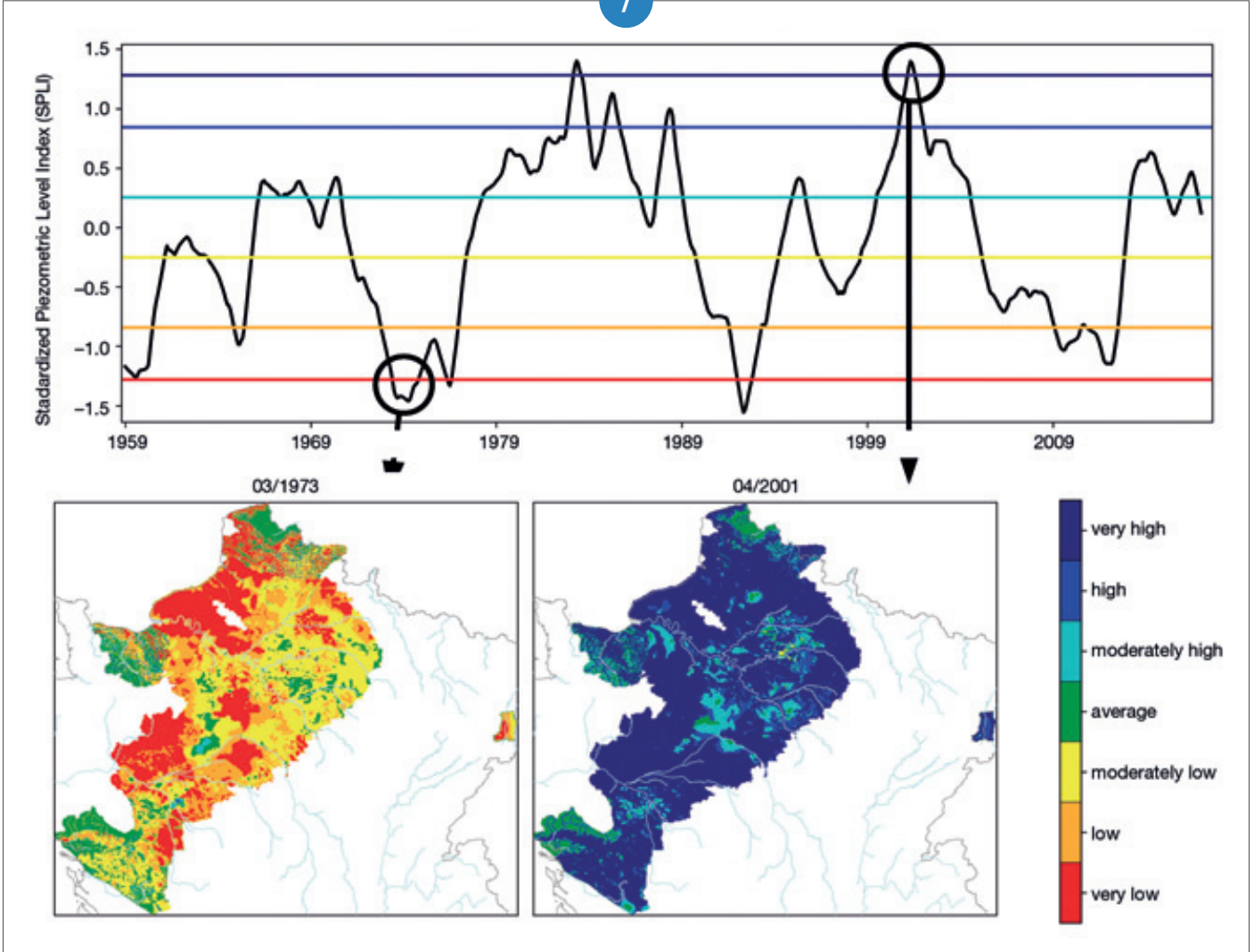
Oceanography

Understanding the finest processes that govern the "Earth system" (The atmosphere, its surrounding components, the ocean being the primary one, and their interactions) is critical. Implemented in advanced numerical models, they drive the operational team progress and contribute to the improvement of deliverables.

As an example, it is noteworthy that taking aerosols into account brings better sea surface temperature retrieval from satellite data, therefore improve the forcing from the ocean to the atmosphere. Similarly, introducing realistic river plumes representation triggers slightly different air-sea interactions. Combining waves and sea level height, namely in case of a storm or cyclonic surge, possibly adding a lagoon, modifies the impact of the ocean on the coastline.

Albeit the methodology still relies on extracting valuable information from the comprehensive observing systems, in situ and remote sensing, and exploiting numerical models, progresses are introduced year after year. Models are continuously improved in order to represent more detailed features and be more realistic and useful. They are validated against the more severe cases that were ever recorded. The February 1953 storm in the North Sea, that led to catastrophic losses in England and the Netherlands stands at the forefront in mid-latitudes. The cyclones that hit the French West Indies in 2017 will play the same role for scientists.

Since the creation of meteorological services, meteorologists and scientists are concerned by what occurs at sea and work hard to improve knowledge and services. They serve all the ocean users, having security in mind, not-forgetting the improvement of activities and economy: Shipping, fishing, industries, or leisure, off and along the shore, in overseas territories and in the mainland. Desert dust, like a grain of sand interfering with the complex Earth mechanism, is also part of the game. A surprise, may be?

1

New operational coastal model for wave forecasting in Reunion Island and Mayotte

Since the end of 2015, the second phase of the project HOMONIM aims to improve the storm surge and waves forecasting in coastal areas of the French overseas. The project is conducted by Météo-France and SHOM, and supported by the French ministry of Ecology (MTES). A first configuration of the coastal wave model WaveWatch 3 (WW3) has been implemented last year in West Indies and Guyana. In November 2017 the coastal wave models for Reunion Island and Mayotte in the Indian Ocean has been implemented in operations.

The configurations in Indian Ocean use a new coastal bathymetry with 100 meters of resolution, which has been produced by SHOM in the framework of the project. Several parametrisations related to the source terms of the model, and in particular the bottom friction, have been evaluated during recent extreme events. Dangerous sea state mostly caused by cyclones conditions such as Felleng case (category 3) during January 2013 (see figure). The first domain covers Reunion Island and Mauritius Island, while the second domain is dedicated to Comoros archipelago. These two coastal systems are driven by the surface winds provided by the atmospheric model AROME for the overseas with grid resolution of 2.5km. The resolution of the coastal model WW3 reaches 100 m in the Mayotte lagoon, which is good enough to describe the wave features in the channels. For Reunion Island, the resolution reaches 200m near the coastlines.

Specific work for the lagoon of Mayotte will need more testing related to sea level and currents forcing from the surge model dedicated to this domain. This latter will be implemented in mid-2018 with a resolution of 200 m. In addition the coastal wave models will be calibrated and evaluated during more events.

2

Storm surges Forecast for Indian Ocean and West Indies-Guyana

In the framework of the HOMONIM project, managed by Météo-France and SHOM, with the support of DGPR and DGSCGC, two storm surges models (Hycom2D), one for the SW of the Indian Ocean, the other for a domain going from the Lesser Antilles to French Guyana, were developed and then installed in the operational suit at Météo-France in 2017. The mesh size of these models is 3.2 km for the Indian Ocean, 2 km for the Guyana coast and 900 m for the Lesser Antilles.

These models were calibrated to reproduce at best, the tides and several extreme events (hurricanes mostly). The most difficult task was to get storm surges measurements: tide gauges are rare and sometimes destroyed when hurricanes pass near. When the Irma Hurricane hit the north of the Lesser Antilles the 6th September 2017, a storm surge of around 2 m was measured at Marigot on the St Martin Island. The storm surge model, driven by the high resolution atmospheric model AROME, simulated a storm surge of 1.70 m (see Figure).

The future work on these models will be directed to the use of the bathymetry which has been recently updated by the project, and to the validation on new and better described events. Moreover, for the Mayotte Island, which presents a large lagoon, nested models will be implemented in 2018 to reach a grid resolution of around 200 meters.

3
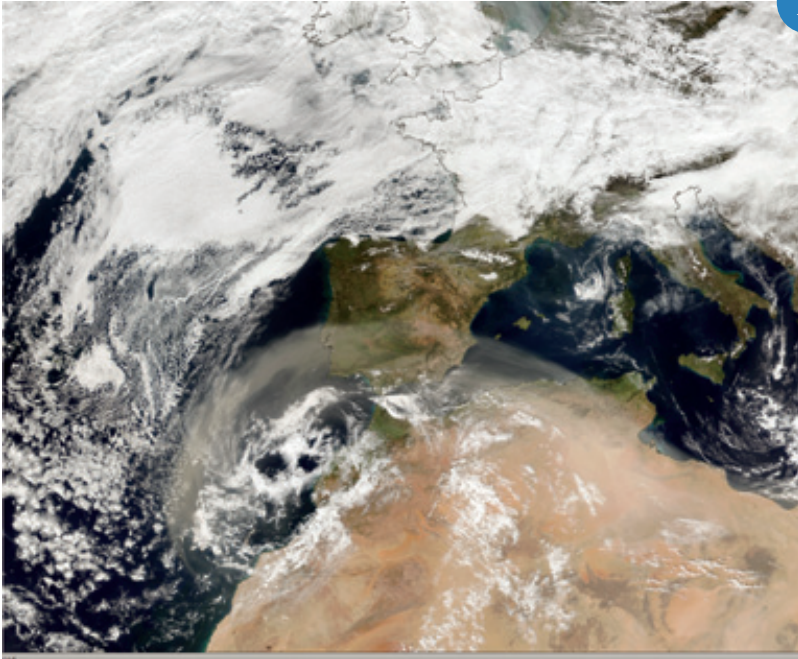
Saharan dust is transported by the storm over the Atlantic Ocean and the Mediterranean Sea.
21st February 2017, 1325 UTC,
Suomi-NPP
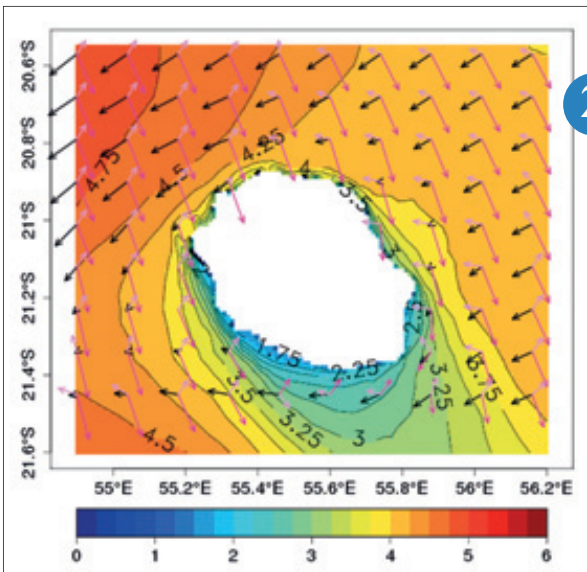
Significant wave height of the total sea (in meters) of WW3 on 31 January 2013 at 18:00 (UTC) in Reunion Island during Felleng hurricane (category 3)
Dark violet arrows describe the direction of primary swell, light arrows the secondary swell and black arrows the wind sea.
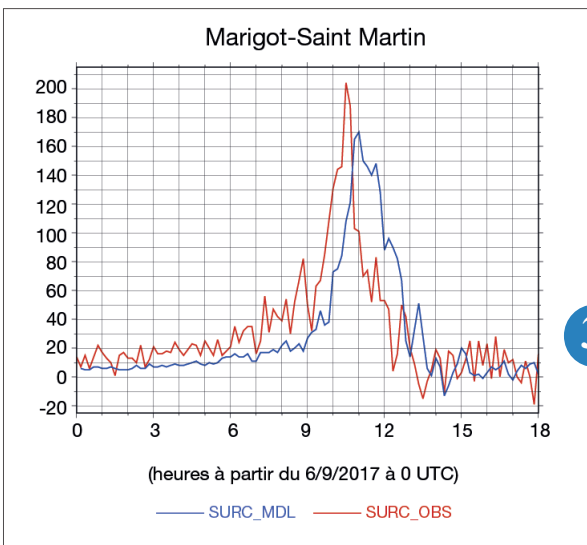
Comparison between the measured (red line) and the modelled (blue line) storm surge at Marigot (in the north of Saint Martin in the Lesser Antilles) during the Irma hurricane path, the 6th September 2017.
The storm surges model is driven by the wind and the atmospheric pressure from the AROME model of Météo-France.

Improvements of the global wave model for open oceans

In the frame of the Copernicus Marine Environment and Monitoring Service (CMEMS-MFC), Météo-France has implemented a new version of the operational wave model MFWAM at global scale. The improvements brought by this upgrade concern first a better resolution of the computing model grid reaching 10 km of resolution and the use of the surface currents provided by the Mercator PSY4 ocean forecasting system with a daily update. The impact of the currents is significant in strong currents area, where the difference of wave height induced by the currents can reach 1 meter, as illustrated in figure a for the Agulhas ocean region.

In addition, the physics of the MFWAM model has been adjusted in order to improve both the description of stress at the air-sea interface for strong winds and a better prediction of high frequency waves. In other respects the assimilation system is updated by using the directional wave spectra provided by the Synthetic Aperture Radar (SAR) of the Sentinel-1A and 1B satellites that are part of the Copernicus space program. With this achievement Météo-France consolidates its leading position in the assimilation of SAR wave spectra. The impact studies have shown that the assimilation of SAR wave spectra significantly improves the directional proper-

ties of swell, with a remarkable reduction of normalized scatter index of the peak period of long waves (larger than 200 m of wavelength) which can reach 20%.

The upgraded operational MFWAM system will also use the altimeter wave heights (Level 3) of Sentinel-3A, which are provided by the Thematic Assembly Centre for waves (TAC-waves) of CMEMS. The combined assimilation of the altimeters data and SAR wave spectra induces globally a normalized scatter index of significant wave height of roughly 8-9% as indicated in the figure b.

④

New ocean model configuration and improved runoff representation for coupled ocean-atmosphere prediction

The Mediterranean Sea plays an important role on the heavy precipitating episodes that frequently affect the region. The large and sudden supply of fresh water from rivers floodings contributes significantly to the water cycle and can influence air-sea interactions.

During the HyMeX first field campaign in fall 2012 (SOP1), numerous observations were collected, including daily and hourly runoff observations. Such dataset allows to better represent the flood peaks and so their impacts on the ocean circulation and stratification.

A new configuration of the NEMO ocean model, named NWMED72, covering the north-western Mediterranean area with a horizontal resolution of ~1.3 km, has been developed and used to study the sensitivity to the runoff representation. Forced in surface by the AROME-WMED real-time forecasts and three sets of river forcing (climatology, daily and hourly observations), ocean simulations show the impact on plume size and surface salinity, which is lower around the plume when observations are used (figure). The stratification is significantly modified locally and the mixing layer becomes thinner, resulting in a stronger

oceanic response to atmospheric forcing that impacts the surface temperature. Diagnostics are also being developed to assess the impact on circulation near the mouths and coupled ocean-atmosphere simulations with the AROME-NEMO system will allow to examine the impact on the prediction of Mediterranean heavy precipitating episodes.

⑤

Processing of old maritime events: the numerical WW3 model goes back in time

For quite many years, the technique and the computation capacities make it possible to re-analyse meteorological events from the past by using modern and operational modelling systems. This method can also be used to re-analyse maritime events. It consists in simply running a very high resolution wave model (here WW3) using the best atmospheric forcing available for a given event.

In this case-study processed by the operational marine forecasting service, we were interested in the dramatic episode of February 1, 1953 which has ravaged the South of the North Sea and more particularly the Netherlands and Belgium. This violent and long-lasting north-western storm occurred during a period of strong tides which greatly increased its coastal impacts.

After verification of the relevance of the atmospheric forcing, provided by the project INCREO at 0.1° resolution, we were able to analyse the outputs of the WW3 model. These outputs have highlighted strong, unusual, short-period waves, mainly coming from the northwest over the southern North Sea area. Thanks to its high resolution and the use of a very fine bathymetry, the WW3 wave model well reproduced the waves near the shore. Focus on short areas has shown realistic unfurling waves on the sandy shoals that dot shallow areas.

⑥

4
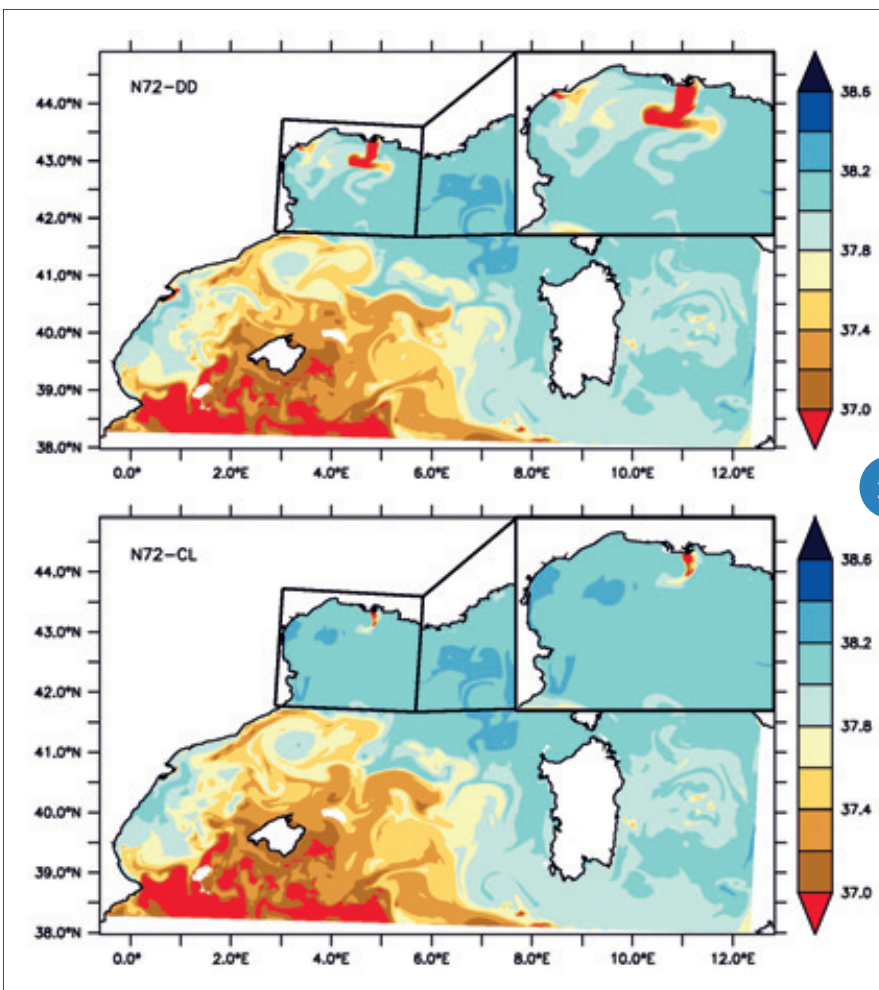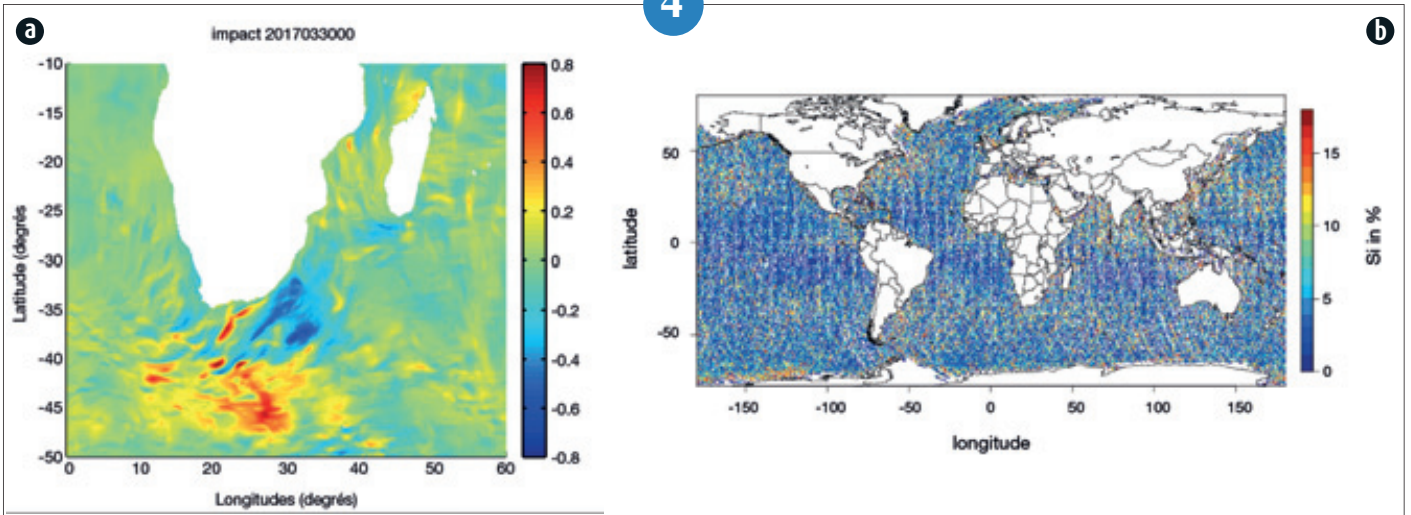
a: Difference of significant wave heights
from runs of the wave model MFWAM with
and without surface currents from the ocean system PSY4
on 30 March 2017 at 0:00 UTC.
b: Global map of scatter index of significant wave heights
from the upgraded MFWAM system for March 2017
The validation is performed with altimeters wave heights
from the satellite Hy-2A.

5

Surface salinity (psu) in the North-Western Mediterranean basin
simulated the 14 October 2012.
The use of observed daily runoffs (N72-DD) improves
the representation of the plume of the Rhône river
and produces additional plumes as those of the Orb
and Aude rivers, both absent in the simulation using
a monthly climatology (N72-CL).

6
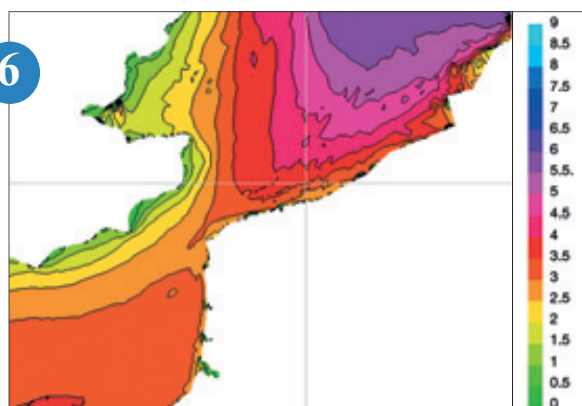
February 1, 1953 - Simulation of H1 / 3 (in metres)
by the WW3 Météo-France model - zoom around
The Pas-de-Calais.

Sea Surface Temperature: a reprocessing of Meteosat Second Generation archive

SEVIRI instrument on board MSG satellites is operating in thermal infra-red domain thus enabling SST retrieval; it is operational since January 2004. The Centre de Météorologie Spatiale is contributing to OSI SAF project funded by EUMETSAT, and as such has reprocessed the SST from MSG/SEVIRI archive from 2004 to 2012. The final product is delivered in the form of hourly synthesis on a 0.05° grid.

SST is computed using a non-linear split window algorithm and brightness temperature at 10.8 and 12.0 μm. Coefficients are determined by regression using simulations of brightness temperature, the algorithm is then de-biased against drifting buoy measurements.

Regional and seasonal biases, mainly due to variation in atmospheric water vapour content, are removed by a bias correction scheme. It relies on atmospheric composition profiles from ECMWF1 reanalysis and a radiative transfer model.

Saharan dusts in the atmosphere do have an import impact on SST retrieval and are taken into account. A Saharan dust index is computed from the 3.9, 8.7, 1.8 and 12.0 μm channels; it enables correcting SST and/or downgrading the pixel-wise quality level in the final product.

The reprocessing has been validated in detail with drifting buoy measurements. The results show that the product is of high quality (mean global bias: -0.02°C; standard deviation: 0.43°C) with a very good temporal stability. The reprocessing dataset is of high interest for long term analysis of highly variable phenomena in time and space such as thermal fronts or diurnal variability of the SST.

7
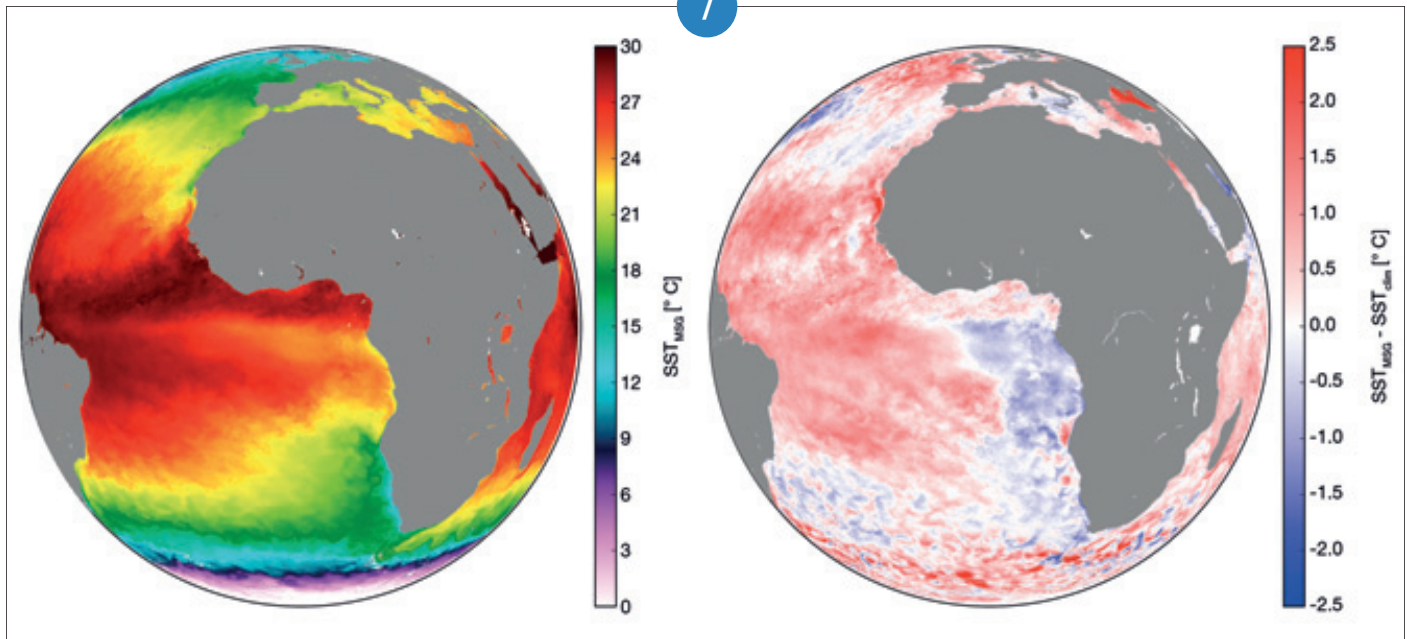
▲
June 2010: on the left, night-time monthly mean SST from the MSG reprocessed data; on the right, monthly mean difference to a climatology of the OSTIA re-analysis from 1985 to 2007.

Campaigns, observation engineering and products

Observing the atmosphere is a prerequisite to improving our understanding of its processes and the way they are simulated by numerical models. This is why research in atmospheric sciences conducts often field campaigns (such as ReNov'Risk for tropical cyclones, Cerdanya-2017 for small-scale, low-level dynamics in mountainous regions, or AEROCLO-SA for aerosols and clouds), or maintain observatories to assess the quality of models on the long run (for instance, the evaluation of surface meteorological parameters and surface exchanges predicted by ARPEGE or AROME with Météopole-Flux) and detect their limits to be overcome by new research studies.

The need to improve models calls for the development of new observations techniques, either new sensors (for instance the development of new air quality sensors tested with a balloon sounding system that allows the recovery of the payload), or new processing techniques that allow the production of new, finer, well-characterized parameters (for the precision of rainfall estimates from weather radars).

Last but not least, observations are a key element of weather prediction systems. Through the assimilation of data from operational observation networks (such as IAGOS), they are used to determine the initial state of the model prediction, the quality of which has a direct impact on the quality of the prediction. Or they can be processed directly by statistical methods for short-term predictions (of cyclones in the Indian Ocean for instance)

1

◄
BASTA cloud radar

Campaigns

Improve understanding and prediction of the cyclonic activity and its impacts in the South-West Indian Ocean: the SWIO-TC Experiment

Tropical cyclones (TCs) may cause huge human, material and environmental losses in tropical and subtropical regions. This is particularly true in the southwest Indian Ocean (SWIO) basin, a poorly studied region that experiences a cyclonic activity roughly as intense as in the North-Atlantic basin. Over the last decades, a large number of storms have indeed caused devastations in the Mascarenes (Mauritius, Reunion Island), Madagascar, Mozambique and other neighbouring countries. In March 2017, TC Enawo and Dineo caused for instance hundreds of fatalities and more than one million refugees in Madagascar and Mozambique, respectively.

The ability to collect high quality observations within and around TC is essential to improve their representation in new high-resolution NWP models currently being developed by most major weather services. This is all the more important in the SWIO basin where observations are extremely limited with, in particular, no routine aircraft observation and very sparse ground-based observation networks. In order to address this problem, the research program ReNov'Risk-Cyclones was funded by EU to reinforce permanent observation capabilities in this basin and to organize a 4-month field campaign dedicated to the study of TCs developing in this area.

This field experiment, referred to as the SWIO-TC Experiment, will be conducted in Jan-Apr 2019 by LACy and its numerous national and international partners (NOAA, SMA, DIROI, IFREMER, CNRS, BOM, ESA, CNES, ...) to better document atmospheric and oceanic impact of TC on inhabited territories of the SWIO basin. It will provide unprecedented observations of TCs and other high impact weather events developing in this basin by coordinating dedicated atmospheric and oceanic measurements in the Mozambique Channel and Mascarene Archipelago.
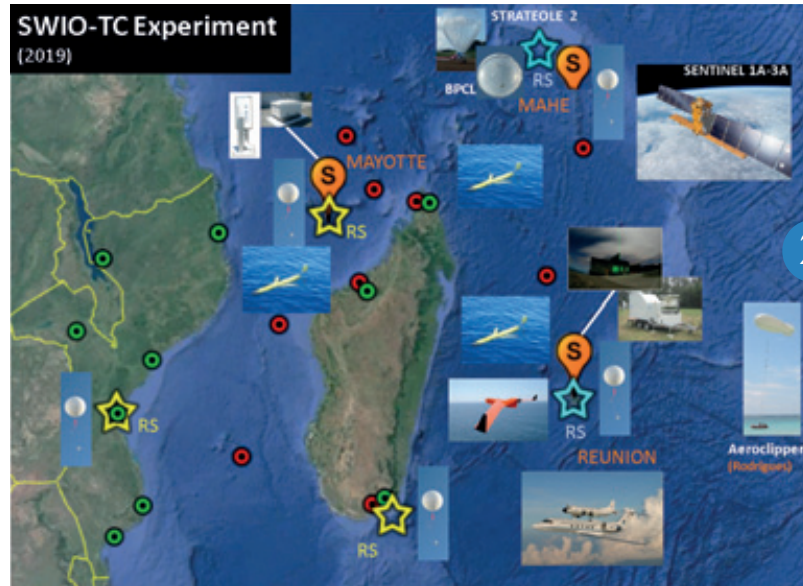
Overview of the experimental setup envisioned for the SWIO-TC Experiment (setup may evolve depending on available funding).

The Cerdanya-2017 field experiment: cold air pools, mountain waves and orographic precipitations

La Cerdanya is one of the largest, sunniest and driest valley of the Pyrenees mountain range, spreading across Spain and France (between Occitanie and Catalunya).

It is about 10 km wide and 35 km long oriented ENE-WSW, whereas most valley in the Pyrenees are oriented N-S, with a relatively flat bottom at about 1000 m above sea level and mountain ridge around rising above 2900 m.

The field experiment Cerdanya-2017 took place in this valley from October 2016 to May 2017, focusing on three meteorological phenomena: cold air pools, mountain waves and orographic precipitations.

It focuses in particular on the detailed inversion structure and the surface energy budget of cold pool, rotors and boundary layer separation in mountain waves situations, and orographic triggering and intensification of precipitations under stratiform and convective regimes.

It is a joint effort of several teams from the Euro-region Pyrenees-Mediterranean; these teams belong to the University of the Balearic Islands, the University of Barcelona, Météo-France and the Meteorological Service of Catalonia.

CNRM deployed ten scientific surface meteorological stations including one surface-atmosphere flux station, a panoramic video camera and several remote sensing instruments (UHF wind profiler radar, scanning Doppler wind lidar, microwave radiometer in collaboration with Laboratoire d'Aérologie). A CNRM UAV profiler was also deployed during intensive observation periods.

CNRM will in particular focus on cold pools. These conditions are still not well represented in NWP models, which leads to severe issues in forecast for associated phenomena such as extreme low temperature, road icing, fog, poor air quality, low level jets (wind energy)...

CNRM/GMEI - METEO FRANCE

3

PPI - 2016/12/30 23:17:46.00 UTC- Elevation 1.0

Vitesse radiale (m/s)
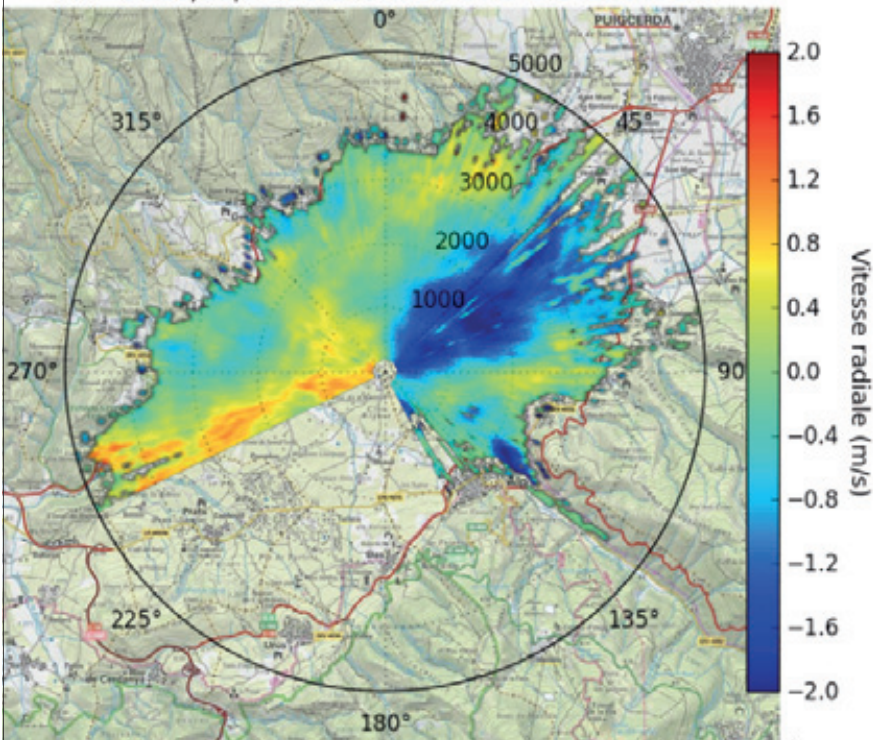
a: Picture of the main measurement site
(La Cerdanya Aerodrome) taken on 20 January 2017
from the tethered balloon and uavs take off platform.
The valley surface was covered by snow which allows to study
its impact on phenomena of interest, in particular cold air pools.
The control tower (wind scanning lidar) and several instruments
(meteorological station, microwave radiometer,
micro rain radar...) may be distinguished in the image centre.
b: Line-of-sight wind observed by the wind scanning lidar
located on the main measurement site (La Cerdanya Aerodrome)
over a quasi-horizontal plane on 30 December 2016 at 11pm.
Negative values (in blue) mean the wind is blowing toward
the image centre, positive values (in red) it is blowing away.
A down-valley wind is observed in the main valley axis
(ENE-WNW) as well as a down-valley wind in a tributary valley
(La Molina, in the SE sector). A study of the impact of these
flows on temperatures minima in the main valley is in progress.

A flying lab to study aerosols in Namibia for Aeroclo-sA project

The AErosol RadiatiOn and CLOuds in southern Africa project (AEROCLO-sA), supported by the French National Research Agency, the French Space Agency (CNES) and The French National Centre Scientific Research (CNRS), seeks to evaluate the interactions between aerosols, clouds and radiation in southern Africa, essential for constraining the current generation of numerical weather prediction and climate models, henceforth to understand their role on the regional climate and global climate. The representation of aerosol-radiation-cloud interactions remains among the greatest uncertainties in climate change, and new sophisticated data sets are needed. AEROCLO-sA is based on a ground and airborne campaign that took place in August-September 2017.

Within, the French Falcon 20 environmental research aircraft of SAFIRE (the French facility for airborne research, an infrastructure of Météo-France, CNRS & CNES)., has performed 10 scientific flights from based in Walvis Bay, Namibia. The aircraft was equipped with different remote sensing instruments, such as the high-resolution backscatter lidar LNG and the demonstrator, called Osiris, of the future 3MI polarimeter on-board EPS-SG , as well as in situ measuring instruments (drop-sondes, aerosol characterization). The Falcon 20 has completed more than 70 flight hours and thanks to the expertise of the French laboratories LISA, LATMOS, LOA, DT-INSU and CNRM many airborne data have been collected. Additional ground-based data were also produced thanks to the complementary participation of IRCELYON and LCE.

This airborne campaign has documented the interactions between aerosols and clouds and studied their impact on radiation. With the additional support of two projects funded by EUFAR (FP7), and the involvement of European researchers from Germany and Greece (TROPOS, NOA), it also provided information on regional sources of pollution such as biomass fires or desert dust Researchers will now analyse these data to improve the representation of aerosols in climate models, to reduce the uncertainty of the direct, semi-direct and indirect radiative effect of aerosols, and their impact on stratocumulus to improve remote sensing algorithms for clouds and aerosols.

Observation engineering and products

Development of statistical-dynamical tools for TC intensity prediction in the Southwest Indian Ocean

To support international efforts toward the improvement of tropical system prediction, operational intensity forecast errors for southwest Indian Ocean (SWIO) systems were examined over the 2001-2016 period at RSMC Reunion Island. Errors are significantly larger at short lead times for rapid intensification (RI) events, defined by a 24-h intensity change $\geq$ 15.4 m/s, with a mean 24-h forecast error of 10.8 m/s versus 4.9 m/s for non-RI events.

Statistical-dynamical tools of the same ilk as those developed in other basins have therefore been designed to improve the prediction of TC intensity change or RI at short range in the SWIO, based on the examination of a total of 26 potential predictors and the RSMC best track data over the 1999-2016 period. An important predictor is the Maximum Potential Intensity (MPI); it was formulated for the first time in the SWIO, based on the statistical relationship between maximum intensity and sea surface temperatures. The second tool developed is a multiple linear regression model for TC intensity change at 24 h based on a multivariate adaptive regression splines (MARS) technique that models nonlinearities and interactions between variables. Finally, a decision tree was built to anticipate rapid intensification in the next 24 h (see figure). These three tools will be used and tested in real-time during the next seasons; they shall offer further guidance to the practical intensity forecasts over the SWIO and help anticipate intensity changes at a short-time range.

Real time transmission of IAGOS data

Many ingredients are playing key roles in the atmosphere, for climate and weather: water, under its various phases, aerosols and chemical species. Greenhouse gases drive climate change, cities are heavily polluted: it is of the utmost importance nowadays to better understand this alchemy. IAGOS (*In-service aircraft for a global observing system www.iagos.org*) aims at measuring these ingredients from civil aircrafts. IAGOS stands as one of the major European climate research infrastructure.

The companies associated to IAGOS – Air France, Lufthansa, China airlines... and recently Hawaiian airlines – operate Airbus A340 and A330 all across de world. Aircraft gather valuable profiles during take-off or landing, but also in flight when they cruise around the critical interface between the upper troposphere and the lower stratosphere.

Air quality is a major challenge. In order to face it, Met services run global and local chemical forecasting models, like Mocage at Météo-France used for the European "Copernicus Atmosphere" programme or the French national Prev'Air initiative. Getting the IAGOS data in real time to improve such systems logically became an obvious objective.

CNRM has installed on board of the Lufthansa A340 D-AIGT a satellite transmission facility. Profiles are now sent in real time to ground, as soon as they are acquired. Reduced profiles are transmitted, the full profiles being kept for delayed processing: They better suit the vertical resolution of numerical models and the transmission costs are more affordable. This simple improvement of a research system for the benefit of operational needs is an example of mutual support between Met services and the Academia. Having in mind the ultimate end users, our citizen!

◄
"Ocean" of biomass fire particles overhanging
Namibia, the huge amount of aerosol makes it
impossible to see the surface.
The aerosol optical thickness is from 1.5 to 500 nm
in Windpoort (north of the country).
Copyright : F. Blouzon, DT-INSU/CNRS

3
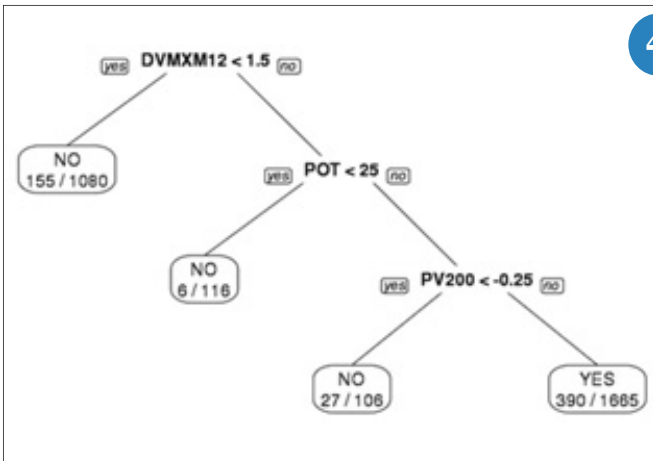
4

◄
The decision tree for the prediction of rapid intensification (class label YES)
in the next 24 hours, based on the values of 3 predictors:
DVMX12 (the previous 12-h intensity change, in m/s),
POT (the Maximum Potential Intensity MPI minus the initial intensity, in m/s),
and PV200 (the 200-hPa potential vorticity averaged in a 200-800-km region
surrounding the storm center, in PVU). The numbers in the leaf nodes indicate
the misclassified samples and the total number of samples from both classes
fulfilling the conditions of each tree path.

5

▲
a: The Real Time Transmission Unit (RTTU) is a gateway between the IAGOS system
and the on-board Satcom telecommunication system.
b: The IAGOS system and the Real Time Transmission Unit (RTTU)
are located in the technical hold. The Lufthansa Technik electrician
carefully follows the specifications for modifying the electrical wires connecting
the RTTU to the Satcom (Satellite communication).

Météopole-Flux: long term measurements to improve modelling of surface-atmosphere exchanges

The measurements system Météopole-Flux has measured continuously heat, water vapour, and CO_2 fluxes between surface and atmosphere, vertical temperature and soil moisture profile, and common meteorological variables, at the experimental field of the Météopole since 2012.

These long term measurements are especially interesting to evaluate in a systematic way the physical parametrization of the numerical models. In 2017, we compared the measurements with surfaces variables from AROME and ARPEGE models while a whole year. The air temperature and humidity at 2 m are well reproduced by the models, but we found significant and systematic differences with the terms of surface energy budget. Going further in data analysis and in particular comparing soil measurements profile, will contribute to improve the representation of surface processes in numerical weather forecast models. This station is also integrated in national research networks: the research infrastructure ACTRIS-France, and ICOS-Ecosystem-France (as associated site). Collaboration with the flux working group of ACTRIS-France enables a standardization of turbulent flux processing with other sites (SIRTA, and P2OA), and shared scientific analysis.

In 2018, the number of measured variables will be increased by means of collaboration with Direction des Systèmes d'Observations of Météo-France which has other complementary sensors close to the experimental field.
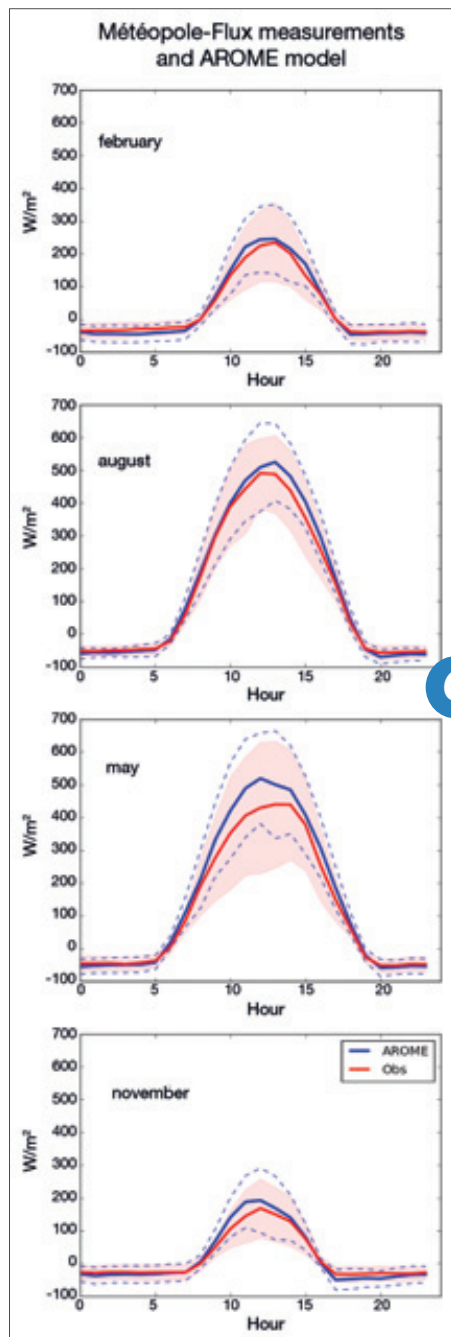
◀ **6**

Monthly meanwhile 2016 year of diurnal cycle of heat fluxes sum measured by Météopole-Flux station (red curve), and produced by AROME model (blue curve). Red shadowed area: standard deviation of measurements. Blue dashed line: standard deviation of model. Measurements enable to highlight a model bias during May.

Recoverable sensors under free balloons

Since 2011, 4M team has developed new lines of flights free balloons, used conventionally for radiosonde, with dual-balloons or parachutes to recover the embarked sensors to allow their reuse to frequently measure the thermodynamic parameters in situ of the atmospheric boundary layer at altitudes up to 30 km.

Today, 4M team is able to realize in the atmospheric boundary layer "high frequency profiling", measured at the ascent and descent, dual-balloons with recovery and immediate reuse of radiosondes (BLLAST 2011, PASSY 2015) with a recovery rate greater than 85% (Fig. a).

4M team also conducts surveys up to 30km under parachute using retractable nacelles that can carry innovative sensors with high added values, such as sensors measuring CO2 and CH4 greenhouse gases, (GSMA Reims collaboration: AMULSE 2013, APOGEE 2017) weighing less than 4 kg.

Technical developments are continuing to improve the delivery systems (dual-balloons separator) or to develop specific parachutes. A profiling simulation interface was also developed, within 4M team, to improve the trajectory forecasts to recover the platform on the ground. Data from the ARPEGE and AROME wind fields (Fig. b) are used as well as in-situ data (radiosonde, wind profiler ...).

7

▶ **7**

a: Release of a recoverable radiosonde with dual balloons during the BLLAST 2011 campaign.
b: Sample simulations of dual-balloons recoverable radiosondes during the PASSY 2015 campaign

Use of ensemble methods to characterise radar quantitative precipitation estimation (QPE) uncertainty

Radar Quantitative Precipitation Estimation (QPE) is increasingly being used in meteorological applications: nowcasting, hydrological hazards, data assimilation, etc. Radars can provide higher temporal and spatial resolution observations of rainfall than rain-gauges. However, radar based quantitative precipitation estimation is affected by uncertainties due to measurements errors and retrieval errors. An increasing demand from users is to have access to a quantitative estimation of the quantitative precipitation estimation uncertainties. This need is all the more important that the horizontal resolution of the radar data will increase.

In order to characterize uncertainties and correct the bias, a stochastic method generating ensemble QPE has been developed at Météo France. This method uses a statistical model of precipitation error variation (one hour cumulation) function of various parameters (precipitation type and intensity, position of the observation relatively to the radar, etc.). The ensemble median gives an estimation of the precipitation measured by radar corrected from the usual bias. The ensemble dispersion gives an estimation of the uncertainty associated to the deterministic QPE.

In the future, the use of these methods has to be extended to five minutes accumulations precipitation in order to respond to the users' needs concerning the temporal component of the uncertainties variations.

8

Ensemble generation to quantify QPE uncertainties.
▼
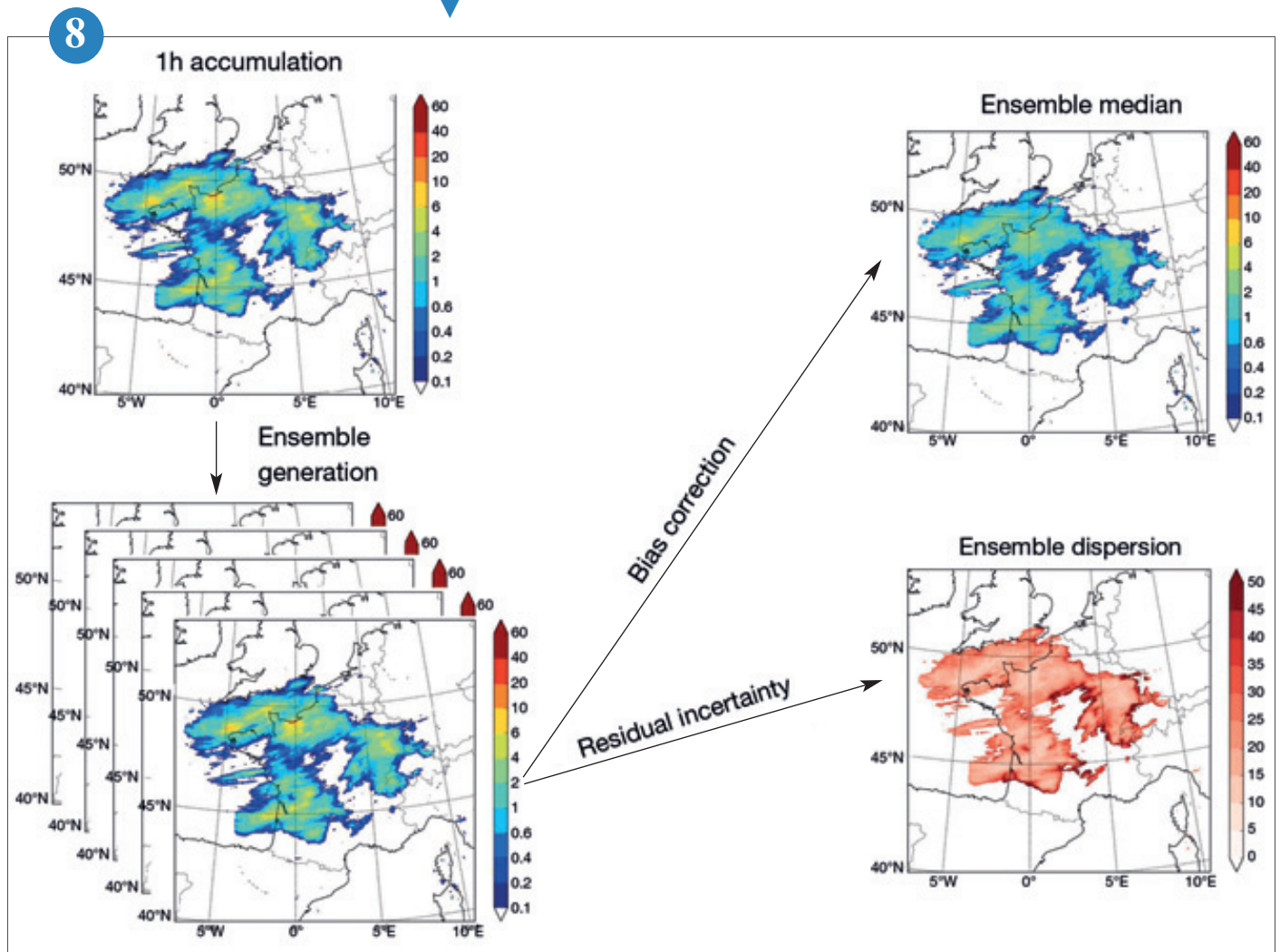
Research and aeronautics

Air traffic growth observed today and foreseen on the 2030 horizon as well as main objectives driving global or regional air navigation plans necessitate a continuous involvement and progress on research on meteorological phenomena with impact on aviation. Thus, Météo-France strengthened its activities for the simulation of turbulence in altitude, and for monitoring and forecast of icing and wind shear, focusing in particular on the approach areas around airports as precursors to future meteorological services for the terminal area in response to foreseen ICAO requirements. In parallel, SESAR projects for the deployment of new innovative MET services, such as those developed and mocked-up during the first part of this European program were launched with a strong involvement of Météo-France.

In 2017, focus was put on functional and technical specifications as well as drafting organization principles and architecture design towards a production effectively harmonized over Europe. Furthermore, activities of the research aircraft unit were focused on air navigation safety through experiments of new on-board equipment. Finally Météo-France had the honour to host the second WMO Aeronautical Meteorology Scientific conference (AeroMetSci-2017) in November at its International Conference Centre. First edition since 1968, attendance reached more than 200 persons coming from many National Meteorological Services and research institutions, from the aviation community (airlines, air navigation service providers, industry, airport managers) and from regulating organizations. Three main themes were presented through orals and poster sessions: research and science in aeronautical meteorology (ice crystals, turbulence, fog, volcanic ash, space weather), users' need and the future service to air navigation, and climate change and its impact on aviation. Expectations of WMO, Météo-France and participants in terms of expertise and knowledge sharing and networking were amply met, and it allowed elaborating recommendations and guidelines for the future in aeronautical meteorology science and research.

1

Use of observed and forecast EDR
for upper-level aeronautical turbulence detection

Turbulence is a dangerous phenomenon for aeronautics. It induces significant costs for airlines due to passengers and crew injuries and damages on airplanes. Moreover the quick spread of events on social network can be generator of negative images for airlines. Observation of turbulence events is based on reports of pilots and EDR (Eddy Dissipation Rate) registered on board. More and more aircrafts are equipped with sensors measuring EDR which allow to build a database of observed events.

For the first semester of 2017, two databases of on board EDR, one over United States and the other one over Europe are analysed (climatology, sensitivity) and compared to pilot reports. It can be noticed that 1% of moderate or severe events are observed over Europe during this period (ICAO Meteorology Panel 2017 criteria, moderate > 0.2 $m^2/^3s^{-1}$). These databases are used in the evaluation of EDR issued by the French numerical weather prediction (NWP) model ARPEGE, as well as in the evaluation of the operational turbulence diagnoses used at Météo-France with different vertical resolutions. It is noticed that EDR from the model has similar skills compared to the other diagnostics. We notice also the positive impact of a best vertical resolution for actual diagnoses. Some case studies complete the verification to explore forecast EDR particularities compared to the other diagnoses (see figure b).

2

Wind shear detection on airports: an experiment
at Clermont-Ferrand Aulnat airport

In the fall of 2017, DSO/DOA has started an experiment on the detection of wind shears on the airport of Clermont-Ferrand with a UHF wind radar. The experiment will last until spring 2018. The UHF profiler has been modified in order to be able to make wind measurements along the air strip at a low elevation.

The challenge is to still be able to measure the wind in spite of the string surface echoes. For the validation of the solution, a scanning Doppler lidar was deployed by CNRM/GMEI. It will serve as a reference. The lidar explores the wind with one azimuthal scan at low elevation (2.5°) followed by 4 vertical scans in four directions including the air strip axes. The whole exploration cycle is repeated every 10 minutes. The maximum range of the lidar is 4 km to 5km depending on the atmospheric conditions.

Several interesting wind shears have already been documented (see figure). The winds measured by the lidar and the radar in the same directions will be systematically compared in order to validate radar measurements as well as its capacity to detect and characterize wind shears. If proven, this capacity will make the UHF radar an all-weather sensor for wind shear detection on airports.

3

AeroMetSci-2017: WMO Aeronautical Meteorology Scientific conference, 6-10 November 2017, Météo-France, Toulouse (France).
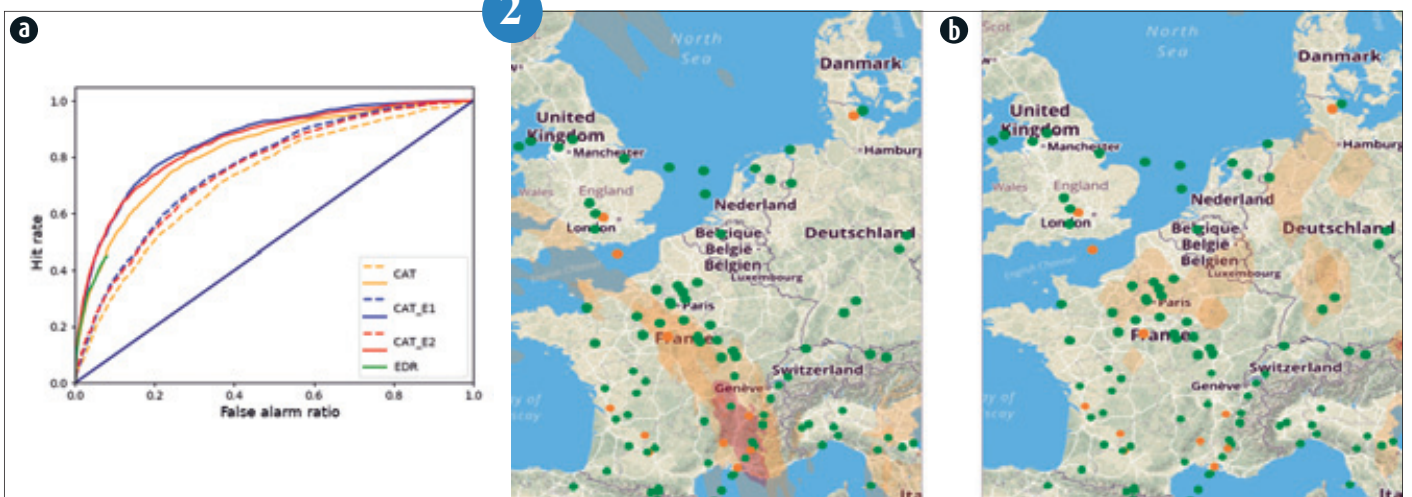
a: ROC curves of EDR and operational Météo-France turbulence diagnoses over Europe based on NWP model ARPEGE with a grid resolution of 0.1° (solid line – vertical resolution ~ 1 km / dotted line ~ vertical resolution ~ 2 km).

b: Situation 5th march 2017 at 06UTC. On board EDR between 04UTC and 08UTC is plotted (green dots = NULL/LIGHT, orange dots = MOD) above turbulence diagnoses calculated from ARPEGE model – run 00UTC / lead time 06h. Left figure: Dutton turbulence diagnosis. Right figure: EDR from the model. Filled contours (orange = MOD, rouge = SEV).

Different turbulence areas are identified (ex : South of France with the Dutton diagnosis – jet diffluence, North Germany with the EDR from the model – jet outlet in front of a thalweg).
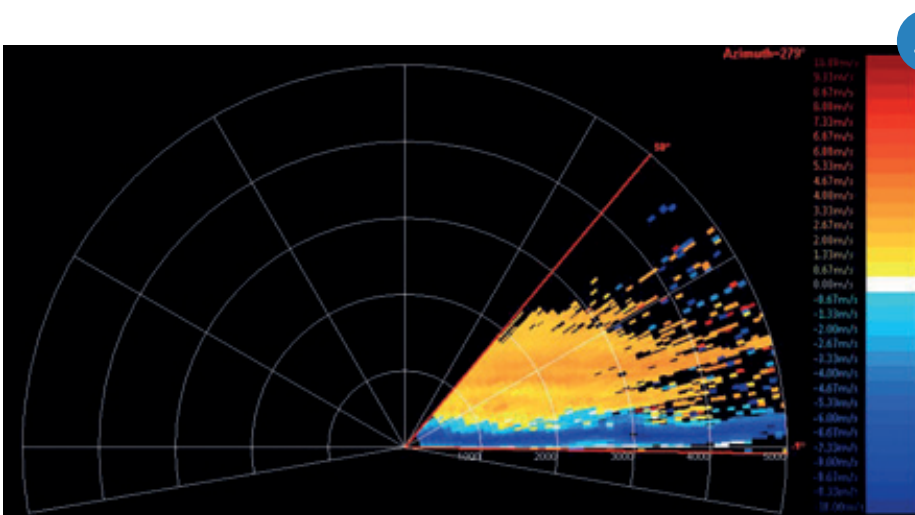
Line-of-sight wind component measured by the lidar in a direction perpendicular to the runway of Clermont-Ferrand airport (azimuth 145°) Warm colors indicate a wind blowing from the North, cold colors are for winds blowing from the South. A string wind shear is visible about 250m above the surface with 10 m/s winds from the South below and 3 m/s winds from the North above.

Flight test of new equipment for air safety

Today, the emergency beacon of aircraft is turned on either automatically by a crash or manually. It often happens that the beacon and its transmission system are damaged during the crash and/or that environmental conditions do not permit a correct transmission; when rescue units search for a missing aircraft, the distress signal cannot be received.

Automatically triggering the distress beacon in flight and as soon as an anomaly has been detected, could permit to record the successive positions of the aircraft in flight and then help to localize the impact area with a greater accuracy. This would enable quicker and more efficient rescue operations and it would increase the chances of recovering survivors. This concept is named Autonomous Distress Tracking (ADT) and is a part of the Aeronautical Distress and Safety System (GADSS) of ICAO. The GRICAS project is funded by the European agency for GNSS (GSA) through the Horizon 2020 program. It consists of various firms and public agencies among which Thales Alenia Space (TAS), the project coordinator. GRICAS aims to develop an end-to-end demonstrator of a distress system that complies with ADT requirements and based on the Medium-Earth Orbit Search And Rescue (MEOSAR) system of COPAS-SARSAT. Additionally, GRICAS operational concept includes the possibility to trigger the distress beacon remotely via the Galileo satellite Return Link: a command of activation is sent to the beacon of a non-cooperative aircraft so it can be tracked in flight (typically the MH-370). The leaders of the project asked SAFIRE (Service des Avions Français Instrumentés pour la Recherche en Environnement), a joint service unit of Météo-France/CNRS/CNES) to test this demonstrator which incudes in particular a new emergency beacon ELT(DT) (Emergency Locator Transmitter for Distress Tracking) during in-flight field trials onboard a twin-jet. The SAFIRE Falcon20 has been especially modified for science and for research and development purposes; it is an ideal platform for this kind of test flights as well because of its flight performance as by its versatility. It already has an antenna for the satellite positioning system «Galileo» and many available slots on its fuselage to integrate a VHF SAR antenna. Various types of equipment permit to record very accurately parameters of its environment or its trajectory. In 2017, Safire has embedded the prototype in its jet in order to fly the third test of the project.

By its involvement in the project and beyond its mission of supporting scientific research in environment, SAFIRE clearly shows its ability to contribute, through aeronautical R&D, to important issues of our society such as the enhancement of air traffic safety.

4

SAFIRE ATR 42, a platform for navigation system readjustment assessments

The position and attitude of an aircraft use an instrument called "inertial system" (INS). The data from such instruments are provided in relation to terrestrial reference systems. The alignment phase of an INS is essential. This is the moment during which it will create its reference axes (horizontal plane and vertical). An inertial unit consists of 3 gyrometers and 3 accelerometers for measuring angular velocities and linear accelerations. The technologies used have changed in recent years. The accuracy of the INS reaches 0.01 degree on the heading, roll or pitch. The position of the INS is computed by integrating the sensors outputs that are affected by errors that induce a drift of the inertial unit. To reduce these errors, also due to the rotundity of the earth, we can use GPS data (American positioning system, or GLONASS and soon GALILEO), we speak of hybridization. In space, the satellites are positioned in their orbit (orientation along the trajectory) using the position of the stars. The purpose of the experiment conducted in collaboration with the DGA is to use the direction of the stars to recalibrate the data of the inertial units in broad daylight. Thus an INS, already autonomous material, would be corrected for the drift error by hybridizing it with a stellar viewfinder. The challenge is to detect and then track the stars in aeronautical flight conditions day or night to readjust the inertial system. During recent flights, a camera architecture developed by CNES (Daytime Visor MIRA) has made it possible to demonstrate that an innovative concept of a daytime viewfinder is capable of acquiring and tracking stars during daytime - a first in France! The tests, of a total duration of approximately fifteen hours, were carried out at various times of the day in order to test several luminous environments according to several flight scenarios. Further tests will be held end of 2017 to test other hybridization methods.

5
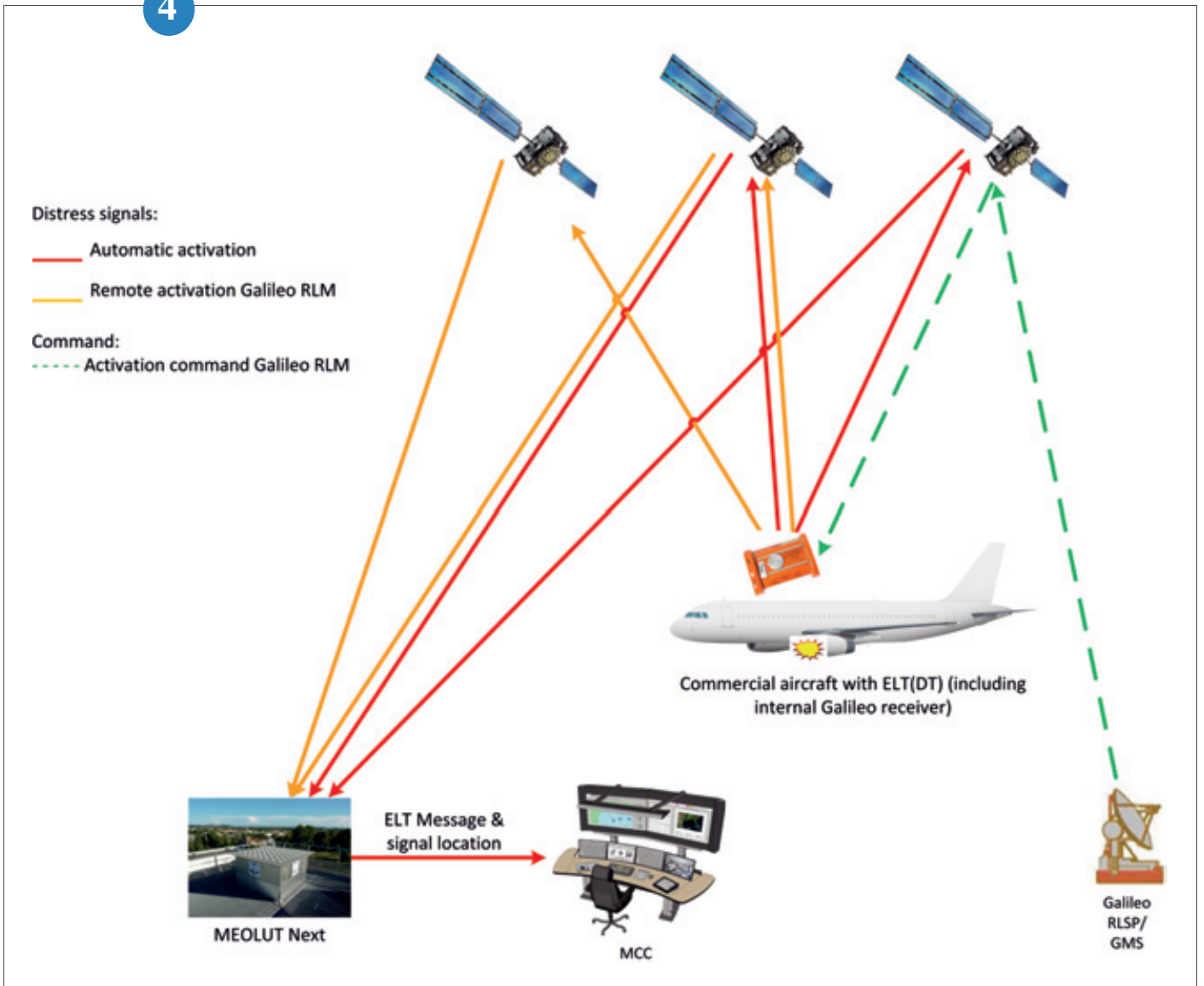
▲
Functional block diagram of GRICAS project

Distress signals:

━━━ Automatic activation

━━━ Remote activation Galileo RLM

Command:

----- Activation command Galileo RLM

Commercial aircraft with ELT(DT) (including internal Galileo receiver)

ELT Message & signal location

MEOLUT Next

MCC

Galileo RLSP/ GMS

◄
SAFIRE ATR 42
Crédit : Jean-Christophe Canonici / Météo-France

Development of a new icing index based on AROME for the aviation forecast

Icing by supercooled water is a serious hazard for aeronautic which can induce loss of control. The availability of new icing observations allowed to carry out two studies contributing to the improvement of icing areas forecasting.

Firstly, AROME operational model forecasts were compared to observations of icing occurrences over mainland France, provided by an airline company for 22 months. Multidimensional icing probability histograms were computed for several simulated variables. The most relevant variables were selected by an objective algorithm to establish a new icing diagnostic (Fig. b). This new index improves the scores (hit rate and false alarm rate) and is now being evaluated by forecasters.

Secondly, a measurement campaign in icing conditions performed during a winter by AIRBUS Hélicoptères has been used to directly compare the observed microphysical properties (liquid water content and mean volume diameter of droplets) to the ones simulated by the Meso-NH research model. Several versions of the one-moment microphysical scheme ICE3, operational in AROME, and the two-moment scheme LIMA, intended for AROME, were evaluated. The ability of the model to forecast icing conditions is limited by the microphysical schemes inclination to transform too much supercooled water in iced species.

The new index could allow to better forecast icing conditions with the current model configuration, while the study on microphysical schemes will participate to the improvement of the icing forecast abilities of future versions of AROME.

6

Potential of dual-polarization radar observations for aircraft icing detection

Dual-polarization radar observations can be particularly helpful in diagnosing ongoing microphysical processes in precipitation, as they provide valuable information about particle sizes, shapes, composition, and orientations. The focus of this study was to examine the potential of these observations for the detection of supercooled liquid water (SLW) in clouds, which is of great interest for aircraft icing hazard monitoring.

Dual-polarization observations measured by the Plabennec radar were examined together with in-situ observations (temperature, liquid water content) from an aircraft campaign during winter 2015-2016. The temporal evolution of the mean vertical profiles of radar variables was explored, as illustrated in the Figure. In particular, four cases with enhanced values of specific differential phase shift K_{dp} (>0.5° km-1) were observed at a temperature of about -5°C, just above a layer with a minimum of differential reflectivity (Z_{dr}), where the aircraft reported SLW. Such signatures were also observed in recent studies, which attributed the enhancement of K_{dp} to very oblate, small and dense crystals (needles), while the weak values of Z_{dr} were explained by the presence of larger and more spherical particles of graupel. Given both types of hydrometeors form when SLW is present, these signatures could be used as indicators of the presence of SLW. These first results suggest that the analysis of the vertical distributions of Z_{dr} and K_{dp} reveals important insights into the cloud microphysical processes that can be associated to the presence of SLW. The use of dual-polarisation observations could thus help improve the current Météo France icing algorithm (SIGMA) in precipitating regions.

7
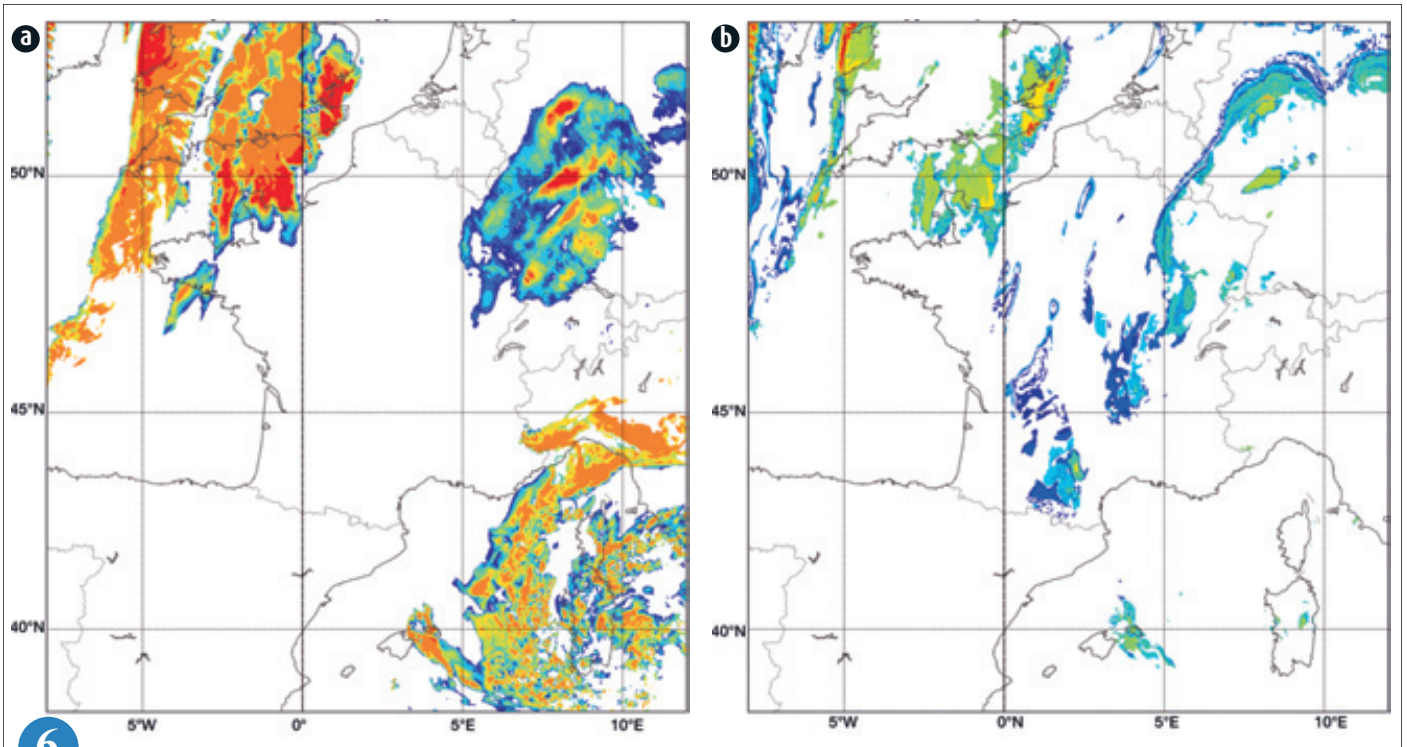
6 ▲ Icing indexes based on AROME forecasts for November 7, 2017 at 9 UTC at 800hPa using (a) the old index and (b) the new index. Because indexes are not calibrated the same way, values cannot be compared, only impacted areas can be compared.
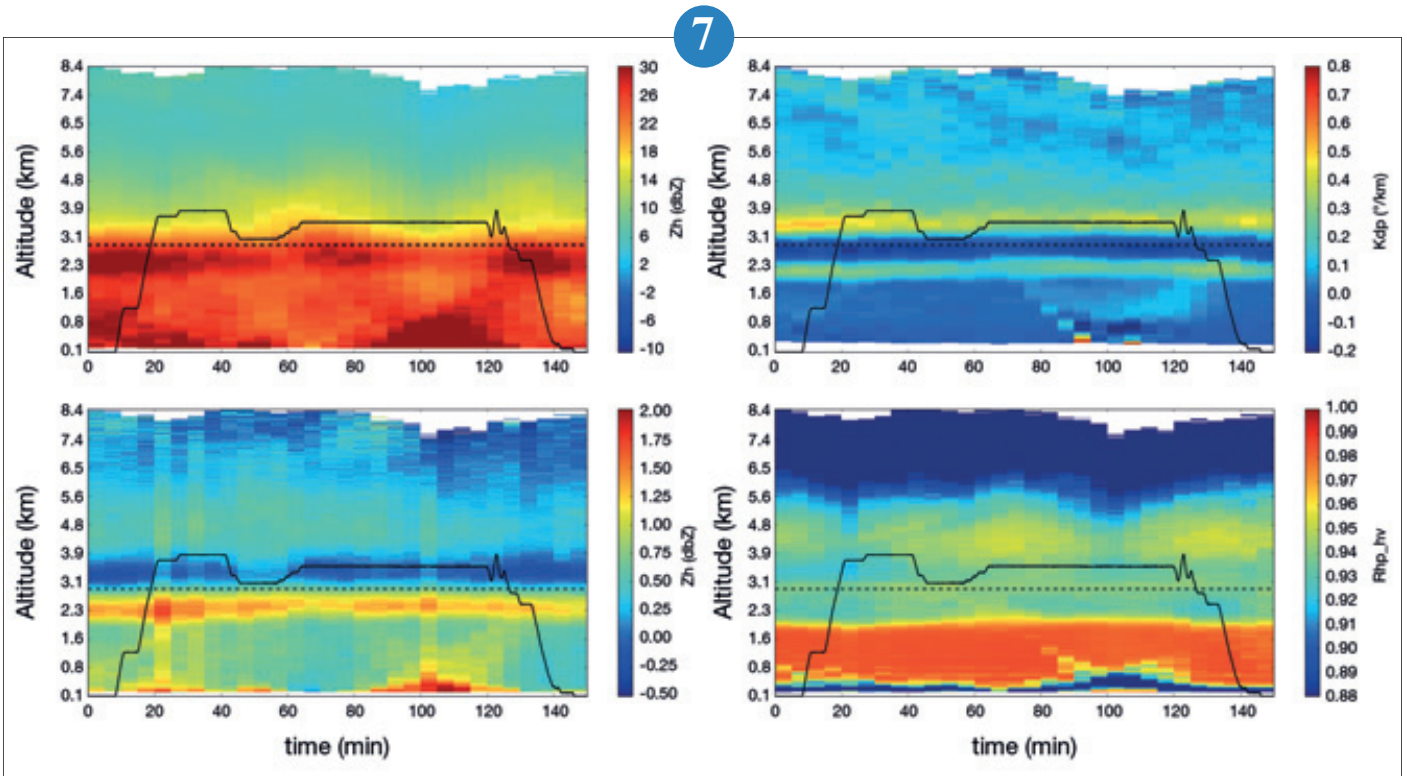
7

▲ Temporal evolution of the pseudo-vertical profiles of reflectivity (Zh), differential phase shift (Kdp), differential reflectivity (Zdr) and copolar correlation coefficient (ρhv), obtained by averaging all azimuths from elevation 2.8° of Plabennec C-band radar. Case 1: 1435 to 1650 UTC. The black plain line indicates the altitude of the aircraft, corresponding to a temperature of about -4°C. The aircraft encountered supercooled liquid water, with liquid water contents (LWC) from 0.1 to 0.6 g m-3 between 40 and 120 minutes of flight. The 0°C isotherm is shown as a black dotted line.

Appendix

2017 Scientific papers list

Papers published in peer-reviewed journals (impact factor > 1)

Abida, R., Attié, J.-L., El Amraoui, L., Ricaud, P., Lahoz, W., Eskes, H., Segers, A., Curier, L., de Haan, J., Kujanpää, J., Nijhuis, A. O., Tamminen, J., Timmermans, R., and Veefkind, P.: Impact of spaceborne carbon monoxide observations from the S-5P platform on tropospheric composition analyses and forecasts. Atmospheric Chemistry and Physics, Volume: 17, Issue: 2, Pages: 1081-1103, Doi: 10.5194/acp-17-1081-2017. Published: JAN 24 2017.

Adam, O., F. Brient et al., 2017: Regional and seasonal variations of the double-ITCZ bias in CMIP5 models, see here.

Adloff, F., G. Jordà, S. Somot, F. Sevault, T. Arsouze, B. Meyssignac, L. Li, S. Planton, 2017: Improving sea level simulation in Mediterranean regional climate models. Climate Dynamics, Doi: 10.1007/s00382-017-3842-3.

Albergel, C., S. Munier, D.J. Leroux, H. Dewaele, D. Fairbairn, A. L. Barbu, E. Gelati, W. Dorigo, S. Faroux, C. Meurey, P. Le Moigne, B. Decharme, J.-F. Mahfouf, J.-C. Calvet, 2017: Sequential assimilation of satellite-derived vegetation and soil moisture products using SURFEX_v8.0: LDAS-Monde assessment over the Euro-Mediterranean area. Geoscientific Model Development, Volume: 10 Issue: 10 Pages: 3889-3912 Published: OCT 25 2017

Anderson, D. C., J. M. Nicely, G. M. Wolfe, T. F. Hanisco, Ross J. Salawitch, T. P. Canty, R. R. Dickerson, E. C. Apel, E. Atlas, S. Baidar, T. J. Bannan, N. J. Blake, D. Chen, B. Dix, R. P. Fernandez, S. R. Hall, R. S. Hornbrook, G. Huey, B. Josse, P. Jöckel, D. E. Kinnison, T. K. Koenig, M. LeBreton, V. Marécal, O. Morgenstern, L. D. Oman, L. L. Pan, C. Percival, D. Plummer, L. Revell, E. Rozanov, A. Saiz-Lopez, A. Stenke, S. Tilmes, K. Ullmann, R. Volkamer, A. J. Weinheimer, G.Zeng, Formaldehyde in the Tropical Western Pacific: Evaluation of controlling mechanisms, models, and its effects on the atmospheric oxidative capacity J. Geophys. Res., vol. 122, 20, 11,201−11,226, 10.1002/2016JD026121, 2017.

Ardilouze, C., Batté, L., Bunzel, F., Decremer, D., Déqué, M., Doblas-Reyes, F.J., Douville, H., Fereday, D., Guemas, V., MacLachlan, C., Müller, W., Prodhomme, C., 2017 : Multi-model assessment of the impact of soil moisture initialization on mid-latitude summer predictability. Clim Dyn. doi:10.1007/s00382-017-3555-7. Published : NOV 2017

Ardilouze, C., Batté, L., Déqué, M., 2017 : Subseasonal-to-seasonal (S2S) forecasts with CNRM-CM : a case study on the July 2015 West-European heat wave, Adv. Sci. Res., 14, 115-121, doi:10.5194/asr-14-115-2017. Published : MAY 2017.

Arndt J., J. Sciare, M. Mallet, G. Roberts, N. Marchand, K. Sartelet, K. Sellegri, F. Dulac, R. M. Healy, and J. C. Wenger, 2017: Sources and mixing state of summertime background aerosol in the northwestern Mediterranean basin. Atmospheric Chemistry and Physics, Volume: 17, Issue: 11, Pages: 6975-7001, Doi: 10.5194/acp-17-6975-2017. Published : JUN 14 2017.

Ayhan, S., M. Pauli, S. Scherr, B. Gottel, A. Bhutani, S. Thomas, T. Jaeschke, J.-M. Panel, F. Vivier, L. Eymard, A. Weill, N. Pohl and T. Zwick, 2017 : Millimeter-Wave Radar Sensor for Snow Height Measurements. IEEE Transactions on Geoscience and Remote Sensing, Institute of Electrical and Electronics Engineers, Volume: 55, Issue: 2, Pages: 854-861, Doi: 10.1109/TGRS.2016.2616441, Published: NOV. 2017.

Bador, M., Terray L., Boé J., Somot S., Alias A., Gibelin A.-L., Dubuisson B., 2017 : Future summer mega-heatwave and record-breaking temperatures in a warmer France climate. Environmental Research Letters, Volume: 12, Issue : 7, Article Number: 074025, Doi: 10.1088/1748-9326/aa751c. Published: JUL 2017.

Barlow, J., M. Best, S.I. Bohnenstengel, P. Clark, S. Grimmond, H. Lean, A. Christen, S. Emeis, M. Haeffelin, I.N. Harman, A. Lemonsu, A. Martilli, E. Pardyjak, M.W. Rotach, S. Ballard, I. Boutle, A. Brown, X. Cai, M. Carpentieri, O. Coceal, B. Crawford, S. Di Sabatino, J. Dou, D.R. Drew, J.M. Edwards, J. Fallmann, K. Fortuniak, J. Gornall, T. Gronemeier, C.H. Halios, D. Hertwig, K. Hirano, A.A. Holtslag, Z. Luo, G. Mills, M. Nakayoshi, K. Pain, K.H. Schlünzen, S. Smith, L. Soulhac, G. Steeneveld, T. Sun, N.E. Theeuwes, D. Thomson, J.A. Voogt, H.C. Ward, Z. Xie, and J. Zhong, 2017: Developing a Research Strategy to Better Understand, Observe, and Simulate Urban Atmospheric Processes at Kilometer to Subkilometer Scales. Bull. Amer. Meteor. Soc., 98, ES261−ES264, https://doi.org/10.1175/BAMS-D-17-0106.1

Barrere, M., F. Domine, B. Decharme, S. Morin, V. Vionnet and M. Lafaysse, 2017: Evaluating the performance of coupled snow−soil models in SURFEXv8 to simulate the permafrost thermal regime at a high Arctic site. Geoscientific Model Development, Volume: 10, Issue: 9, Pages: 3461-3479, Doi: 10.5194/gmd-10-3461-2017 (https:// doi.org/10.5194/gmd-10-3461-2017), Published: SEP 2017.

Bellprat, O., J. García-Serrano, N. Fučkar, F. Massonnet, V. Guemas, and F. J. Doblas-Reyes, 2017 : The Role of Arctic Sea Ice and Sea Surface Temperatures on the Cold 2015 February Over North America AMS.

Benedetti, F., Guilhaumon F., Adloff F., Ayata S.-D. (2017) Investigating uncertainties in zooplankton composition shifts under climate change scenarios in the Mediterranean Sea. Ecography (accepted)

Berner J., U. Achatz, L. Batté, L. Bengtsson, A. de la Cámara, Antje Weisheimer, Michael Weniger, Paul D. Williams, J.-I. Yano and al., 2017: Stochastic Parameterization: Toward a New View of Weather and Climate. Bulletin of the American Meteorological Society, Volume: 98, Issue: 3, Pages: 565-587, Doi: 10.1175/BAMS-D-15-00268.1. Published: MAR 2017.

Berthou, S., Mailler, S., Drobinski, P., Arsouze, T., Bastin, S., Béranger, K., C. Lebeaupin Brossier, 2017: Lagged effects of the Mistral wind on heavy precipitation through ocean-atmosphere coupling in the region of Valencia. Climate Dynamics, Doi: 10.1007/s00382-016-3153-0.

Birman, C., F. Karbou, J. Mahfouf, M. Lafaysse, Y. Durand, G. Giraud, L. Mérindol and L. Hermozo, 2017 : Precipitation Analysis over the French Alps Using a Variational Approach and Study of Potential Added Value of Ground-Based Radar Observations. Journal of Hydrometeorology, Volume: 18, Pages: 1425-1451, Doi: 10.1175/JHM-D-16-0144.1, Published : MAY 2017.

Blanchard-Wrigglesworth, E., A. Barthélemy, M. Chevallier, R. Cullather, N. Fu kar, F. Massonnet, P. Posey, W. Wang, J. Zhang, C. Ardilouze, M. Bitz, G. Vernieres, A. Wallcraft and M. Wang, 2017 : Multi-model seasonal forecast of Arctic sea-ice: forecast uncertainty at pan-Arctic and regional scales. Climate Dynamics, Volume: 49, Issue: 4, Pages: 1399-1410, Doi: 10.1007/s00382-016-3388-9. Published : AUG 2017.

Boone, A., P. Samuelsson, S. Gollvik, A. Napoly, L. Jarlan, E. Brun, and B. Decharme, 2017 : The interactions between soil−biosphere−atmosphere land surface model with a multi-energy balance (ISBA-MEB) option in SURFEXv8 − Part 1: Model description. Geoscientific Model Development, Volume: 10, Issue: 2, Pages: 843-872, Doi: 10.5194/gmd-10-843-2017. Published: FEB 21 2017.

Bordois, L., F. Auclair, A. Paci, Y. Dossmann and C. Nguyen (2017). Non-linear processes generated by supercritical tidal ow in shallow straits. Physics of Fluids.

Bouin, M.-N., Redelsperger, J.-L. and Lebeaupin Brossier, C., 2017: Processes leading to deep convection and sensitivity to sea-state representation during HyMeX IOP8 heavy precipitation event.Quaterly journal of the Royal Meteorological Society. Volume: 143 Issue: 707 Pages : 2600-2615 Part: B Published: JUL 2017. doi: 10.1002/qj.3111

Bourgeois, D. Bouniol, F. Couvreux, F. Guichard, J. Marsham, L. Garcia-Carreras, C. Birch and D. Parker, 2017: Characteristics of mid-level clouds over West Africa. Accepted manuscript online: 24 nov 2017 - Doi: 10.1002/qj.3215.

Brooks, I. M., Tjernström, M., Persson,P. O. G., Shupe, M. D., Atkinson, R. A., Guylaine Canut, Cathryn E. Birch, Thorsten Mauritsen, Joseph Sedlar, and Barbara J. Brooks, 2017 : The turbulent structure of the Arctic summer boundary layer during The Arctic Summer Cloud-Ocean Study. Journal of Geophysical Research: Atmospheres, 122.

Calvet, J.-C., Fritz, N., Berne, C., Piguet, B., Maurel, W., and Meurey, C.: Deriving pedotransfer functions for soil quartz fraction in southern France from reverse modeling, SOIL, 2, 615-629, Doi : 10.5194/soil-2-615-2016.

Canal, N., O. Deudon, X. Le Bris, P. Gate, G. Pigeon, M. Regimbeau, J.-C. Calvet , 2017: Anticipation of the winter wheat growth using the seasonal weather forecast over France. Meteorological Applications, Volume: 24, Issue: 3, Pages: 432-443, Doi: 10.1002/met.164. Published: JUL 2017.

Cariolle, D., P. Moinat, H. Teyssèdre, L. Giraud, B. Josse, and F. Lefèvre, 2017 : ASIS v1.0: an adaptive solver for the simulation of atmospheric chemistry.

Geoscientific Model Development, Volume: 10, Issue: 4, Pages: 1467-1485, Doi: 10.5194/gmd-10-1467-2017, Published: APR 11 2017.

Cavicchia, L., Scoccimarro E., Gualdi S., Ahrens B., Berthou S., Conte D., Dell'Aquila A., Drobinski P., Djurdjevic V., Dubois C., Gallardo C., Li L., Oddo P., Sanna A., Torma C. (2016) Spatiotemporal characterisation of Mediterranean extreme precipitation events: a multi-model assessment. Climate Dynamics, doi : 10.1007/s00382-016-3245-x

Cesana, G., K. Suselj and F. Brient, 2017 : On the Dependence of Cloud Feedbacks on Physical Parameterizations in WRF Aquaplanet Simulations. Geophysical Research Letters, Volume : 44, Issue : 20, Pages : 10762-10771, Doi : 10.1002/2017GL074820. Published : OCT 28 2017.

Chadwick, R., H. Douville and C.B. Skinner, 2017: Timeslice experiments for understanding regional climate projections: Applications to the tropical hydrological cycle and European winter circulation. Climate Dynamics, Volume 49, Issue: 9-10, Pages: 3011-3029, Doi: 10.1007/s00382-016-3488-6. Published: NOV 2017.

Chadwick, R., G. M. Martin, D. Copsey, G. Bellon, M. Caian, F. Codron, C. Rio, and R. Roehrig (2017): Examining the West African Monsoon circulation response to atmospheric heating in a GCM dynamical core. Journal of Advances in Modeling Earth Systems, Volume: 9, Issue: 1, Pages: 149-167, Doi: 10.1002/2016MS000728. Published: MAR 2017.

Chauvin F, H. Douville and A. Ribes, 2017: Atlantic tropical cyclones water budget in observations and CNRM-CM5 model. Climate Dynamics, Volume: 49, Issue: 11-12, Pages: 4009-4021, Doi: 10.1007/s00382-017-3559-3. Published: DEC 2017.

Chevallier, M., Smith, G., Lemieux, J.-F., Dupont, F., Forget, G., Fujii, Y., Hernandez, F., Msadek, R., Peterson, K.A., Storto, A., Toyoda, T., Valdivieso, M., Vernieres, G., Zuo, H., Balmaseda, M., Chang, Y.-S., Ferry, N., Garric, G., Haines, K., Keeley, S., Kovach, R.M., Kuragano, T., Masina, S., Tang, Y., Tsujino, H., Wang, X, 2016. Intercomparison of the Arctic sea ice cover in global ocean-sea ice reanalyses from the ORA-IP project. Climate Dynamics, Volume: 49, Issue: 3, Special Issue: SI, Pages: 1137-1138, Doi: 10.1007/s00382-016-2985-y. Published: AUG 2017.

Coppola, L., L. Prieur, I. Taupier-Letage, C. Estournel, P. Testor, D. Lefevre, S. Belamari, S. LeReste, and V. Taillandier (2017), Observation of oxygen ventilation into deep waters through targeted deployment of multiple Argo-O2 floats in the northwestern Mediterranean Sea in 2013, J. Geophys. Res. Oceans, 122, doi:10.1002/2016JC012594.

Couto, F., V. Ducrocq, R. Salgado and M. J. Costa, 2017 : Understanding significant precipitation in Madeira island using high-resolution numerical simulations of real cases. Quarterly Journal of the Royal Meteorological Society, Volume: 143, Issue: 702, Special Issue: UNDEFINED, Supplement: UNDEFINED, Pages: 251-264, Part: A, Doi: 10.1002/qj.2918. Published: JAN 2017.

D'Amboise, C. J. L., K. Müller, L. Oxarango, S. Morin and T. V. Schuler, 2017 : Implementation of a physically based water percolation routine in the Crocus/SURFEX (V7.3) snowpack model. Geoscience Model Development, Volume: 10, Issue: 9, Pages: 3547-3566, Doi: 10.5194/gmd-10-3547-2017, Published: SEP 2017.

Daniel, M., A. Lemonsu, V. Viguié: "Role of watering practices in large-scale urban planning strategies to face the heat-wave risk in future climate", Urban Climate, Available online 15 November 2016, http://dx.doi.org.insu.bib.cnrs.fr/10.1016/j.uclim.2016.11.001

Dayan, U., P. Ricaud, R. Zbinden and F. Dulac : Atmospheric pollution over the eastern Mediterranean during summer - a review. Atmospheric Chemistry and Physics, Volume: 17, Issue: 21, Pages: 13233-13263, DOI: 10.5194/acp-17-13233-2017. Published: NOV 8 2017.

De Angelis, F., Cimini, D., Lohnert, U., Caumont, O., Haefele, A., Pospichal, B., Martinet, P., Navas-Guzman, F., Klein-Baltink, H., Dupont, J.C., Hocking, J., 2017: Long-term observations minus background monitoring of ground-based brightness temperatures from a microwave radiometer network. Atmospheric Measurement Techniques, Volume: 10, Issue: 10, Pages: 3947-3961, Doi: 10.5194/amt-10-3947-2017. Published: OCT 25 2017

Dell'Aquila, A, A. Mariotti, S. Bastin, S. Calmanti, L. Cavicchia, M. Déqué, V. Djurdjevic, M. Dominguez, M. Gaertner, and S. Gualdi, 2017: Evaluation of simulated decadal variations over the Euro-Mediterranean region from ENSEMBLES to Med-CORDEX, Climate Dynamics, Volume: , Issue: , Pages: , Doi : 10.1007/s00382-016-3143-2

Demuzere, S. Harshan, L. Järvi, M. Roth, C. S. B. Grimmond, V. Masson, K. W. Oleson, E. Velasco and H. Wouters, 2017: Impact of urban canopy models and external parameters on the modelled urban energy balance in a tropical city . Quarterly Journal of the Royal Meteorological Society, Volume: 143, Issue: 704, Pages: 1581-1596, Part: A, Doi: 10.1002/qj.3028. Published : APR 2017.

Déqué, M., S. Calmanti, O. Christensen, A. Dell Aquila, C. Maule, A. Haensler, G. Nikulin, C. Teichmann, 2017: A multi-model climate response over tropical Africa at +2 °C, Climate Services, Doi: 10.1016/j.cliser.2016.06.002.

Dewaele, H., Munier, S., Albergel, C., Planque, C., Laanaia, N., Carrer, D., and Calvet, J.-C.: Parameter optimisation for a better representation of drought by LSMs: inverse modelling vs. sequential data assimilation, Hydrol. Earth Syst. Sci., 21, 4861–4878, https://doi.org/10.5194/hess-21-4861-2017, 2017.

Diallo, F. B., Hourdin, F., Rio, C., Traore, A.-K., Mellul, L., Guichard, F., Kergoat, L., 2017: The surface energy budget computed at the grid-scale of a climate model challenged by station data in West Africa. Journal of Advances in Modeling Earth Systems, 9, 2710–2738. https://doi.org/10.1002/ 2017MS001081

Dorigo, W., W. Wagner, C. Albergel, F. Albrecht, G. Balsamo, L. Brocca, D. Chung, M. Ertl, M. Forkel, A. Gruber, E. Haas, P. D. Hamer, M. Hirschi, J. Ikonen, R. de Jeu, R. Kidd, W. Lahoz, Y. Y. Liu, D. Miralles, T. Mistelbauer, N. Nicolai-Shaw, R. Parinussa, C. Pratola, C. Reimer, R. van der Schalie, S. I. Seneviratne, T. Smolander and P. Lecomte, 2017: ESA CCI Soil Moisture for improved Earth system understanding: State-of-the art and future directions. Remote Sensing of Environment, Volume: 203, Pages: 185-215, Doi: 10.1016/ j.rse.2017.07.001. Published: DEC 15 2017.

Dorigo, W., W. Wagner, C. Albergel, F. Albrecht, G. Balsamo, L. Brocca, D. Chung, M. Ertl, M. Forkel, A. Gruber, E. Haas, P. D. Hamer, M. Hirschi, J. Ikonen, R. de Jeu, R. Kidd, W. Lahoz, Y. Y. Liu, D. Miralles, T. Mistelbauer, N. Nicolai-Shaw, R. Parinussa, C. Pratola, C. Reimer, R. van der Schalie, S. I. Seneviratne, T. Smolander and P. Lecomte, 2017: ESA CCI Soil Moisture for improved Earth system understanding: State-of-the art and future directions, Remote Sensing of Environment, Volume: 203 Pages: 185-215 Published: DEC 15 2017

Douville H., Y. Peings and D. Saint-Martin, 2016: Snow-(N)AO relationship revisited over the whole 20th century. Geophysical Research Letters, Volume: 44, Issue: 1, Pages: 569-577, Doi: 10.1002/2016GL071584. Published: JAN 2017.

Douville H., M. Plazzotta, 2017: Midlatitude summer drying: An underestimated threat in CMIP5 models ? Geophysical Research Letters, Volume : 44, Issue: 19, Pages: 9967-9975, Doi: 10.1002/ 2017GL075353. Published: OCT 16 2017.

Drobinski, P., Da Silva N., Panthou G., Bastin S., Muller C., Ahrens B., Borga M., Conte D., Fosser G., Giorgi F., Güttler I., Kotroni V., Li L., Morin E., Onol B., Quintana-Segui P., Romera R., Torma C.Z. (2016) Temperature-precipitation extremes relationship in the Mediterranean: past climate assessment and projection in anthropogenic scenarios. Climat Dynamics, Doi: 10.1007/s00382-016-3083-x

Dubois G., Céron J.-P., Dubois C., Frias M.D., Herrera S. (2016) Reliability and usability of tourism climate indices. Earth Perspectives (2016) 3:2, Doi: 10.1186/s40322-016-0034-y

Duffourg F., K.-O. Lee, V. Ducrocq, C. Flamant, P. Chazette and P. Di Girolamo, 2017: Role of moisture patterns in the backbuilding formation of HyMeX IOP13 heavy precipitation systems. Quarterly Journal of the Royal Meteorological Society. DOI: 10.1002/qj.3201.

Dumont, M., L. Arnaud, G. Picard, Q. Libois, Y. Lejeune, P. Nabat, D. Voisin and S. Morin, 2017: In situ continuous visible and near-infrared spectroscopy of an alpine snowpack. The Cryosphere, Volume: 11, Issue: 2, Pages: 1091-1110, Doi: 10.5194/tc-11-1091-2017, Published: MAY 2017.

Dunic N., Vilibic I., Šepic J., Somot S., Sevault F. (2016) Dense water formation and BiOS-induced variability in the Adriatic Sea simulated using an ocean regional circulation model. Climate Dynamics, Med-CORDEX special issue, Doi: 10.1007/s00382-016-3310-5

Eeckman, J., P. Chevallier, A. Boone, L. Neppel, A. De Rouw, F. Delclaux, and D. Koirala, 2017 : Providing a non-deterministic representation of spatial variability of precipitation in the Everest region. Hydrol. Earth Syst. Sci., 21, 4879–4893.

Fairbairn, D., A. L., Barbu, A. Napoly, C. Albergel, J.-F. Mahfouf, & J.-C. Calvet (2016) : The effect of satellite-derived surface soil moisture and leaf area index land data assimilation on streamflow simulations over France. Hydrology and Earth System Sciences, Volume: 21, Issue: 4 Pages: 2015-2033, Published: APR 13 2017.

Faisal H., M. Srinivasan, C. Peterson, M. Gosset, P. Le Moigne, L. Li and al., 2017 : Engaging the User Community for Advancing Societal Applications of the Surface Water Ocean Topography (SWOT) mission. BAMS -D-17-0161.

Field, P. R., Brožková, R., Chen, M., Dudhia, J., Lac, C., Hara, T., Honnert, R., Olson, J., Siebesma, P., de Roode, S., Tomassini, L., Hill, A. and McTagart-Cowan, R., 2017: Exploring the convective grey zone with regional simulations of a cold air outbreak. Quaterly journal of the Royal Meteorological Society, Volume: 143, Issue: 707, Pages: 2537-2555, Part: B, Doi: 10.1002/qj.3105. Published: JUL 2017.

Flaounas, E., F. Kelemen, H.Wernli, M.A. Gaertner, M. Reale, E. Sanchez-Gomez, P. Lionello, S. Calmanti, Z. Podrascanin, S. Somot, N. Akhtar, R. Romera and D. Conte, 2016 : Assessment of an ensemble of ocean-atmosphere coupled and uncoupled regional climate models to reproduce the climatology of Mediterranean cyclones. Climate Dynamics, Med-

CORDEX special issue, Doi: 10.1007/s00382-016-3398-7.

Freney, E., K. Sellegri, M. Chrit, K..Adachi, J. Brito, A. Waked, A. Borbon, A. Colomb, R. Dupuy, J.-M. Pichon, L. Bouvier, C. Delon, C. Jambert, P. Durand, T. Bourianne, C. Gaimoz, S. Triquet, A. Féron, M. Beekmann, F. Dulac and K. Sartelet, 2017 : Aerosol composition and the contribution of SOA formation over Mediterranean forests, Atmospheric Chemistry and Physics.

Fučkar, N., F. Massonnet, V. Guemas, J. García-Serrano, O. Bellprat, M. Acosta, and F. J. Doblas-Reyes, 2017 : Record low northern hemisphere sea ice extent in march 2015, AMS

Gaertner M.A., J.J. Gonzalez-Aleman , R. Romera, M. Dominguez, V. Gil, E. Sanchez C. Gallardo M.M. Miglietta , K. Walsh D. Sein S. Somot , A. dell'Aquila, B. Ahrens, A. Colette, S. Bastin, E. van Meijgaard and G. Nikulin, 2017: Simulation of medicanes over the Mediterranean Sea in a regional climate model ensemble impact of ocean-atmosphere coupling and increased resolution. Climate Dynamics, Med-CORDEX special issue. Doi: 10.1007/s00382-016-3456-1.

García-Serrano, J., C. Cassou, H. Douville, A. Giannini, F. J. Doblas-Reyes, 2017: Revisiting the ENSO teleconnection to the tropical North Atlantic. Journal of Climate, Volume: 30, Issue : 17, Pages: 6945-6957, Doi: 10.1175/JCLI-D-16-0641.1. Published: SEP 2017.

Garrigues, S., A. Boone, B. Decharme, A. Olioso, C. Albergel, J. Calvet, S. Moulin, S. Buis, and E. Martin, 2017: Impacts of the Soil Water Transfer Parametrization on the Simulation of Evapotranspiration over a 14-Year Mediterranean Crop Succession. J. Hydrometeor. doi: 10.1175/JHM-D-17-0 058. in press. See here.

Getirana, A., A. Boone, C. Peugeot, and, 2017: Streamflows over a West African Basin from the ALMIP2 Model Ensemble. J. Hydrometeor., 18, 1831–1845, https://doi.org/10.1175/JHM-D-16-0233.1

Giordani, H., C. Lebeauoin-Brossier, F. Léger, G. Caniaux, 2017 : A PV-approach for dense water formation along fronts : Application to the Northwestern Mediterranean. Journal of Geophysiacl Research-Oceans, Volume: 122, Issue: 2, Pages: 995-1015, Doi: 10.1002/2016JC012019. Published: FEB 2017.

Grippa, M.; Kergoat, L.; Boone, A.; Peugeot, C.; Demarty, J.; Cappelaere, B.;Gal, L.; Hiernaux, P.; Mougin, E; Ducharne, A; Dutra, E; Anderson, M; Hain, C., 2017: Modeling Surface Runoff and Water Fluxes over Contrasted Soils in the Pastoral Sahel: Evaluation of the ALMIP2 Land Surface Models over the Gourma Region in Mali. Journal of Hydrometeorology, Volume: 18, Issue: 7, Pages: 1847-1866, Doi: 10.1175/JHM-D-16-0170.1. Published: JUL 2017.

Guichard, F., Couvreux, F., 2017: A short review of numerical cloud-resolving models. TELLUS SERIES A-Dynamic Meteorolgy and Oceanography, Volume: 69, Article Number: 1373578, Published: SEP 19 2017.

Guth, J., V. Marécal, B. Josse and J. Arteta, 2017 : Primary aerosols and secondary inorganic aerosols budget over the Mediterranean basin during 2012 and 2013.

Harzallah, A., Jordà G., Dubois C., Sannino G., Carillo A., Li L., Arsouze T., Beuvier J., Akthar N., Ahrens B. (2016) Long term evolution of the heat budget in the Mediterranean Sea from Med-CORDEX forced and coupled simulations. Clim Dyn. 1-21, doi: 10.1007/s00382-016-3363-5

Hermozo, L., L. Eymard and F. Karbou, 2017: Modeling Sea Ice Surface Emissivity at Microwave Frequencies: Impact of the Surface Assumptions and Potential Use for Sea Ice Extent and Type Classification. IEEE Transactions on Geoscience and Remote Sensing, Volume: 55, Issue: 2, Pages: 943-961, Doi: 10.1109/TGRS.2016.2616920, Published: FEB 2017.

Horemans J.A., A. Henrot, C. Delire, C. Kollas, P. Lasch-Born, C. Reyer, F. Suckow, L. Francois, and R. Ceulemans, Combining multiple statistical methods to evaluate the performance of process-based vegetation models across three forest stands. Central European Forestry Journal 63,4,, doi:10.1515/forj-2017-0025, Nov 2017.

Jaidan, N., L. El Amraoui, J.-L. Attié, P. Ricaud, and F. Dulac, Future changes in surface ozone over the Mediterranean basin in the framework of the Chemistry-Aerosol Mediterranean Experiment (ChArMEx), Atmospheric Chemistry and Physics Discussions, acp-2017-553, 2017.

Jomelli, V., F. Mokadem, I. Schimmelpfennig, E. Chapron, V. Rinterknecht, V. Favier, D. Verfaillie, D. Brunstein, C. Legentil, E. Michel, D. Swingedouw, A. Jaoen, G. Aumaître, D.L. Bourles, K. Keddadouche, 2017 : Sub Antarctic glacier extensions in the Kerguelen region (49ºS, Indian Ocean) over the past 23 000 years constrained by 36Cl moraine dating. Quaternary Science Reviews, Volume: 162, Pages: 128-144, Doi: 10.1016/j.quascirev.2017.03.010 Published: APR 2017.

Kangah, Y., P. Ricaud, J.-L. Attié, N. Saitoh, D. A. Hauglustaine, R. Wang, L. El Amraoui, R. Zbinden, and C. Delon, Summertime upper tropospheric nitrous oxide over the Mediterranean as a footprint of Asian emissions. Journal of Geophysiacal Research-Atmospheres, Volume : 122, Issue : 8, Pages : 4746-4759, Doi : 10.1002/2016JD026119. Published : APR 27 2017.

Kergoat, L., Guichard, F; Pierre, C; Vassal, C, 2017: Influence of dry-season vegetation variability on Sahelian dust during 2002-2015 : Geophysical Research Letters, Volume: 44, Issue: 10, Pages: 5231-5239, Doi: 10.1002/2016GL072317. Published : MAY 28 2017.

Lacressonnière, G., Watson, L., Gauss, M., Engardt, M., Andersson, C., Beekmann, M., Colette, A., Foret, G., Josse, B., Marécal, V., Nyiri, A., Siour, G., Sobolowski, S., and Vautard, R.: Particulate matter air pollution in Europe in a +2 ºC warming world. Atmospheric Environment, Volume: 154, Pages: 129-140, Doi: 10.1016/j.atmosenv.2017.01.037. Published: APR 2017.

Lafaysse, M., B. Cluzet, M. Dumont, Y. Lejeune, V. Vionnet and S. Morin, 2017: A multiphysical ensemble system of numerical snow modelling. The Cryosphere, Volume: 11, Issue: 2, Pages: 1173-1198, Doi: 10.5194/tc-11-1173-2017, Published: MAY 2017.

Lafore, J.-P., Beucher, F., Peyrillé, P., Diongue-Niang, A., Chapelon, N., Bouniol, D., Caniaux, G., Favot, F., Ferry, F., Guichard, F., Poan, E., Roehrig, R. and Vischel, T., 2017: The extreme rain event of Ougadougou in 2009 Part I: multi-scale analysis and conceptual model. Q. J. R. Meteorol. Soc. Volume: 143 Issue: 709 Pages: 3094-3109 Part: B Published: OCT 2017. Doi: 10.1002/qj.3165

Le Gall, A., C. Leyrat, M. A. Janssen, G. Choblet, G. Tobie, O. Bourgeois, A. Lucas, C. Sotin, C. Howett, R. Kirk, R. D. Lorenz, R. D. West, A. Stolzenbach, M. Massé, A. H. Hayes, L. Bonnefoy, G. Veyssière and F. Paganelli, 2017: Thermally anomalous features in the subsurface of Enceladus's south polar terrain. Nature Astronomy, Volume: 1, Article number: 0063, Doi: 10.1038/s41550-017-0063, Published: MAR. 2017.

Leauthaud, C., Cappelaere, B.; Demarty, J.; Guichard, F; Velluet, C.; Kergoat, L.; Vischel, T.; Grippa, M.; Mouhaimouni, M.; Bouzou Moussa, I.; Mainassara, I.; Sultan, B., 2017: A 60-year reconstructed high-resolution local meteorological data set in Central Sahel (1950-2009) : evaluation, analysis and application to land surface modelling. International Journal of Climatology, Volume: 37, Issue: 5, Pages: 2699-2718, Doi: 10.1002/joc.4874. Published: APR 2017.

Lebeaupin Brossier, C., F. Léger, H. Giordani, J. Beuvier, M-N. Bouin, V. Ducrocq, N. Fourrié, 2017 : Dense water formation in the north-western Mediterranean area during HyMeX-SOP2 in 1/36º ocean simulations: Ocean-atmosphere coupling impact.Journal of Geophysical Research-Oceans, 122 (7), 5749-5773,

Lee, K.-O, Flamant, C., Ducrocq, V., Duffourg, F., Fourrié, N., Delanoë, J. and Bech, J., 2016 : Initiation and development of a mesoscale convective system in the Ebro River Valley and related heavy precipitation over north-eastern Spain during HyMeX IOP 15a. Quaterly journal of the Royal Meteorological Society, Volume : 143, Issue : 703, Pages : 942-956, Part : B, Doi : 10.1002/qj.2978. Published : JAN 2017.

Llasses, J., G. Jordà, D. Gomis, F. Adloff, D. Macías, A. Harzallah, T. Arsouze, N. Akthar, L. Li, A. Elizalde, G. Sannino (2017), Heat and salt redistribution within the Mediterranean Sea in the Med-CORDEX model ensemble, Climate dynamics, doi : 10.1007/s00382-016-3242-0.

Lunet, T., C. Lac, F. Auguste, F. Visentin, V. Masson, and J. Escobar, 0: Combination of WENO and Explicit Runge-Kutta methods for wind transport in Meso-NH model. Monthly Weather Review, Volume: 145 Issue: 9 Pages: 3817-3838 Published: SEP 2017

Martin, G.M., P. Peyrillé, R. Roehrig, C. Rio, M. Caian, G. Bellon, F. Codron, J.-P. Lafore, D. E. Poan, A. Idelkadi, 2017: Understanding the West African Monsoon from the analysis of diabatic heating distributions as simulated by climate models. Journal of Advances in Modeling Earth Systems, Volume : 9, Issue : 1, Pages : 239-270, Doi : 10.1002/2016MS000697. Published : MAR 2017.

Martinet, M., Nuissier, O., Duffourg, F., Ducrocq, V. and Ricard, D., 2017:Fine-scale numerical analysis of the sensitivity of the HyMeX IOP16a heavy precipitating event to the turbulent mixing-length parametrization. Quaterly journal of the Royal Meteorological Society, Volume: 143 Issue: 709 Pages: 3122-3135 Part: B Published: OCT 2017

Martinet, P., Cimini, D., De Angelis, F., Canut, G., Unger, V., Guillot, R.,Tzanos, D., and Paci, A., : Combining ground-based microwave radiometer and the AROME convective scale model through 1DVAR retrievals in complex terrain: an Alpine valley case study. Atmospheric Measurment Techniques, Volume : 10, Issue : 9, Pages : 3385-3402, Doi : org/10.5194/amt-10-3385-2017. Published : SEP 18 2017.

Martoia, F., L. Orgeas, P. Dumont, J.-F. Bloch, F. Flin and J. Viguie, 2017 : Crumpled paper sheets : low-cost biobased cellular materials for structural applications. Materials and Design, Volume: 136, Pages: 150-164, Doi: 10.1016/j.matdes.2017.09.031, Published: DEC. 2017.

Mazoyer, M., C. Lac, O. Thouron, T. Bergot, V. Masson, and L. Musson-Genon, 2017 : Large eddy simulation of radiation fog : impact of dynamics on the fog life cycle. Atmospheric Chemistry and Physics, Volume: 17 Issue: 21 Pages: 13017-13035 Published: NOV 6 2017

Morgenstern, O., M. I. Hegglin, E. Rozanov, B. Josse, V. Marécal, M. Michou, L. D. Oman, G. Pitari, D. Saint-Martin and al., 2017 : Review of the global models

used within phase 1 of the Chemistry–Climate Model Initiative (CCMI). Geoscientific Model Development, Volume: 10, Issue: 2, Pages: 639-671, Doi: 10.5194/gmd-10-639-2017. Published: FEB 13 2017.

Munier, S. and F. Aires, 2017 : A new global method of satellite dataset merging and quality characterization constrained by the terrestrial water budget. Remote Sensing of Environment, 205, 119-130. See here.

Napoly, A., Boone, A., P. Samuelsson, S. Gollvik, E. Martin, R. Seferian, D. Carrer, B. Decharme and L. Jarlan, 2017 : The Interactions between Soil-Biosphere-Atmosphere (ISBA) land surface model Multi-Energy Balance (MEB) option in SURFEX - Part 2: Model evaluation for local scale forest sites. Geoscientific Model Development, Volume : 10, Issue : 4, Pages : 1621-1644, Doi : 10.5194/gmd-10-1621-2017. Published : APR 18 2017.

Nicolet, G., N. Eckert, S. Morin and J. Blanchet, 2017 : A multi-criteria leave-two-out cross-validation procedure for max-stable process selection. Spatial Statistics, Vol: 22, Part 1, Pages: 107-128, https://doi.org/10.1016/j.spasta.2017.09.004, Published : OCT 2017.

Nord, G., Boudevillain, B., Berne, A. Branger, F., Braud, I., Dramais, G., Gerard, S., Le Coz, J., Legout, C., Molinie, G., Van Baelen, J., Vandervaere, JP, Andrieu, J., Aubert, C., Calianno, M., Delrieu, G., Grazioli, J., Hachani, S., Horner, I., Huza, J., Le Boursicaud, R., Raupach, T.H., Teuling, A.J., Uber, M., Vincendon, B., Wijbrans, A .,2017: A high space-time resolution dataset linking meteorological forcing and hydro-sedimentary response in a mesoscale Mediterranean catchment (Auzon) of the Ardeche region, France. Earth System Science Data, Volume: 9 Issue: 1 Published: MAR 22 2017

Obermann, A., Bastin S., Belamari S., Conte D., Gaertner MA, Li L., Ahrens B. (2017) : Mistral and Tramontane wind speed and wind direction patterns in regional climate simulations. Clim Dyn. doi : 10.1007/s00382-016-3053-3

Omrani, H., Drobinski, P., Arsouze, T., Bastin, S., Lebeaupin-Brossier, C., Mailler, S., 2017: Spatial and temporal variability of wind energy resource and production over the North Western Mediterranean Sea: Sensitivity to air-sea interactions. Renewable Energy, Volume: 101 Pages: 680-689 Published: FEB 2017

Osinski, R. and F. Bouttier, 2017 : Short-range probabilistic forecasting of convective risks for aviation based on a LAF-ensemble approach. Met. Apps, Volume 25, Issue 1, January 2018105-118. doi : 10.1002/met.1674.

Oudar, T., E. Sanchez-Gomez, F. Chauvin, J. Cattiaux, C. Cassou and L. Terray, Respective effects of Arctic sea ice loss and GHGs increase on the Northern Hemisphere atmospheric circulation, Climate Dynamics, Volume: 49, Issue: 11-12, Pages: 3693-3713, Doi: 10.1007/s00382-017-3541. Published: DEC 2017.

Ouzeau, G., J.-M. Soubeyroux, M. Schneider, R. Vautard, and S. Planton, 2016: Heat waves analysis over France in present and future climate: application of a new method on the EURO-CORDEX ensemble. Climate Services, Doi: 10.1016/j.cliser.2016.09.002.

Ovadnevaite J., A. Zuend, A. Laaksonen, K. J. Sanchez, G. Roberts, D. Ceburnis, S. Decesari, M. Rinaldi, N. Hodas, M. C. Facchini, J. H. Seinfeld & C. O' Dowd 2017: Surface tension prevails over solute effect in organic-influenced cloud drople activation. Nature, Volume: 546, Issue: 7660, Pages: 637-641, Doi: 10.1038/ nature22806. Published: JUN 29 2017.

Parodi, A., D. Kranzlmueller, A. Clematis, E. Danovaro, A. Galizia, L. Garrote, M. C. Llasat, O. Caumont, E. Richard, Q. Harpham, F. Siccardi, L. Ferraris, N. Rebora, F. Delogu, E. Fiori, L. Molini, E. Foufoula-Georgiou, D. D'Agostino, 2017 : DRIHM(2US): an e-Science environment for hydro-meteorological research on high impact weather events. Bulletin American Meteorological Society, Volume 98, Issue: 10, Pages: 2149-2166, Doi: 10.1175/BAMS-D-16-0279.1. Published: OCT 2017.

Parsons, D.B., M. Beland, D. Burridge, P. Bougeault , G. Brunet, J. Caughey, S. M. Cavallo, M. Charron, H. C. Davies, A. Diongue Niang, V. Ducrocq, P. Gauthier, T. M. Hamill, P. A. Harr, S. C. Jones, R. H. Langland, S. J. Majumdar, B. N. Mills, M. Moncrieff, T. Nakazawa, T. Paccagnella, F. Rabier, J.-L. Redelsperger, C. Riedel, R. W. Saunders, M. A. Shapiro, R. Swinbank, I. Szunyogh, C. Thorncroft, A. J. Thorpe, X. Wang, D. Waliser, H. Wernli, Z. Toth, 2017: THORPEX Research and the Science of Prediction. Bulletin of the American Meteorological Society, Volume: 98, Issue 4, Pages: 807-830, Doi: 10.1175/BAMS-D-14-00025.1. Published : APR 2017.

Peings, Y., J. Cattiaux, S. Vavrus and G. Magnusdottir, 2017: Late Twenty-First-Century Changes in the Midlatitude Atmospheric Circulation in the CESM Large Ensemble. Journal of Climate, Volume: 30, Issue: 15, Pages: 5943-5960, Doi: 10.1175/JCLI-D-16-0340.1. Published: AUG 2017.

Phillips, V.T.J. , Yano, J.I., Formenton, M., Ilotoviz, E., Kanawade, V., Kudzotsa, I., Sun, J.M., Bansemer, A., Detwiler, A.G., Khain, A., Tessendorf, S.A., 2017: Ice Multiplication by Breakup in Ice-Ice Collisions. Part II: Numerical Simulations. Journal of Atmospheric Sciences, Volume: 74 Issue: 9 Pages: 2789-2811 Published: SEP 2017

Phillips, Vaughan T. J.; Yano, Jun-Ichi; Khain, Alexander, 2017: Ice Multiplication by Breakup in Ice-Ice Collisions. Part I: Theoretical Formulation. Journal of the Atmospheric Sciences, Volume : 74, Issue: 6, Pages : 1705-1719, Doi : 10.1175/JAS-D-16-0224.1. Published : JUN 2017.

Pineau-Guillou L., F. Ardhuin, M.-N. Bouin, J.-L. Redelsperger, B. Chapron, J.R. Bidlot and Y. Quilfen, 2017: Strong winds in a coupled waveatmosphere model during a North Atlantic storm event: evaluation against observations. Quarterly Journal of the Royal Meteorological Society. DOI: 10.1002/qj.3205.

Planque, C., Carrer, D., and Roujean, J.-L., : Analysis of MODIS albedo changes over French steady woody covers during the period 2001-2013, Remote Sensing of Environment, Volume: 191, Pages: 13-29, Doi: 10.1016/j.rse.2016.12.019. Published: MAR 15 2017.

Planton, Y., A. Voldoire, H. Giordani, G. Caniaux, Main processes of interannual variability of the atlantic cold tongue, Climate Dynamic, Doi: 10.1007/s00382-017-3701-2, online.

Puy, M., J. Vialard, M. Lengaigne, E. Guilyardi, P. Di Nezio, A. Voldoire, M. Balmaseda, G. Madec, C. Menkes, M. McPhaden, 2017: The lottery El Niño?, Clim. Dyn., doi: 10.1007/s00382-017-3938-9, online.

Rabatel, A., P. Sirguey, V. Drolon, P. Maisongrande, Y. Arnaud, E. Berthier, L. Davaze, J.-P. Dedieu and M. Dumont, 2017: Annual and Seasonal Glacier-Wide Surface Mass Balance Quantified from Changes in Glacier Surface State: A Review on Existing Methods Using Optical Satellite Imagery. Remote Sensing, Volume: 9, Issue:5, Pages: 507, Doi: 10.3390/rs9050507, Published: MAY 2017.

Raimonet, M., Oudin, L., Vautard, R., Le Moigne, P., Silvestre, M., Rabouille, C., Garnier, J., Thieu, V., 2017 : Evaluation of reanalysis datasets for hydrological modeling. Journal of Hydrometeorology, Volume: 18 Issue: 11,Pages: 3027-3041, Published: NOV 2017

Rainaud, R., Lebeaupin Brossier, C., Ducrocq, V. and Giordani, H. (), High-resolution air-sea coupling impact on two heavy precipitation events in the Western Mediterranean. Quaterly journal of the Royal Meteorological Society, Volume: 143, Issue: 707, Pages: 2448-2462, Part: B, Doi: 10.1002/qj.3098. Published: JUL 2017.

Raynaud, L. and F. Bouttier, 2017: The impact of horizontal resolution and ensemble size for convective-scale probabilistic forecasts. Quarterly Journal Royal Meteorological Society, Volume : 143, Issue: 709, Pages: 3037-3047, Part: B, Doi: 10.1002/qj.3159. Published: OCT 2017.

Redon, E., Aude Lemonsu, Valéry Masson, Benjamin Morille, and Marjorie Musy, 2017 : Implementation of street trees within the solar radiative exchange parameterization of TEB in SURFEX v8.0. Geoscientific Model Development, Volume: 10, Issue: 1, Pages: 385-411, Doi: 10.5194/gmd-10-385-2017. Published: JAN 25 2017.

Reindert, J., M. Roberts, P. Vidale, C. Senior, A. Bellucci, Q. Bao, P. Chang, S. Corti, N. Fučkar, V. Guemas, J. von Hardenberg, W. Hazeleger, C. Kodama, T. Koenigk, L. Leung, J. Lu, J. Luo, J. Mao, M. Mizielinski, R. Mizuta, P. Nobre, M. Satoh, E. Scoccimarro, T. Semmler, J. Small and J. von Storch, 2016 : High Resolution Model Intercomparison Project (HighResMIPv1.0) for CMIP6. GMD article.

Revuelto, J., C. Azorin-Molina, E. Alonso-González, A. Sanmiguel-Vallelado, F. Navarro-Serrano, I. Rico, and J. I. López-Moreno, 2017: Meteorological and snow distribution data in the Izas Experimental Catchment (Spanish Pyrenees) from 2011 to 2017. Earth System Science Data, Volume: 9, Pages: 993-1005, Doi: 10.5194/essd-9-993-2017, Published: DEC 2017.

Ribes A., F. Zwiers, J.-M. Azaïs, P. Naveau (2017): A new statistical method for climate change detection and attribution. Climate Dynamics, Volume: 48, Issue: 1-2, Pages: 367-386. Doi: 10.1007/s00382-016-3079-6. Published: JAN 2017.

Ricaud P., E. Bazile, M. del Guasta, C. Lanconelli, P. Grigioni, and A. Mahjoub, 2017: Genesis of diamond dust, ice fog and thick cloud episodes observed and modelled above Dome C, Antarctica. Atmospheric Chemistry and Physics, Volume: 17, Issue: 8, Pages: 5221-5237, Doi: 10.5194/acp-17-5221-2017. Published: APR 21 2017.

Richon, C., Dutay, J.-C., Dulac, F., Wang, R., Balkanski, Y., Nabat, P., Aumont, O., Desboeufs, K., Laurent, B., Guieu, C., Raimbault, P., Beuvier, J., 2017 : Modeling the impacts of atmospheric deposition of nitrogen and desert dust–derived phosphorus on nutrients and biological budgets of the Mediterranean Sea, Progress in Oceanography.

Roca, R., Fiolleau, T., Bouniol, D., 2017: A Simple Model of the Life Cycle of Mesoscale Convective Systems Cloud Shield in the Tropics. JOURNAL OF CLIMATE Volume: 30 Issue: 11 Pages: 4283-4298 Published: JUN 2017

Rochetin, N., F. Couvreux and F. Guichard, 2017 Morphology of breeze circulations induced by surface flux heterogeneities and their impact on convection initiation. Quarterly Journal of the Royal Meteorological Society, Volume: 143, Issue: 702, Special Issue: UNDEFINED, Supplement: UNDEFINED, Pages: 463-478, Part: A, Doi: 10.1002/qj.2935. Published: JAN 2017.

Rodier, Q., V. Masson, F. Couvreux and A. Paci, 2017: Evaluation of a Buoyancy and Shear based Mixing Length for a Turbulence Scheme. Frontiers in Earth Science, Volume: 5, Article Number: UNSP 65,

Doi: 10.3389/feart.2017.00065. Published: AUG 9 2017.

Rodríguez-Fernández, N. J., Muñoz Sabater, J., Richaume, P., de Rosnay, P., Kerr, Y. H., Albergel, C., Drusch, M., and Mecklenburg, S., 2017: SMOS near-real-time soil moisture product: processor overview and first validation results, Hydrol. Earth Syst. Sci., 21, 5201-5216, see here.

Rottner, L., Baehr, C., Couvreux, F., Canut, G., Rieutord, T., 2017: A new downscaling method for sub-grid turbulence modeling. Atmospheric Chemistry and Physics, Volume: 17 Issue: 11 Pages: 6531-6546 Published: JUN 2 2017

Sachsperger, J., S. Serafin, V. Grubiši, I. Stiperski and A. Paci, 2017: The amplitude of lee waves on the boundary-layer inversion (pages 27–36). Quarterly Journal of the Royal Meteorological Society, Volume: 143, Issue: 702, Special Issue: UNDEFINED, Supplement: UNDEFINED, Pages: 27-36, Part: A, Doi: 10.1002/qj.2915. Published : JAN 2017.

Sarrat, C., Aubry, S., Chaboud, T., Lac, C., 2017: Modelling Airport Pollutants Dispersion at High Resolution. Aerospace, Volume: 4 Issue: 3 Article Number: 46 Published: SEP 2017.

Schellekens, J., Dutra, E; Martinez-de la Torre, A; Balsamo, G; van Dijk, A; Weiland, FS; Minvielle, M; Calvet, JC; Decharme, B; Eisner, S; Fink, G; Florke, M; Pessenteiner, S; van Beek, R; Polcher, J; Beck, H; Orth, R; Calton, B; Burke, S; Dorigo, W; Weedon, GP, 2017: A global water resources ensemble of hydrological models: the eartH2Observe Tier-1 dataset. Earth System Science Data, Volume: 9, Issue: 2, Pages: 389-413, Doi: 10.5194/essd-9-389-2017. Published: JUL 3 2017.

Schoetter, R., V. Masson, A. Bourgeois, M. Pellegrino, and J.-P. Lévy, 2017: Parametrisation of the variety of human behaviour related to building energy consumption in TEB (SURFEX v. 8.2). Geoscientific Model Development, Volume: 10, Issue: 7, Pages: 2801-2831, Doi: 10.5194/gmd-10-2801-2017. Published: JUL 21 2017.

Séférian, R., S. Baek, O. Boucher, J.-L. Dufresne, B. Decharme, D. Saint-Martin and R. Roehrig, 2017 : An interactive ocean surface albedo scheme : formulation and evaluation in two atmospheric models, Geoscientific Model Development.

Sherpa, S., P. Wagnon, F. Brun, E. Berthier, C. Vincent, Y. Lejeune, Y. Arnaud, R. Kayastha and A. Sinisalo, 2017: Contrasted surface mass balances of debris-free glaciers observed between the southern and the inner parts of the Everest region (2007-2015). Journal of Glaciology, Pages: 1-15, Doi: 10.1017/jog. 2017.30, Published: JUL 2017.

Silva R. A , J. J. West, J.-F. Lamarque, D. T. Shindell, W. J. Collins, G. Faluvegi, G. A. Folberth, L. W. Horowitz, T. Nagashima, V. Naik, S. T. Rumbold, K. Sudo, T. Takemura, D.Bergmann, P.Cameron-Smith, R.M. Doherty, B. Josse, I. A. MacKenzie, D.S. Stevenson and G. Zeng : Future global mortality from changes in air pollution attributable to climate change. Nature Climate Change, Volume: 7, Issue: 9, Pages: 647-+, Doi: 10.1038/nclimate3354. Published: SEP 2017.

Slangen, A., F. Adloff, S. Jevrejeva, P. W. Leclercq, B. Marzeion, Y. Wada, R. Winkelmann (2016), A review of recent updates of sea-level projections at global and regional scales. Surveys in Geophysics, Volume: 38, Issue : 1, Special Issue: SI, Pages: 385-406, Doi: 10.1007/s10712-016-9374-2. Published: JAN 2017.

Somot, S., Houpert, L., Sevault, F., Testor, P., Bosse, A., Taupier-Letage, I., Bouin, M.-N., Waldman, R., Cassou, C., Sanchez-Gomez, E., Durrieu de Madron, X., Adloff, F., Nabat, P., Herrmann, M., 2016: Characterizing, modelling and understanding the climate variability of the deep water formation in the North-Western Mediterranean Sea. Climate Dynamics, DOI: 10.1007/s00382-016-3295-0.

Spandre, P., H. François, E. Thibert, S. Morin and E. George-Marcelpoil, 2017 : Determination of snowmaking efficiency on a ski slope from observations and modelling of snowmaking events and seasonal snow accumulation. The Cryosphere, Volume: 11, Issue: 2, Pages: 891-909, Doi: 10.5194/tc-11-891-2017, Published: APR 2017.

Stavropulos-Laffaille, X., Chancibault, K., Andrieu, H., Lemonsu, A., Masson, V., 2017: Hydrological validation of an urban hydro-microclimate model (TEB-Hydro): Sensitivity analysis on the catchment of Reze (Nantes, France). Houille Blanche-Revue Internationale de L'Eau, Issue: 3 Pages: 14-21 Published JUN 2017

Stiperski I., S. Seran, A. Paci, H. Ágústsson, A. Belleudy, R. Calmer, K. Horvath, C. Knigge, J. Sachsperger, L. Strauss and V. Grubisic (2017). Water tank experimentt on stratied ow over double mountain-shaped obstacles at high Reynolds number. Atmosphere 8 (13). http://dx.doi.org/10.3390/atmos8010013

Stoffelen, A., S. Aaboe, J.-C. Calvet, J. Cotton, G. De Chiara, J. Figua-Saldana, A. A. Mouche, M. Portabella, K. Scipal, W. Wagner: Scientific developments and the EPS-SG scatterometer, IEEE Journal of Selected Topics in applied Earth Observations and Remote Sensing, Volume: 10, Issue: 5, Pages: 2086-2097, Part: 2, Doi: 10.1109/JSTARS.2017.2696424. Published: MAY 2017.

Taylor, CM; Belusic, D; Guichard, F; Arker, DJP; Vischel, T; Bock, O;Harris, PP; Janicot, S; Klein, C; Panthou, G, 2017: Frequency of extreme Sahelian storms tripled since 1982 in satellite observations. Nature, Volume: 544, Issue: 7651, Pages: 475-+, Doi: 10.1038/nature22069. Published: APR 27 2017.

Teixeira, M, A. Paci and A. Belleudy (2017). Drag produced by waves trapped at a density interface in non-hydrostatic ow over an axisymmetric hill. J. Atmos. Sci., 74, 1839-1857, https://doi.org/10.1175/JAS-D-16-0199.1

Termonia, P., C. Fischer, E. Bazile, F. Bouyssel, R. Brožková, Pierre Bénard, B. Bochenek, D. Degrauwe, M. Derkova, R. El Khatib, R. Hamdi, J. Mašek, P. Pottier, N. Pristov, Y. Seity, P. Smolíková, O. Spaniel, M. Tudor, Y. Wang, C. Wittmann and A. Joly, 2017: The ALADIN System and its Canonical Model Configurations AROME CY41T1 and ALARO CY40T1, GMD. See here.

Testor P., Bosse A., Houpert L., Margirier F., Mortier L., Lego H., Dausse D., Labaste M., Karstensen J., Hayes D., Olita A., Ribotti A., Schroeder K., Chiggiato J., Onken R., Heslop E., Mourre B., D'Ortenzio F., Mayot N., Lavigne H., de Fommervault O., Coppola L., Prieur L., Taillandier V., Durrieu de Madron X., Bourrin F., Many G., Damien P., Estournel C., Marsaleix P., Taupier-Letage I., Raimbault P. Waldman R., Bouin M.-N., Giordani H., Caniaux G., Somot S., Ducrocq V., Conan P. (2017) Multiscale observations of deep convection in the northwestern Mediterranean Sea during winter 2012-2013 using multiple platforms. JGR-Oceans, Special Issue HyMeX-Mermex (accepted), doi:10.1002/2016JC012671.

Tornay, N., R. Schoetter, M. Bonhomme, S. Faraut, A. Lemonsu and V. Masson (2017): GENIUS: A methodology to define a detailed description of buildings for urban climate and building energy consumption simulations, Urban Climate, Volume : 20, Pages: 75-93, Doi: 10.1016/j.uclim.2017.03.002. Published: JUN 2017.

Tommasi, D., Stock, C. A., Hobday, A. J., Methot, R., Kaplan, I. C., Paige Eveson, J., Holsman, K., Miller, T. J., Gaichas , S., Gehlen, M., Pershing, A., Vecchi, G. A., Msadek, R., Delworth, T., Mark Eakin, C., Haltuch, M. A., Séférian, R., Spillman, C. M., Hartog, J. R., Siedlecki, S., Samhouri, J. F., Muhling, B., Asch, R. G., Pinsky, M. L., Saba, V. S., Kapnick, S. B., Gaitan, C. F., Rykaczewski, R. R., Alexander, M. A., Xue, Y., Pegion, K. V., Lynch, P., Payne, M. R., Kristiansen, T., Lehodey, P. and Werner, F. E., 2017: Managing living marine resources in a dynamic environment: the role of seasonal to decadal climate forecasts. Progress in Oceanography, Volume: 152, Pages: 15-49, Doi: 10.1016/j.pocean.2016. 12.011. Published: MAR 2017.

Tompkins, A.M., Ortiz de Zárate, M.I., Saurral, R.I., Vera, C., Saulo, C., Merryfield, W.J., Sigmond M., Lee, W.S., Baehr, J., Braun, A., Butler, A., Déqué, M., Doblas-Reyes, F.J., Gordon, M., Scaife, A.A., Imada, Y., Ishii, M., Ose, T., Kirtman, B., Kumar, A., Müller, W.A., Pirani, A., Stockdale, T., Rixen, M., and T. Yasuda, 2017 : The Climate-system Historical Forecast Project: providing open access to seasonal forecast ensembles from centers around the globe . Bull. Amer. Meteor. Soc., https://doi.org/10.1175/BAMS-D-16-0209.1

Tramblay Y., Jarlan L., Hanich L., Somot S. (2017) Future scenarios for surface water resources availability in North African dams. Water Resources Management (published on line), https://doi.org/10.1007/s11269-017-1870-8

Tuzet, F., M. Dumont, M. Lafaysse, G. Picard, L. Arnaud, D. Voisin, Y. Lejeune, L. Charrois, P. Nabat and S. Morin, 2017: A multilayer physically based snowpack model simulating direct and indirect radiative impacts of light-absorbing impurities in snow. The Cryosphere, Volume: 11, Issue: 6, Pages: 2633-2653, https://doi.org/10-5194/tc-11-2633-2017, Published: NOV 2017.

Vavrus, S., F. Wang, J. Martin, J. Francis, Y. Peings and J. Cattiaux (2017), Changes in North American Atmospheric Circulation and Extreme Weather. Journal of Climate, Volume: 30, Issue: 11, Pages: 4317-4333, Doi: 10.1175/JCLI-D-16-0762.1. Published : JUN 2017.

Verfaillie, D., M. Déqué, S. Morin and M. Lafaysse, 2017 : The method ADAMONT v1.0 for statistical adjustement of climate projections applicable to energy balance land surface models. Geoscientific Model Development, Volume: 10, Issue: 11, Pages: 4257-4283, Doi: 10.5194/gmd-10-4257-2017, Published: NOV 24 2017.

Verrelle, A., D. Ricard, and C. Lac, 2017 : Evaluation and improvement of turbulence parameterization inside deep convective clouds at kilometer-scale resolution. Monthly Weather Review, Volume: 145, Issue: 10, Pages: 3947-3967, Doi: 10.1175/MWR-D-16-0404.1. Published: OCT 2017.

Vidot, J., B. Bellec, M. Dumont and P. Brunel, 2017 : A daytime VIIRS RGB pseudo composite for snow detection. Remote Sensing of Environment, Volume: 196, Pages: 134-139, Published: NOV 2017.

Vidot, J., P. Brunel, M. Dumont, C. Carmagnola and J. Hocking, 2017: The VIS/NIR land and snow BRDF atlas for RTTOV: Comparaison between MODIS MCD43C1 C5 and C6. Remote Sensing, Volume: 10, Issue: 1, Page: 21, Doi: 10.3390/rs10010021, Published: DEC 2017.

Vignon, E., van de Wiel, B. J. H., van Hooijdonk, I. G. S., Genthon, C., van der Linden, S. J. A., van Hooft, J. A., Baas, P., Maurel, W., Traullé, O. and Casasanta, G. (2017), Stable boundary-layer regimes at Dome C, Antarctica: observation and analysis. Quarterly Journal of the Royal Meteorological Society, Volume: 143, Issue: 704, Pages: 1241-1253, Part : A, Doi: 10.1002/qj.2998. Published: APR 2017.

Vionnet, V., E. Martin, V. Masson, C. Lac, F. Naaim Bouvet and G. Guyomarc'h, 2017 : High-resolution Large Eddy simulation of snow accumulation in alpine terrain. Journal of Geophysical Research: Atmospheres, Volume: 122, Doi: 10.1002// 2017JD026947, Published: OCT 2017.

Vitart, F., C. Ardilouze, A. Bonet, A. Brookshaw, M. Chen, C. Codorean, M. Deque, L. Ferranti, E. Fucile, M. Fuentes, H. Hendon, J. Hodgson, H. Kang, A. Kumar, H. Lin, G. Liu, X. Liu, P. Malguzzi, I. Mallas, M. Manoussakis, D. Mastrangelo, C. MacLachlan, P. McLean, A. Minami, R. Mladek, T. Nakazawa, S. Najm, Y. Nie, M. Rixen, A. Robertson, P. Ruti, C. Sun, Y. Takaya, M. Tolstykh, F. Venuti, D. Waliser, S. Woolnough, T. Wu, D. Won, H. Xiao, R. Zaripov, and L. Zhang, 2016 : The Sub-seasonal to Seasonal Prediction (S2S) Project Database. Bulletin of the American Meteorological Society, Volume: 98, Issue: 1, Pages: 163-+, Doi: 10.1175/BAMS-D-16-0017.1. Published: JAN 2017.

Voldoire A., B. Decharme, J. Pianezze, C. Lebeaupin Brossier, F. Sevault, A. Alias, V. Ducrocq, S. Faroux, H. Giordani, F. Léger, P. Marsaleix, R. Rainaud, .., Evelyne Richard, S. Riette and al., 2017 : SURFEX v8.0 interface with OASIS3-MCT to couple atmosphere with hydrology, ocean, waves and sea-ice models, from coastal to global scales. Geoscientific Model Development, Volume: 10, Issue: 11, Pages: 4207-4227, Doi: 10.5194/gmd-10-4207-2017. Published NOV 20 2017.

Waldman R., Somot S., Herrmann M., Bosse A., Caniaux G., Estournel C., Houpert L., Prieur L., Sevault F., Testor P. (2016): Modelling of the intense 2012-2013 dense water formation event in the northwestern Mediterranean Sea: evaluation with an ensemble simulation approach. Journal of

Geophysical Research-Oceans, Volume : 122, Issue: 2, Pages: 1297-1324, Doi: 10.1002/ 2016JC012437. Published: FEB 2017.

Watson. L., Michou M, Nabat P, Saint-Martin D (2017) Assessment of CNRM coupled ocean-atmosphere model sensitivity to the representation of aerosols. Climate Dynamics DOI: 10.1007 s00382-017-4054-6, URL https://doi.org/10.1007/s00382-017-4054-6

Wautier, A., C. Geindreau and F. Flin, 2017: Numerical homogenization of the viscoplastic behavior of snow based on X-ray tomography images. The Cryosphere, Volume: 11, Issue: 3, Pages: 1465-1485, Doi: 10.5194/tc-11-1465-2017, Published: JUN 2017.

Webb, M. J., T. Andrews, A. Bodas-Salcedo, S. Bony, C. S. Bretherton, R. Chadwick, H. Chepfer, H. Douville, P. Good, J. E. Kay, S. A. Klein, R. Marchand, B. Medeiros, A. P. Siebesma, C. B. Skinner, B. Stevens, G. Tselioudis, Y. Intercomparison Project (CFMIP) contribution to CMIP6. Geoscientific Model Development, Doi: 10.5194/gmd-2016-70.

Xia, J., A. McGuire, D. Lawrence, E. Burke, G. Chen, X. Chen, C. Delire, C. Koven, A. MacDougall, S. Peng, A. Rinke, K.Saito, W. Zhang, R. Alkama, T. Bohn, P. Ciais, B. Decharme, I. Gouttevin, T. Hajima, D. Hayes, D. Ji, G. Krinner, D. Lettenmaier, P. Miller, M. John, B. Smith, T. Sueyoshi, Z. Shi, L. Yan, J. Liang, L. Jiang,Y. Luo, Terrestrial ecosystem model performance in simulating productivity and its vulnerability to climate change in the northern permafrost region. Journal of Geophysical Research-Biogeosciences, Volume: 122, Issue: 2, Pages: 430-446, Doi: 10.1002 /2016JG003384. Published: FEB 2017.

Yano J-I and J. Tribbia, 2017: Tropical Atmospheric Madden–Julian Oscillation: A Strongly Nonlinear Free Solitary Rossby Wave? Journal of the Atmospheric Sciences - Volume: 74, Number: 10 (October 2017).

Yano, J.-I. and Ambaum, M. H.P. (), Moist Static Energy: Definition, Reference Constants, a Conservation Law, and Effects on Buoyancy. Quaterly journal of the Royal Meteorological Society, Volume: 143, Issue: 708, Pages: 2727-2734, Part: A, Doi: 10.1002/qj.3121. Published : OCT 2017.

Yano, J-I and E. Ouchtar, 2017: Convective initiation uncertainties without trigger or stochasticity: probabilistic description by the Liouville equation and Bayes' theorem, Quarterly Journal of the Royal Meteorological Society, Volume: 143, Issue: 705, Pages: 2025-2035, Part : B, Doi: 10.1002/qj.3064. Published: APR 2017.

Yano, J.I., 2017: Inertio-gravity waves under the non-traditional f-plane approximation: singularity in the large-scale limit. Journal of Fluid Mechanics, Volume: 810, Pages: 475-488 Published: JAN 2017

Zhang, S., Roussel, N., Boniface, K., Ha, M. H., Frappart, F., Darrozes, J., Baup, F., and Calvet, J.-C.: Use of GNSS SNR data to retrieve either soil moisture or vegetation height from a wheat crop, Hydrol. Earth Syst. Sci., 21, 4767–4784, https://doi.org/ 10.5194/hess-21-4767-2017, 2017.

Zhang, WM., Brandt, M; Guichard, F; Tian, QJ; Fensholt, R, 2017: Using long-term daily satellite based rainfall data (1983-2015) to analyze spatio-temporal changes in the sahelian rainfall regime. Journal of Hydrology, Volume: 550, Pages: 427-440, Doi: 10.1016/j.jhydrol.2017. 05.033. Published : JUL 2017.

Other scientific papers

Calvet, J.-C., Ceschia, E., Courault, D., Dewaele, H., Goulas, Y., Inglada, J., Le Toan, T., and Maignan, F. : Observation de la végétation depuis l'espace, La Météorologie, 97, 86-93, 2017.

Chambon P., Geer A. : All-sky assimilation of Megha-Tropiques/SAPHIR radiances in the ECMWF numerical weather prediction system. ECMWF Technical Memorandum n° 802

Dombrowski-Etchevers, I., V. Vionnet, , 2017 : Pertinence des prévisions météorologiques à l'échelle kilométrique pour la modélisation du manteau neigeux en montagne. La Météorologie, Numéro : 99, Série: 8, Pages : 25-34, https://hdl.handle.net/2 042/63587, Published: NOV 2017.

Dombrowski-Etchevers, I., V. Vionnet, L. Quéno : La prévision météorologique à l'échelle kilométrique au service de la nivologie, La Météorologie, soumis

Labadie C., P. Cébron, P. Raynaud, L. Descamps, P. Arbogast : Le vendeur de glaces et le chaos : Expliquer la prévision probabiliste à travers un jeu. La Météorologie, 96, 21.

Mahfouf J-F., J-M. Moisselin, F. Autonès, J. Vidot : Apport de l'observation satellitaire pour la prévision du temps, La Météorologie, 97, 27.

Mahfouf J-F. « Les modèles de prévision numérique à aire limitée opérationnels de Météo-France » par C. Fischer, en préparation pour le numéro 100 de La Météorologie

Menut, L., J.-L. Attié, M. Beekmann, B. Bessagnet, C. Clerbaux, J. Cuesta, G. Dufour, G. Foret, L. El Amraoui, M. Mallet, F. Melleu, P. Ricaud, D. Tanré, S. Turquety, Apport de l'observation satellite à l'analyse et à la prévision de la qualité de l'air, La Météorologie, 97, 34-45, doi:10.4267/2042/62165, 2017.

Rabatel, A., E. Berthier, Y. Arnaud, J.-P. Dedieu, M. Dumont, S. Gascoin, M. Gay, K. Guerreiro, F. Karbou, A. Douraev, G. Picard, F. Rémy, P. Sirguey, E. Trouvé and E. Zakharova, 2017 : Télédétection satellitaire des surfaces enneigées et englacées. La Météorologie, n° 97, Pages: 78-85, Doi: 10.4267/2042/62170, Published : MAI 2017.

Vionnet, V., F. Naaim-Bouvet, Y. Deliot, H. Bellot, F. Karbou, M. Naaim, G. Guyomarc'h et Y. Durand, 2017 : Col du lac Blanc : un site pour l'observation et la modélisation de la neige en haute montagne. La Météorologie, Numéro : 99, Série : 8, Pages : 35-44, https://hdl.handle.net/2042/63588, Published: NOV 2017.

2017 Papers published in peer-reviewed journals (outside CNRM)

Andrey-Andrés, J., Fourrié, N., Guidard, V., Armante, R., Brunel, P., Crevoisier, C., and Tournier, B.: A simulated observation database to assess the impact of the IASI-NG hyperspectral infrared sounder, Atmos. Meas. Tech., 11, 803818, https://doi.org/ 10.5194/ amt-11-803-2018, 2018.

Bador M., Terray L., Boé J., Somot S., Alias A., Gibelin A.-L., Dubuisson B. (2017): "Future summer mega-heatwave and record-breaking temperatures in a warmer France climate". Environ. Res. Lett. 12 074025.

Buizza R., S. Brönnimann, L. Haimberger, P. Laloyaux, J. Martin, M. Fuentes, M. Alonso-Balmaseda, A. Becker, Michael Blaschek, Per Dahlgren, E. de Boisseson, Dick Dee, M. Doutriaux, Boucher (3), X. Feng, Keith Haines , S. Jourdain, Y. Kosaka (1), D. Lea,

M. Mayer, P. Messina, C. Perruche, P. Peylin, J. Pullainen, N.Rayner, E. Rustemeier, D. Schepers, R. Saunders, J. Schulz, A. Sterin, S. Stichelberger, A. Storto (12), C.E. Testut, M-A. Valente, A. Vidard (15), N. Vuichard (16), A. Weaver, J. While and M. Ziese: "The EU-FP7 ERA-CLIM2 project contribution to advancing science and production of Earth-system climate reanalyses". Doi: 10.1175/BAMS-D-17-0199.1.

Canal, N., Deudon, O., Le Bris, X., Gate, P., Pigeon, G., Regimbeau, M. and Calvet, J.-C. (2017), Anticipation of the winter wheat growth based on seasonal weather forecasts over France. Met. Apps, 24: 432–443. Doi: 10.1002/met.1642

Hersbach, H., S. Brönnimann, L. Haimberger, M. Mayer, L. Villiger, J. Comeaux, A. Simmons, D. Dee, S. Jourdain, C. Peubey, P. Poli, N. Rayner, A.M. Sterin, A. Stickler, M.A. Valente, and S.J. Worley, 2017: The potential value of early (1939-1967) upper-air data in atmospheric climate reanalysis. Quarterly Journal of the Royal Meteorological Society, 143:1197-1210, doi: 10.1002/qj.3040.

Jeannin, N., L.Castanet, I.Dahman, V.Pourret, B.Pouponneau: "Smart Gateways Switching Control Algorithms Based on Tropospheric Propagation Forecasts", International Journal of Satellite Communications and Networking, 2017,1-13.

Laurent, Victoire ; Varney, Patrick ; Chewtchouk, Jonathan ; Tardy, Marc ; Flohr, Michaël ; Dubuisson, Brigitte ; Piquemal, Jean-Michel : « Les évolutions passées et futures du climat des îles Marquises et de la Société », La Météorologie - n° 96 - février 2017, DOI : 10.4267/2042/61972.

Platt T., Sathyendranath S., White III GN, Jackson T., Saux Picart S. and Bouman H. (2017) Primary Production: Sensitivity to Surface Irradiance and Implications for Archiving Data. Front. Mar. Sci. 4:387. Doi: 10.3389/fmars.2017.00387.

Poli, P., D.P. Dee, R. Saunders, V.O. John, P. Rayer, J. Schulz, K. Holmlund, D. Coppens, D. Klaes, J.E. Johnson, A.E. Esfandiari, I.V. Gerasimov,

E.B. Zamkoff, A.F. Al-Jazrawi, D. Santek, M. Albani, P. Brunel, K. Fennig, M. Schröder, S. Kobayashi, D. Oertel, W. Döhler, D. Spänkuch, and S. Bojinski, 2017: Recent Advances in Satellite Data Rescue. Bulletin of the American Meteorological Society, 98, 1471-1484, doi:10.1175/BAMS-D-15-00194.1.

Pouponneau, B., V. Pourret, E. Faucou, O. Mestre, M.Sorel, R.Bellini, M. Barthod, C. Dubois, S. Martinoni-Lapierre: « Évaluation de la ressource éolienne terrestre en France », La Météorologie, 2017, 98, 28-35.

Saux, S., Picart, P. Tandeo, E. Autret, B. Gausset, 2018. "Exploring machine learning to correct satellite-derived sea surface temperatures", Remote Sens., 10 (2), 224; doi:10.3390/rs10020224

Shinya Kobayashi, Paul Poli, Viju O. John. (2017) Characterisation of Special Sensor Microwave Water Vapor Profiler (SSM/T-2) radiances using radiative transfer simulations from global atmospheric reanalyses. Advances in Space Research 59: 4, 917-935.

Su, Z., W. Timmermans, Y. Zeng, J. Schulz, V. John, R. Roebeling, P. Poli, D. Tan, F. Kaspar, A. Kaiser-Weiss, E. Swinnen, C. Toté, H. Gregow, T. Manninen, A. Riihelä, J. Calvet, Y. Ma, and J. Wen, 2017: An overview of European efforts in generating climate data records. Bulletin of the American Meteorological Society, Early Online Release, doi: 10.1175/BAMS-D-16-0074.1.

Thorne, P.W., R. J. Allan, L. Ashcroft, P. Brohan, R.J.H Dunn, M. J. Menne, P. R. Pearce, J. Picas, K. M. Willett, M. Benoy, S. Bronnimann, P. O. Canziani, J.

Coll, R. Crouthamel, G. P. Compo, D.. Cuppett, M. Curley, C. Duffy, I. Gillespie, J. Guijarro, S. Jourdain, E. C. Kent, H. Kubota, T. P. Legg, Q. Li , J. Matsumoto, C. Murphy, N. A. Rayner, J. J. Rennie, E. Rustemeier, L. C. Slivinski, V. Slonosky, A. Squintu, B. Tinz, M. A. Valente, S. Walsh, X. L. Wang, N. Westcott, K. Wood, S. D. Woodruff and S. J. Worley, "Towards an integrated set of surface meteorological observations for climate science and applications". Doi: 10.1175/BAMS-D-16-0165.1.

Vidot J., B. Bellec, M. Dumont, P. Brunel, 2017, "A daytime VIIRS RGB pseudo composite for snow detection", Remote Sensing of Environment, 196, 134-139, doi:10.1016/j.rse.2017.04.028.

Vidot, J., Brunel, P., Dumont, M., Carmagnola, C., Hocking, J., 2018, "The VIS/NIR Land and Snow BRDF Atlas for RTTOV: Comparison between MODIS MCD43C1 C5 and C6". Remote Sens., 2018, 10, 21.

Vignon, E., Bas J.H. van de Wiel, Ivo G. S. van Hooijdonk, C. Genthon, S. J.A. van der Linden, J. Antoon van Hooft, P. Baas, W. Maurel, O. Traullé, G. Casasanta, 2017: Stable boundary-layer regimes at Dome C, Antarctica: observation and analysis. Q.J.R. Meteorol. Soc. Doi: 10.1002/qj.2998.

Zamo, M. and Philippe Naveau. "Estimation of the Continuous Ranked Probability Score with Limited Information and Applications to Ensemble Weather Forecasts." Mathematical Geosciences (2017): 1-26.

PHD defended in 2017

Barbier, J., 2017 : "Extrêmes climatiques : les vagues de chaleur au printemps sahélien". Thèse soutenue le 15 décembre 2017.

Boukachaba, N., 2017 : "Apport des observations satellitaires hyperspectrales infra rouges IASI au-dessus des continents dans le modèle météorologique à l'échelle convective AROME". Thèse soutenue le 25 septembre 2017.

Bourgeois, E., 2017 : Les nuages de mi-niveau en Afrique de l'Ouest : observation, caractérisation, modélisation. Thèse soutenue le 7 décembre 2017.

Brioulet, P.-E., 2017 : "Thermodynamique et turbulence dans les épisodes de vents forts sur le Golfe du Lion". Thèse soutenue le 28 novembre 2017.

Daniel, M., 2017 : "Ville, climat urbain et climat régional sur la France : étude par une approche de modélisation climatique couplée". Thèse soutenue le 17 novembre 2017.

Dewaele, H., 2017 : "Intégration de données satellitaires dans SURFEX pour le suivi de la végétation à l'échelle mondiale". Thèse soutenue le 4 décembre 2017.

Kangah, Y., 2017 : "Mesure du protoxyde d'azote (N2O) depuis l'espace". Thèse soutenue le 1er décembre 2017.

Martinet, M., 2017 : Initiation et organisation d'un système fortement précipitant méditerranéen dans le cadre de la période d'observation spéciale HyMeX : simulations aux échelles hectométriques. Thèse Soutenu le 11 décembre 2017.

Queno L., 2017 : "Apport de prévisions météorologiques à échelle kilométrique pour la modélisation du manteau neigeux en montagne". Thèse soutenue le 24 novembre 2017.

Redon, E., 2017 : "Modélisation de la végétation urbaine comme régulateur thermique". Thèse soutenue le 20 juin 2017.

Rieutord, T., 2017 : "Analyse de sensibilité d'un algorithme de filtrage des mesures de vent par lidar". Thèse soutenue le 13 novembre 2017.

Rodier, Q., 2017 : Paramétrisation de la turbulence atmosphérique dans le couche limte stable. Thèse soutenue le jeudi 14 décembre 2017.

Taillardat, M., 2017 : "Méthodes Non-Paramétriques de Post-Traitement des Prévisions d'Ensemble". Thèse soutenue le lundi 11 décembre 2017.

Tav J., 2017 : "Étude du dépôt de radionucléides par les gouttelettes de brouillards et de nuages sur les végétaux à partir d'expérimentations in situ". Thèse soutenue le 12 octobre 2017.

Varino F., 2017 : "Typologie des tempêtes du XXe siècle". Thèse soutenue le 22 septembre 2017.

« Habilitations à diriger des recherches » defended in 2017

Bouniol, D., 2017 : Contributions à l'étude des processus physiques dans les nuages. HDR soutenue le mardi 14 novembre 2017.

Couvreux, F., 2017 : Contribution à l'analyse des processus de couche limite et à leur représentation dans les modèles à partir de simulations explicites. HDR soutenue le 9 juin 2017.

Dumont, M., 2017 : « De la couleur de la neige : mesure, modèle et applications ». HDR soutenue le lundi 20 novembre 2017.

El Amraoui, L., 2017 : « Apport de l'assimilation de données dans la chimie atmosphérique : De l'environnement stratosphérique vers la prévision de la qualité de l'air » le 10 janvier 2017.

Mallet, M., 2017 : "Interaction : "Aérosol, rayonnement et climat" à l'échelle régionale" le jeudi 14 décembre 2017.

Plu, M., 2017 : "Prévisibilité des tempêtes, des cyclones tropicaux et de la composition chimique de l'atmosphère" le jeudi 9 novembre 2017.

Glossary

Organisms and Laboratories

Organisms

ADEME	Agence de l'Environnement et de la Maîtrise de l'Energie
AIEA	Agence Internationale de l'Energie Atomique
ANELFA	Association Nationale d'Etude et de Lutte contre les Fléaux Atmosphériques (Association to Suppress Atmospheric Plagues)
ANR	Agence Nationale de la Recherche
BEC	Bureau d'Etudes et de Consultance
CDM	Centre Départemental de la Météorologie
CDMA	Cellule de développement Météo-Air
CEH	Centre for Ecology and Hydrology
CEMAGREF	CEntre national du Machinisme Agricole, du Génie Rural, des Eaux et Forêts (Institut national de Recherche en Sciences et Technologies pour l'Environnement et l'Agriculture)
CEN	Centre d'Etudes de la Neige
CEPMMT	Centre Européen pour les Prévisions Météorologiques à Moyen Terme
CERFACS	Centre Européen de Recherche et de Formation Avancée en Calcul Scientifique
CMM	Centre de Météorologie Marine
CMRS	Centre Météorologique Régional Spécialisé
CMS	Centre de Météorologie Spatiale
CNES	Centre National d'Études Spatiales
CNP	Centre National de Prévision
DGA	Délégation générale pour l'armement
DGPR	Direction Générale de la Prévention des Risques (Head Office of the Hazard Prevention)
DGSCGC	Direction générale de la Sécurité Civile et de la Gestion de Crise (Head Office of the Civil Security and of the Crisis Management)
EALAT	Ecole de l'Aviation Légère de l'Armée de Terre
EASA	European Aviation Safety Agency
ECMWF	European Centre for Medium-range Weather Forecasts
EEA	Agence Environnementale Européenne
ENAC	Ecole Nationale de l'Aviation Civile
ENM	Ecole Nationale de la Météorologie
ESA	European Space Agency
ETNA	Division Ecoulements Torrentiels, Neige et Avalanches du CEMAGREF
EU	European Union
EUFAR	EUropean Facility for Airborne Research in environmental and geo-sciences
EUMETNET	EUropean METeorological NETwork
EUMETSAT	European Organisation for the Exploitation of Meteorological Satellites
FAA	US Federal Aviation Agency
FAAM	Facility for Airborne Atmospheric Measurements (Royaume-Uni)
FMI	Finnish Meteorological Institute
ICARE	International Conference on Airborne Research for the Environment
IFREMER	Institut Francais de Recherche pour l'Exploitation de la MER
INERIS	Institut National de l'Environnement et des Risques
INRIA	Institut National de Recherche en Informatique et en Automatique
INSU	Institut National des Sciences de l'Univers
IPEV	Institut Paul Emile Victor
IRD	Institut de Recherche pour le Développement
IRSTEA	Institut national de Recherche en Sciences et Technologies pour l'Environnement et l'Agriculture (anciennement CEMAGREF)
JAXA	Japan Aerospace eXploration Agency
JMA	Japan Meteorological Agency
KNMI-TNO	Royal Netherlands Meteorological Institute and Netherlands Organization for Applied Scientific Research
MEEM	Ministère de l'Environnement, de l'Energie et de la Mer
MERCATOR-OCEAN	Société Civile Française d'océanographie opérationnelle
MetOffice	United Kingdom Meteorological Office
MPI	Max Planck Institut
NASA	National Aeronautics and Space Administration
NCAR	National Center for Atmospheric Research
NEC	Nippon Electric Company
NIWA	National Institute for Water and the Atmosphere (New-Zeland)
NOAA	National Ocean and Atmosphere Administration
OACI	Organisation de l'Aviation Civile Internationale
OMM	Organisation Météorologique Mondiale
OMP	Observatoire Midi-Pyrénées
ONERA	French Aerospace Lab
RSMC	Regional Specialized Meteorological Centre
RTRA-STAE	Réseau Thématique de Recherche Avancée - Sciences et Technologies pour l'Aéronautique et l'Espace
SCHAPI	French national hydrological service
SHOM	Service Hydrographique et Océanographique de la Marine (Marine Hydrographical and Oceanographical Service)
SMHI	Swedish Meteorological and Hydrological Institute
UKMO	United Kingdom Meteorological Office
VAAC	Volcanic Ash Advisory Centre
WHO	World Health Organization
WMO	World Meteorological Organization

Laboratories or R&D units

3SR	Laboratoire Sols – Solides – Structures – Rhéologie, UJF Grenoble / CNRS / Grenoble INP
BRGM	Bureau de Recherches Géologiques et Minières (Geological and Mining Research Office)
CEREA	Centre d'Enseignement et de Recherche en Environnement Atmosphérique
CESBIO	Centre d'Etudes Spatiales de la BIOsphère
CNRM	Centre National de Recherches Météorologiques
CNRM-GAME	Groupe d'études de l'Atmosphère MÉTéorologique
CNRS	Centre National de Recherches Scientifiques
CRA	Centre de Recherches Atmosphériques
DSO	Direction des Systèmes d'Observation (Météo-France)
GAME	Groupe d'Etude de l'Atmosphère Météorologique
GSMA	Groupe de spectrométrie moléculaire et atmosphérique, UMR 7331 CNRS Université de Reims Champagne Ardennes
IFSTTAR	Institut Français des Sciences et Technologies des Transports, de l'Aménagement et des Réseaux
IGN	Institut Géographique National
IPSL	Institut Pierre Simon Laplace
LaMP	Laboratoire de Météorologie Physique
LATMOS	Laboratoire ATmosphères, Milieux, Observations Spatiales
LAVUE	Laboratoire Architecture, Ville, Urbanisme, Environnement
LCP	Laboratoire Chimie et Procédés
LEGI	Laboratoire des écoulements physiques et industriels
LGGE	Laboratoire de Glaciologie et de Géophysique de l'Environnement
LHSV	Laboratoire d'Hydraulique Saint-Venant
LIRIS	Laboratoire d'InfoRmatique en Image et Systèmes d'information
LISST	Laboratoire Interdisciplinaire Solidarités, Sociétés, Territoires
LMD	Laboratoire de Météorologie Dynamique
LOCEAN	Laboratoire d'Océanographie et du Climat : Expérimentations et Approches Numériques
LPCEE	Laboratoire de Physique et Chimie de l'Environnement et de l'Espace
LPED	Laboratoire Population Environnement Développement
LRA	Laboratoire de Recherche en Architecture
LSCE	Laboratoire des Sciences du Climat et de l'Environnement
RIU	Rhenish Institute for environmental research at the University of Cologne
SAFIRE	French group of Aircraft Equipped for Environmental Research - Unit of the CNRS, Meteo-France and the CNES which operates the 3 French research aircraft
WUT	Warsaw University of Technology (Politechnika Warszawska)

National or international programs or projects

BACCHUS	Impact of Biogenic versus Anthropogenic emissions on Clouds and Climate: towards a Holistic UnderStanding
BAMED	BAlloons in the MEDiterranean
C3AF	Changement Climatique et Conséquences sur les Antilles Françaises

CHFP	Climate Historical Forecasting Project
CHROME	Coupling Hydro-meteorological Regional Multi-Ensemble
CIDEX	Calibration and Icing Detection EXperiment
CMIP	Coupled Model Intercomparaison Project
COPERNICUS	European Earth observation system http://www.copernicus.eu/pages-principales/services/ climate-change/
CYPRIM	projet Cyclogénèse et précipitations intenses dans la zone méditerranéenne
ERA-CLIM	European Reanalysis of Global Climate Observations
ESURFMAR	Eumetnet SURFace MARine programme
EUFAR2	2nd EUFAR project under FP7 and 4th since 2000
EUREQUA	Evaluation mUltidisciplinaire et Requalification Environnementale des QUArtiers, projet financé par l'Agence Nationale pour la Recherche, ANR-2011-VILD-006. Partenaires : GAME, IFSTTAR, CEREA, LISST, LAVUE, LPED.
EURO4M	European reanalysis and observations for monitoring http://www.euro4m.eu/
FP7	7th Framework Programme for Research
GeoMIP	Geoengineering Model Intercomparison Project
GHRSST	International Group for High Resolution SST
GLOSCAL	GLobal Ocean Surface salinity CALibration and validation
H2020	Framework Programme for Research and Innovation (2014-2020)
HOMONIM	Historique Observation MOdélisation des Niveaux Marins (History, Observation, Modelisation of Sea Level)
HyMeX	Hydrological cYcle in the Mediterranean EXperiment
IMAGINES	Implementing Multi-scale Agricultural Indicators Exploiting Sentinels
IncREO	Increasing Resilience through Earth Observation
LEFE	programme national « Les Enveloppes Fluides et l'Environnement »
MACC	Monitoring Atmospheric Composition and Climate
METOP	METeorological Operational Polar satellites
PLUVAR	Variabilité sub-saisonnière des pluies sur les iles du Pacifique Sud
PNRA	Programma Nazionale di Recerche in Antartide
QUANTIFY	Programme QUANTIFYing the climate impact of global and European transport systems
RHYTMME	Risques HYdro-météorologiques en Territoires de Montagnes et MEditerranéens
SCAMPEI	Scénarios Climatiques Adaptés aux Montagnes : Phénomènes extrêmes, Enneigement et Incertitudes - projet de l'ANR coordonné par le CNRM
SMOS	Soil Moisture and Ocean Salinity
Suomi-NPP	US program for meteorological polar orbiting satellites
THORPEX	THe Observing system Research and Predictability EXperiment
UERRA	Uncertainties in Ensembles of Regional Re-Analyses
USAP	United States Antarctic Program
VOLTIGE	Vecteur d'Observation de La Troposphère pour l'Investigation et la Gestion de l'Environnement
WCRP	World Climate Research Programme

Campaigns

AMMA	Analyses Multidisciplinaires de la Mousson Africaine
CAPITOUL	Canopy and Aerosol Particles Interactions in Toulouse Urban Layer
CORDEX	COordinated Regional climate Downscaling EXperiment
EUREQUA	Evaluation mUltidisciplinaire et Requalification Environnemental des QUArtiers
HAIC	High Altitude and Ice Crystals (www.haic.eu)
MEGAPOLI	Megacities : Emissions, urban, regional and Global Atmospheric POLlution and climate effects, and Integrated tools for assessment and mitigation
SMOSREX	Surface MOnitoring of the Soil Reservoir EXperiment

Other acronyms

AIRS	Atmospheric Infrared Sounder
ALADIN	Aire Limitée Adaptation Dynamique et développement InterNational
ALIDS	Airborne Laser Interferometric Drop Sizer
AMSR	Advanced Microwave Scanning Radiometer
AMSU	Advanced Microwave Sounding Unit
AMSU-A	Advanced Microwave Sounding Unit-A
AMSU-B	Advanced Microwave Sounding Unit-B
AMULSE	Atmospheric Measurements by Ultra-Light SpEctrometer
ANASYG	ANAlyse Synoptique Graphique
ANTILOPE	ANalyse par spaTIaLisation hOraire des PrEcipitations
ARAMIS	Application Radar A la Météorologie Infra-Synoptique
ARGO	Array for Real time Geostrophic Oceanography
AROME	Application of Research to Operations at Mesoscale
AROME-COMB	AROME - COMBinaison
AROME-PERTOBS	AROME (OBServations PERTurbées aléatoirement)

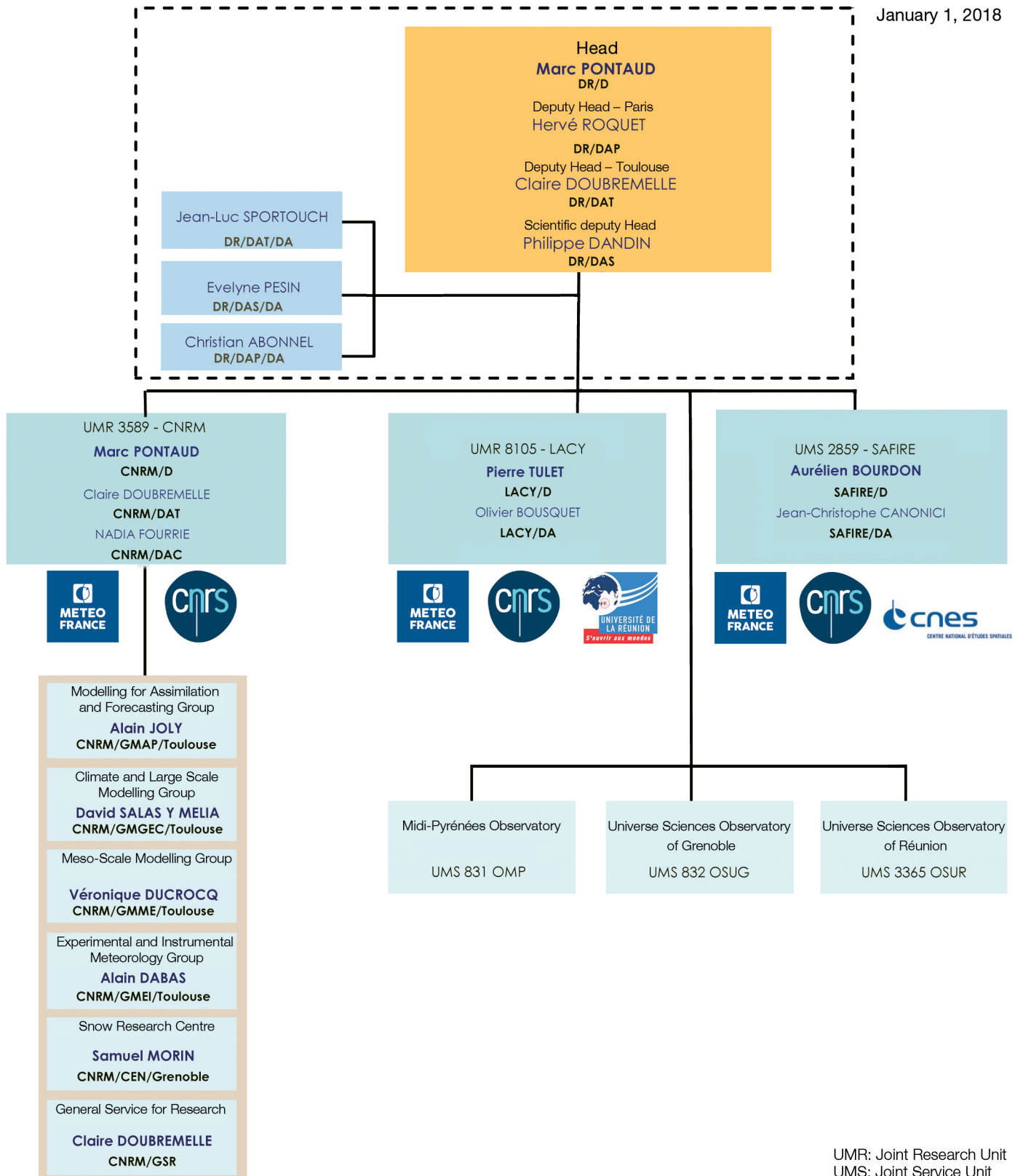|	
AROME-WMED	AROME configuration over the Western Mediterranean region
ARPEGE	Action de Recherche Petite Échelle Grande Échelle
AS	Adaptations Statistiques
ASAR	Advanced Synthetic Arperture Radar
ASCAT	Advanced SCATterometer
ASTEX	Atlantic Stratocumulus Transition EXperiment
ATM	Air Traffic Management
ATMS	Advanced Technology Microwave Sounder
AVHRR	Advanced Very High Resolution Radiometer
BAS	British Antarctic Survey
BLLAST	Boundary Layer Late Afternoon and Sunset Turbulence
BLPB	Boundary Layer Pressurized Balloon
BPCL	Ballon Pressurisé de Couche Limite
BSS	Probabilistic score « Brier Skill Score »
CALIOP	Cloud-Aerosol Lidar with Orthogonal Polarization
CALIPSO	Cloud-Aerosol Lidar and Infrared Pathfinder Satellite Observations
CANARI	Code d'Analyse Nécessaire à ARPEGE pour ses Rejets et son Initialisation
CAPE	Convective Available Potential Energy
CAPRICORNE	CAractéristiques PRIncipales de la COuveRture NuageusE
CARIBOU	Cartographie de l'Analyse du RIsque de Brume et de brOUillard
CAROLS	Combined Airborne Radio-instruments for Ocean and Land Studies
Cb	Cumulonimbus
CFMIP	Cloud Feedback Intercomparison Project
CFOSAT	Chinese-French SATellite
ChArMEx	Chemistry-Aerosol Mediterranean Experiment
CISMF	Centre Inter-armées de Soutien Météorologique aux Forces
CLAS	Couches Limites Atmosphériques Stables
CMC	Cellule Météorologique de Crise
CMIP6	6th phase of the Coupled Model Inter-comparison Project
CMIP5	5th phase of the Coupled Model Inter-comparison Project
CNRM-CM5	Version 5 du Modèle de Climat du CNRM
CNRM-RCSM	Regional Climate System Model
COP	Objectives and Performance Contract
COPAL	COmmunity heavy-PAyload Long endurance instrumented aircraft for tropospheric research in environmental and geo-sciences
CPR	Cloud Profiling Radar
CrIS	Cross-track Infra-Red Sounder
CROCUS	Modèle de simulation numérique du manteau neigeux développé par Météo-France
CTRIP	CNRM-Total Routing Integrated Pathway
DCSC	Direction de la Climatologie et des Services Climatiques
DCT	Diffraction Contrast Tomography
DEM	Discrete Element Method
DMT	Dropplet Measurement Technologies
DOA	Upper Air Observation Department
DP	Direction de la Production
DPR	Dual frequency Precipitation Radar
DPrévi	Direction de la Prévision
DSI	Direction des Systèmes d'Information (Météo-France)
DSNA	Direction des Services de la Navigation Aérienne
ECOCLIMAP	Base de données de paramètres de surface
ECUME	Exchange Coefficients from Unified Multi-campaings Estimates
EGEE	Etude du golfe de GuinEE
ENVISAT	ENVIronmental SATellite
ERA	European Re-Analysis
ESRF	European Synchrotron Radiation Facility
EUCLIPSE	European Union Cloud Intercomparison, Process Study & Evaluation
FAB	Fonctionnal Aerospace Block
FABEC	Functional Airspace Block Europe Central
FAR	Fausse AleRte
FSO	Forecast Sensitivity to Observations
FSOi	Forecast Sensitivity to Observations-based impact
GABLS4	Gewex Atmospheric Boundary Layer Study
GELATO	Global Experimental Leads and ice for ATmosphere and Ocean
GEV	Generalized extreme value (GEV) distribution
GIEC	Groupe Intergouvernemental d'experts sur l'Evolution du Climat
GMAP	Modelling and Assimilation for Forecasting Group
GMEI	Experimental and Instrumental Meteorology Group
GMES	Global Monitoring for Environment and Security
GMME	Meso-Scale Modelling Group
GNSS-R	Global Navigation by Satellite System - Reflectometry
GPM	Global Precipitation Measurement
GPP	Gross Primary Production
GPS	Global Positionning System
High IWC	High Ice Water Content
HIRLAM	HIgh Resolution Limited Area Model
HISCRTM	HIgh Spectral resolution Cloudy-sky Radiative Transfer Model

HSS	Measurement of improvement of the forecast
HYCOM	HYbrid Coordinate Ocean Model
IAGOS	In-service Aircraft for Global Observing System
IASI	Infrared Atmospheric Sounding Interferometer
IAU	Incremental analysis update
IFS	Integrated Forecasting System
IIR	Infrared Imaging Radiometer
INDARE	Indian Ocean Data Rescue Initiative
IOP	Intensive Observation Period
IPR	Intellectual Property Rights
IPS	Indice Piézométrique Standardisé (Standardized Piezometric Level Index)
ISBA	Interactions Soil Biosphere Atmosphere
ISBA-A-gs	Interactions Soil-Biosphere-Atmosphere model, including photosynthesis and vegetation growth
ISBA - ES	Numerical model developped at CNRM to represent soil-vegetation evolution, with a refined snow pack tretament
ISBA-TOP	Coupling between the surface scheme ISBA and a « mediterranean » version of the hydrological TOPMODEL model
ISFC	Indice de Segmentation de la Composante de Fourier
ISIS	Algorithme de suivi automatique des systèmes identifiés à partir de l'imagerie infra-rouge de Météosat
IWC	Ice Water Content
LAI	Leaf Area Index
Land-SAF	LAND Satellite Application Facilities
LAURE	Air and Rational Use of Energy Act (Loi sur l'Air et l'Utilisation Rationnelle de l'Energie)
LCCS	Land Cover Classification System
LES	Large Eddy Simulation model
LISA	LIdar SAtellite
4M	Mobile Means for Meteorological Measurements
Med-CORDEX	Mediterranean Coordinated Regional Climate Downscaling Experiment
MEDUP	MEDiterranean intense events : Uncertainties and Propagation on environment
Megha-Tropiques	Satellite fanco-indien dédié à l'étude du cycle de l'eau et des échanges d'énergie dans la zone tropicale
MEPRA	Modèle Expert de Prévision du Risque d'Avalanche (modélisation)
MERSEA	Marine EnviRonment and Security for the European Area
MESCAN	Combinaison de MESAN (nom du système suédois) et de CANARI
MESO-NH	Modèle à MESO-échelle Non Hydrostatisque
MFWAM	Météo-France WAve Model
MHS	Microwave Humidity Sounder
MISR	Multi-angle Imaging SpectroRadiometer
MNPCA	Microphysique des Nuages et de Physico-Chimie de l'Atmosphère
MOCAGE	MOdélisation de la Chimie Atmosphérique de Grande Echelle (modélisation)
MODCOU	MODèle hydrologique COuplé surface-souterrain.
MODIS	MODerate-resolution Imaging Spectro-radiometer (instrument)
MoMa	Méthodes Mathématiques pour le couplage modèles et données dans les systèmes non-linéaires stochastiques à grand nombre de degrés de liberté
MOTHY	French Oil Spill drift Model
MRR	Micro Rain Radars
MSG	METEOSAT Second Generation
NAO	North Atlantic Oscillation
NEMO	Nucleus for European Modelling of Ocean
NEMO-WMED36	NEMO configuration of the Western Mediterranean Sea
NSF	Norges StandardiseringsForbund
NWCSAF	Satellite Application Facility for Nowcasting
NWP	Numerical Weather Prediction
OASIS	Ocean Atmosphere Sea Ice Soil
OPIC	Objets pour la Prévision Immédiate de la Convection
ORACLE	Opportunités et Risques pour les Agro-ecosystèmes et les forêts en réponse aux changements CLimatiquE, socio-économiques et politiques en France
ORCHIDEE	ORganizing Carbon and Hydrology in Dynamic EcosystEms
OSCAT	OCEANSAT-2 Scatterometer
OSTIA	Operational Sea surface Temperature sea Ice Analysis
OTICE	Organisation du Traité d'Interdiction Complète des Essais nucléaires
PALM	Projet d'Assimilation par Logiciel Multi-méthodes
PDO	Pacific Decadal Oscillation
PEARO	Prévision d'Ensemble AROME
PEARP	Prévision d'Ensemble ARPège
PI	Prévision Immédiate
PN	Prévision Numérique
POD	PrObabilité de Détection
POI	Période d'Observation Intensive
PRESYG	PREvision Synoptique Graphique
Prev'Air	Plateforme nationale de la qualité de l'air

PREVIBOSS	PREvisibilité à courte échéance de la variabilité de la VIsibilité dans le cycle de vie du Brouillard, à partir de données d'Observation Sol et Satellite
Prévi-Prob	Projet sur les prévisions probabilistes
PSI	Pollutant Standard Index
PSR	Plan Submersions Rapides (Rapid Submersion Plan)
PVM	Particulate Volume Monitor
PVs	Moist-air Potential Vorticity
RADOME	Réseau d'Acquisition de Données d'Observations Météorologiques Etendu
RCP8.5	8.5 W/m² Representative Concentration Pathway corresponding to a 8.5 W/m² radiative forcing at the end of the 21st century compared to preindustrial climate
RDI	Référent Départemental Inondation (Flooding Departmental Reference)
RDT	Rapidly Developing Thunderstorm
RHI	Range Height Indicator (coupe verticale)
ROC	Relative Operating Characteristic curve
RRTM	Rapid Radiative Transfer Model
RTTOV	Radiative Transfer for TOVS
SAFNWP	Satellite Application Facility for Numerical Weather Prediction
SAF OSI	Satellite Application Facility for Ocean and Sea Ice
SAFRAN	Système d'Analyse Fournissant des Renseignements Atmosphériques pour la Neige - Set of reconstructed data from observations over France for 1958 to present at high horizontal, vertical and temporal resolution
SAPHIR	Sondeur Atmosphérique du Profil d'Humidité Intertropicale par Radiométrie
SARA	Spectroscopy by Amplified Resonant Absorption
SATOB	Satellite Observation
SCM	Single-Column Model
SESAR	Single European Sky ATM Research
SEVIRI	Spinning Enhanced Visible and Infra-Red Imager
SFRI	Système Français de Recherche et d'Innovation
S2M	SAFRAN - SURFEX/ISBA-Crocus – MEPRA
SIM	SAFRAN ISBA MODCOU
SIRTA	Site Instrumental de Recherche par Télédétection Atmosphérique
SMOSMANIA	Soil Moisture Observing System – Meteorological Automatic Network Integrated Application
SMT	Système Mondial de Télécommunications
SOERE/GLACIOCLIM	Système d'Observation et d'Expérimentation sur le long terme pour la Recherche en Environnement : "Les GLACIers, un Observatoire du CLIMat".
SOP	Special Observing Period
SPC	Service de Prévision des Crues (Flooding Forecasting Service)
SPI	Standardized Precipitation Index
SPIRIT	SPectromètre Infra-Rouge In situ Toute altitude
SPPT	Stochastically Perturbed Parametrization Tendencies
SSI	Solar Surface Irradiance
SSMI/S	Special Sounder Microwave Imager/Sounder
SURFEX	code de SURFace Externalisé (externalized land surface parameterization)
SVP	Surface Velocity Program
SWI	Soil Wetness Index
SWIM	Surface Wave Investigation and Monitoring
SYMPOSIUM	SYstème Météorologique de Prévision Orienté Services, Intéressant des Usagers Multiples - split of French territory into climate heterogeneous areas, the size of which is to 10 to 30 km
TACTIC	Tropospheric Aerosols for ClimaTe In CNRM
TCU	Towering Cumulus
TRL	Technology Readiness Level
TEB	Town Energy Budget
TRIP	Total Runoff Integrating Pathways
TSM	Températures de Surface de la Mer
UHF	Ultra-Haute Fréquence
UNIBAS	Modèle de précipitations
UTLS	Upper Troposphere - Lower Stratosphere
VARPACK	Current tool for diagnostic analysis in Meteo-France
VHF	Very High Frequency
VOS	Voluntary Observing Ships
WWLLN	World Wide Lightning Location Network

Research Department (DR) Management structure

METEO FRANCE

Head
Marc PONTAUD
DR/D

Deputy Head – Paris
Hervé ROQUET
DR/DAP
Deputy Head – Toulouse
Claire DOUBREMELLE
DR/DAT
Scientific deputy Head
Philippe DANDIN
DR/DAS

Jean-Luc SPORTOUCH
DR/DAT/DA

Evelyne PESIN
DR/DAS/DA

Christian ABONNEL
DR/DAP/DA

UMR 3589 - CNRM
Marc PONTAUD
CNRM/D
Claire DOUBREMELLE
CNRM/DAT
NADIA FOURRIE
CNRM/DAC

METEO FRANCE   cnrs

UMR 8105 - LACY
Pierre TULET
LACY/D
Olivier BOUSQUET
LACY/DA

METEO FRANCE   cnrs   UNIVERSITÉ DE LA RÉUNION S'ouvrir aux mondes

UMS 2859 - SAFIRE
Aurélien BOURDON
SAFIRE/D
Jean-Christophe CANONICI
SAFIRE/DA

METEO FRANCE   cnrs   cnes CENTRE NATIONAL D'ÉTUDES SPATIALES

Modelling for Assimilation and Forecasting Group
Alain JOLY
CNRM/GMAP/Toulouse

Climate and Large Scale Modelling Group
David SALAS Y MELIA
CNRM/GMGEC/Toulouse

Meso-Scale Modelling Group
Véronique DUCROCQ
CNRM/GMME/Toulouse

Experimental and Instrumental Meteorology Group
Alain DABAS
CNRM/GMEI/Toulouse

Snow Research Centre
Samuel MORIN
CNRM/CEN/Grenoble

General Service for Research
Claire DOUBREMELLE
CNRM/GSR

Midi-Pyrénées Observatory

UMS 831 OMP

Universe Sciences Observatory of Grenoble

UMS 832 OSUG

Universe Sciences Observatory of Réunion

UMS 3365 OSUR

UMR: Joint Research Unit
UMS: Joint Service Unit

Liberté • Égalité • Fraternité
RÉPUBLIQUE FRANÇAISE

MINISTÈRE
DE LA TRANSITION
ÉCOLOGIQUE
ET SOLIDAIRE

Creation DIRCOM/CGN